Malin Alise Sandmoe

Integrated stress response pathways induced by DHA in human colon cancer cell lines

Master thesis in Molecular Medicine

Trondheim, June 2016

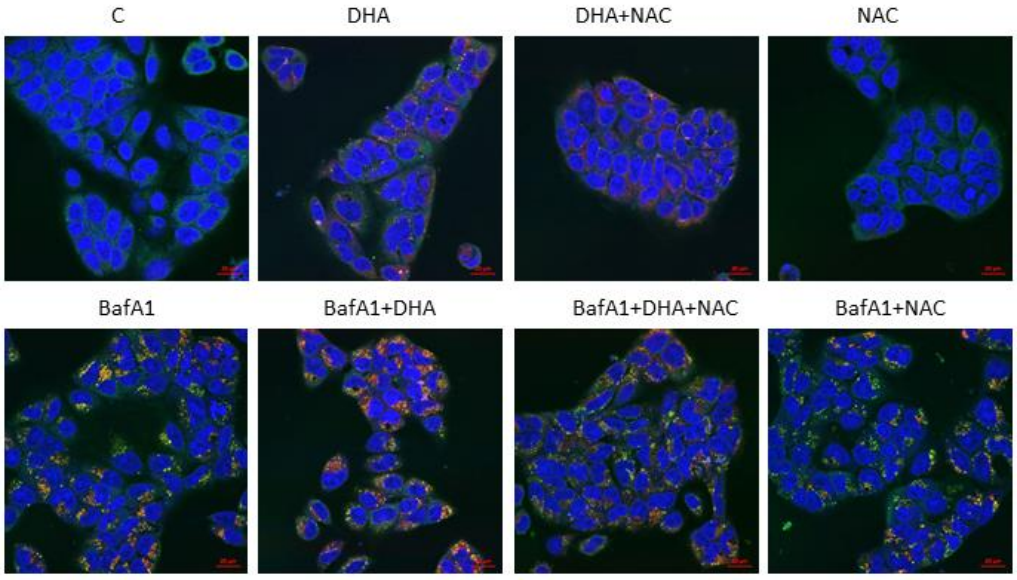

NTNU
Norwegian University of
Science and Technology

Contents

Acknowledgements

This work was performed during the years 2015-2016 at the Department of Laboratory Medicine, Children's and Women's Health, Faculty of Medicine, Norwegian University of Science and Technology (NTNU).

First and foremost, I would like to thank my main supervisor Professor Svanhild Schønberg for giving me the opportunity to be part of your research group and for patiently guiding me through this project. I am very grateful for your support and good advices throughout this work.

I would also like to express my very great appreciation to my co-supervisor Caroline Hild Pettersen. Your door was always open whenever I had a question or needed advice, even in the busiest of times. Thank you for always helping me and steering me in the right direction.

My gratitude also goes to the members of our research group. I am particularly thankful to Helle Samdal for patiently teaching and helping me through all the laboratory work, and for always taking the time to answer my questions. I have really appreciated our good collaboration.

Finally, I am very grateful to my mum and dad, family and friends for their support and encouragement. Thank you for always believing in me.

Trondheim, June 2016

Malin Alise Sandmoe

Abstract

Estimates show that 95% of all cancers can be attributed to environmental factors, and diet represents 30-35% of this. The omega-3 polyunsaturated fatty acid docosahexaenoic acid (DHA, 22:6 n-3) is an essential fatty acid that has been shown to have anticancer properties. Many molecular mechanisms have been proposed to be involved, including increased oxidative stress, alterations in membrane composition or function, changes in eicosanoid production, and regulation of gene expression. Our group has previously shown that ER stress is induced in response to DHA in several human colon cancer cell lines. ER stress is a part of the integrated stress response, which responds to various types of cellular stressors and coordinates a response throughout cellular structures. The aim of this study was to elucidate the molecular mechanisms involved in the anticancer properties of DHA, with special focus on pathways involved in the integrated stress response.

The two human colon cancer cell lines DLD-1 and LS411N were chosen based on their different sensitivity to DHA treatment and the fact that they are cultured in the same growth medium. DHA-effect on cell growth was measured by cell counting. About 40% growth inhibition was observed after 48 h in DLD- cells, whereas LS411N cells showed very little growth inhibition. Co-treatment with the antioxidants BHA and BHT did not counteract the growth inhibition, but growth inhibition was partly counteracted after NAC treatment, indicating a role of oxidative stress in DHA-induced growth inhibition. Protein expression analyses of ER-stress- and Golgi-stress-related proteins showed that ER stress was induced DLD-1 cells, but not in LS411N cells. Golgi stress was not induced in either cell line. Mitochondrial oxidative stress and reactive oxygen species (ROS) were measured by flow cytometry, and results showed an increase in both mitochondrial oxidative stress and ROS levels. Whereas NAC did not reduce mitochondrial oxidative stress, it did reduce ROS levels. The fluorescence intensity of the autophagy marker Cyto-ID was measured by flow cytometry to measure autophagic structures in the cells. Results showed an increase in autophagy after DHA treatment in DLD-1 cells. Protein expression analyses showed an increase in autophagic flux in the same cell line. Autophagy levels increased in LS411N cells, but an increase in autophagic flux was not observed. The basal autophagy level in LS411N cells was found to be 2.5 fold higher than in DLD-1 cells, indicating a possible connection between basal autophagy levels and DHA sensitivity. DLD-1 expresses mutant p53, while p53 is not expressed in LS411N cells. Protein levels of p53 in DLD-1 cells were affected after DHA treatment, but SiRNA-mediated knockdown of p53 in DLD-1 cells did not affect the DHA sensitivity. This

suggests that DHA sensitivity does not depend on p53 status. Together, results suggest that oxidative stress and pathways of the integrated stress response are involved in DHA-induced growth inhibition and that autophagy levels are important for the DHA sensitivity of colon cancer cells.

Abbreviations

AA	Arachidonic acid
Akt	Protein kinase B
ALA	α-linoleic acid
AMPK	AMP-activated protein kinase
APC	Adenomatous polyposis coli
ARF4	ADP-ribosylation factor 4
ATF4	Activating transcription factor 4
ATF6	Activating transcription factor 6
ATG	Autophagy-related genes
BafA1	Bafilomycin A1
Bax	Bcl-2-like protein 4
Bcl-2	B-cell lymphoma 2
BFA	Brefeldin A
BHA	Butylated hydroxyanisole
BHT	Butylated hydroxytoluene
CHOP	C/EBP homologous protein
cMyc	V-myc avian myeocytomatosis viral oncogene homolog
CoA	Coenzyme A
COX	Cyclooxygenase
CREB-3	Cathelicidin antimicrobial peptide responsive element binding protein 3
DCF	Dichlorofluorescein
DHA	Docosahexaenoic acid
DTT	Dithiotreitol
eIF2α	Eukaryotic initiation factor 2
EPA	Eicosapentaenoic acid
ER	Endoplasmic reticulum
ERSE	ER stress response element
EtOH	Ethanol
FA	Fatty acid
FAS	Fatty acid synthase
GA	Golgi apparatus
GADD34	Growth arrest and DNA damage-inducible protein 34
GASE	Golgi apparatus stress response element
GRP	Glucose-related protein
H2DCF	Dichlorohydrofluorescein diacetate
HSP	Heat shock protein
IRE1	Inositol-requiring enzyme 1
ISR	Integrated stress response
LA	Linoleic acid
LC3	Ubiquitin-like microtubule associated protein 1 light chain 3
LOX	Lysyl oxidase
MAG	Monoacylglycerol
MeOH	Methanol
mTOR	Mammalian target of rapamycin

MUFA	Monounsaturated fatty acid
NAC	N-acetyl cysteine
NADPH	Nicotinamide adenine dinucleotide phosphate
NFE2L2	Nuclear factor (erythroid-derived 2)-related factor 2
NF-κB	Nuclear factor kappa light chain enhancer of activated B-cells
OA	Oleic acid
p53	Tumour protein 53
p62/SQSTM1	Sequestosome 1
pATF6	Phosphorylated ATF6
PBS	Phosphate saline buffer
PE	Phosphatidyl-ethanolamine
peIF2α	Phosphorylated eIF2α
PERK	PKR-like ER kinase
PFA	Paraformaldehyde
PGE_2	Prostaglandin E2
PGE_3	Prostaglandin E3
PI3K	Phosphatidyl inositol-3-kinase
PI3P	Phosphatidyl inositol-3-phosphate
PPAR	Proliferator-activated receptors
PUFA	Polyunsaturated fatty acid
RAS	Rat-sarcoma family of genes
ROS	Reactive oxygen species
RT	Room temperature
SFA	Saturated fatty acid
siRNA	Small interfering RNA
TAG	Triacylglycerol
TBS	Tris buffered saline
TBST	Tris buffered saline with tween
TFE3	Transcription factor binding to IGHM enhancer 3
TG	Thapsigargin
TRIB3	Tribbles-related protein 3
UBD	Ubiquitin-binding domain
UFA	Unsaturated fatty acid
ULK	ATG1/unc-51-like kinase
UPR	Unfolded protein response
VEGF-A	Vascular endothelial growth factor A
VPS	Vacuolar protein sorting
XBP1	X-box binding protein-1

1. Introduction

Cancer is one of the leading causes of death worldwide, causing approximately 8.2 million deaths each year (reviewed in [1]). Research shows that 95% of the cases are caused by environmental factors, including external factors such as pollution and infections, and lifestyle factors such as tobacco, alcohol and diet. It has been estimated that the diet represents 30-35% of the risk factors involved in the onset of cancer (reviewed in [2]).

A western diet is characterized by a high intake of omega-6 (n-6) polyunsaturated fatty acids (PUFAs) compared to omega-3 (n-3) PUFAs, and a high intake of saturated fatty acids (SFAs). Many studies have investigated the possible health effects of an increased intake of n-3 PUFAs, and possible benefits have been reported for several diseases such as cardiovascular diseases, inflammatory diseases, and neurodegenerative diseases, as well as a number of different cancer types (reviewed in [3]). Even though epidemiological studies are inconsistent in showing a the relationship between an increased intake of n-3 PUFAs and cancer risk, both *in vivo* and *in vitro* studies have demonstrated that n-3 PUFAs can inhibit cancer cell growth. The mechanisms behind the anticancer properties of n-3 PUFAs probably involve initiation of cell death, inhibition of cell proliferation, or a combination of both of these mechanisms (reviewed in [4]).

1.1 Cancer

Cancer is a group of diseases that is caused by uncontrolled cell growth and division of abnormal cells that also have the ability to invade other tissues in the body. It is caused by both genetic and epigenetic alterations, which in turn can be caused by both inherited mutations and environmental factors (reviewed in [1]). In 2014 over 30,000 new cases of cancer were registered in Norway, with the most common cancer forms being prostate cancer, breast cancer, colon cancer and lung cancer. Almost 11,000 cancer-related deaths were registered the same year, half of which were caused by the cancer forms previously mentioned [5].

1.1.1 Carcinogenesis

Carcinogenesis is defined as the initiation of cancer formation, and it describes the process where normal cells are transformed into cancer cells. It is considered to be a multistage process with four steps: tumour initiation, tumour promotion, malignant conversion, and tumour progression (figure 1). The stepwise process of carcinogenesis is due to an

accumulation of genetic and/or epigenetic changes, with a gradual increase in the number of changes as carcinogenesis advances. The changes include activation of proto-oncogenes, inactivation of tumour-suppressor genes, and changes that allow the cancer cells to invade other tissues [6].

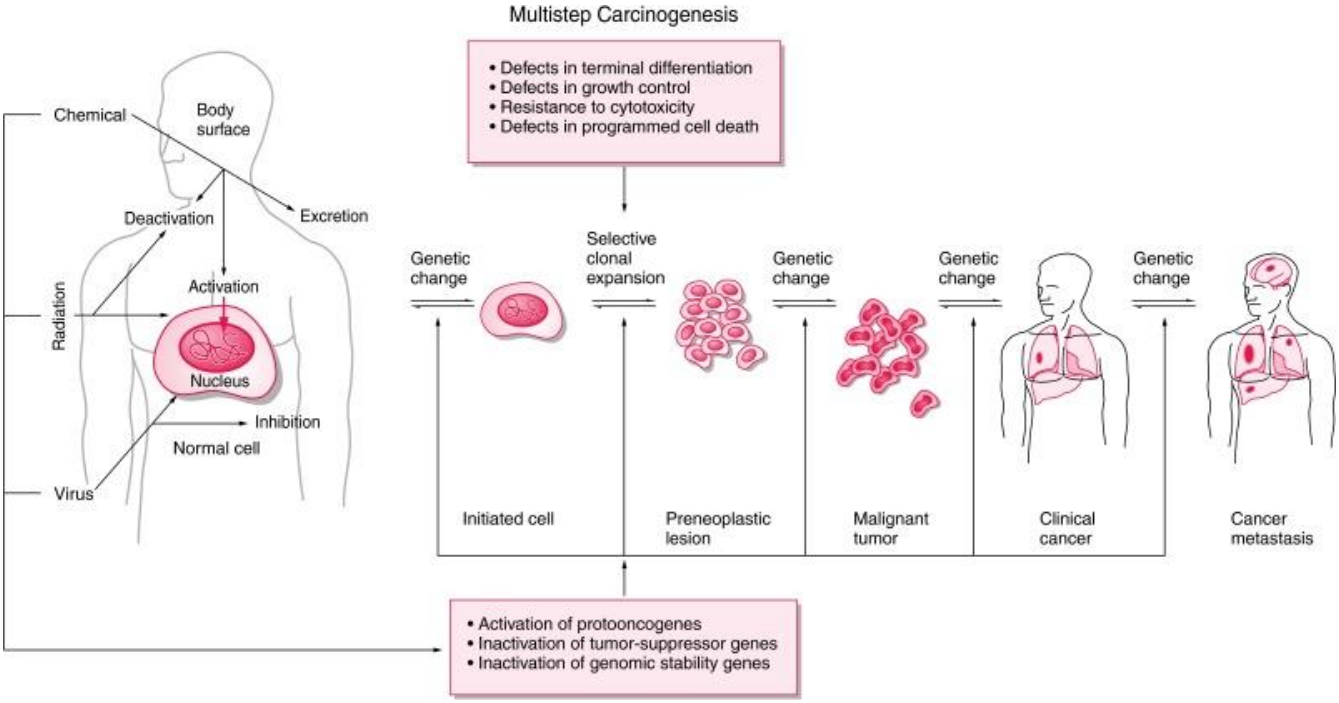

Figure 1: The multistage process of carcinogenesis. Carcinogenesis is initiated by genetic changes in the cells, and a clonal expansion of these cells initiates a tumour. Further genetic alterations promote growth and spread of the cancer cells (the figure is copied from [6]).

Cancer cells do not operate on their own; they are part of a tumour microenvironment that comprises both transformed cancer cells and non-transformed cells such as immune cells and vascular cells. They communicate via cellular messengers such as chemokines, cytokines and growth factors, and are often connected by a strong extracellular matrix (reviewed in [7]). Therefore, it is important to understand the biology not only of the malignant cells itself, but of the tumour microenvironment as a whole. Several capabilities are necessary to enable tumour growth and metastatic spread, and Hanahan and Weinberg have listed ten hallmarks of cancer that in addition to the properties of the malignant cells also includes the tumour microenvironment (figure 2) (reviewed in [8]).

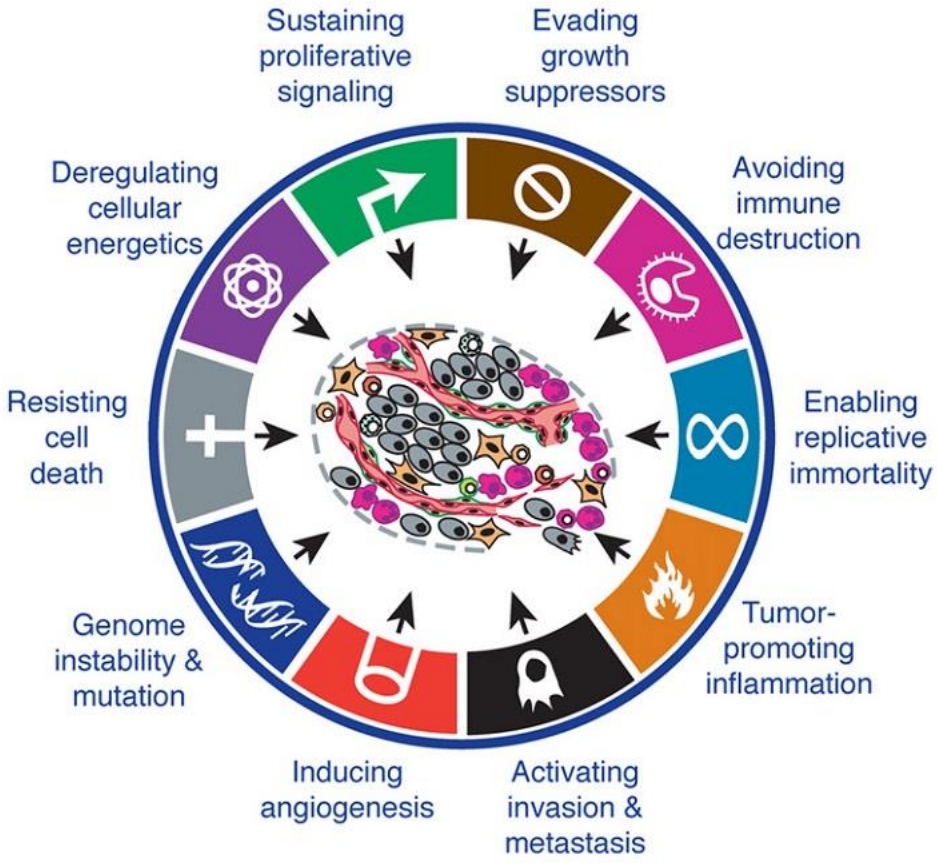

Figure 2: The hallmarks of cancer, consisting of ten proposed alterations in cell physiology and tumour microenvironment that contribute to malignant growth (the figure is adapted with permission from [8]).

Sustaining proliferative signalling

One of the most important traits of cancer cells is that they are able to proliferate an infinite number of times. In normal cells the cell number is tightly regulated by a number of mechanisms, but cancer cells are able to avoid this regulation. One way they are able to sustain the proliferation is by producing growth factors that regulate the progression through the cell cycle, both in the cancer cells itself and in normal cells in the tumour microenvironment. The normal cells will then produce various growth factors that affect the cancer cells. Another possible mechanism to sustain the proliferative signalling is by increasing the number of receptors to the growth factors on the cell membrane, thus enabling signalling even though the levels of growth factors are limited (reviewed in [8]).

Evading growth suppressors

In general, cell proliferation is negatively regulated by several mechanisms, including tumour-suppressor genes and contact inhibition. Cancer cells are often able to evade these suppressor mechanisms due to mutations in the genes responsible. Contact inhibition is often deregulated

in cancer cells, making them able to grow even though the cell density is already high. One tumour-suppressor that is often found mutated in cancers is tumour protein 53 (p53), a protein that in normal cells is responsible for halting cell cycle progression if the stress level becomes too high. Another such protein is the retinoblastoma-associated (RB) protein, which normally regulates cell cycle progression in response to a number of intracellular- and extracellular signals. The loss-of-function of these regulators will therefore enable the cancer cell to evade growth suppression (reviewed in [8]).

Genome instability and mutation

As previously mentioned, the multistage process of carcinogenesis can be considered as a gradual increase in mutations or epigenetic changes as the cancer progresses. Cancer cells often have increased rates of mutations, caused by an increased sensitivity to mutagens or a fault in the genomic maintenance system. One central protein is p53, which is considered to be “the guardian of the genome” due to its function in sensing and repairing DNA-damage. Mutations in p53 leading to a loss of function can therefore lead to an accumulation of other mutations because the DNA-damage is not discovered and repaired (reviewed in [8]).

Resisting cell death

Apoptosis is triggered in response to certain cellular stresses, leading to a programmed cell death to protect the organism from further damage. One way for cancer cells to resist cell death is by avoiding apoptosis. Several mechanisms are involved in inducing apoptosis, but one that is often found deregulated is the p53-pathway. Normally, DNA-damage or other stresses will induce expression of phorbol-12-myristate-13-acetate-induced protein 1 (Noxa) and p53 upregulated modulator of apoptosis (Puma) via p53, which in turn inhibits B-cell lymphoma 2 (Bcl-2). Bcl-2 works as an inhibitor of apoptosis by controlling the pro-apoptotic protein bcl-2-like protein 4 (Bax), but when inhibited itself, Bax is free to initiate apoptosis. Thus, a loss-of-function of p53 will result in the cell being able to survive even though it is damaged in some way. Other mechanisms to avoid cell death include an increase in the expression of anti-apoptotic regulators or a downregulation of pro-apoptotic signals (reviewed in [8]).

Deregulating cellular energetics

Cancer cells are actively growing and proliferating, and this requires large amounts of energy. In order to meet the demands, the metabolism of cancer cells is often reprogrammed. One such mechanism is by changing the glucose metabolism. Instead of oxidative phosphorylation

of pyruvate, the energy is produced solely by glycolysis, even if oxygen is present. The energy-yielding process is therefore termed “aerobic glycolysis”. This switch produces less energy than by the complete oxidation of glucose, but the cancer cells compensate for the lower energy yield by upregulating the number of glucose transporters. Also, it has been found that the glycolytic intermediates are used in a number of biosynthetic pathways in the cancer cells, leading to more available building blocks for organelles and macromolecules necessary for cell growth and division (reviewed in [8]).

Inducing angiogenesis

All cells are dependent on a system that delivers O_2 and nutrients, and that removes CO_2 and waste products. This is done by the vascular system. The growth of new vessels, angiogenesis, is normally turned off in adults, but in a tumour this system is often switched on. One signal molecule involved in blood vessel growth is vascular endothelial growth factor-A (VEGF-A), which can be upregulated both by hypoxia and by oncogene signalling. Thrombospondin-1 is another signalling molecule, but opposed to VEGF-A, its normal function is to inhibit angiogenesis. Thus, a deregulation of thrombospondin-1 may enable the growth of new blood vessels (reviewed in [8]).

Activating invasion and metastasis

The path to invasion and metastasis is considered to be a multistep process, starting with an invasion in nearby tissues, and continuing to spread in the body via blood and lymphatic vessels. A characteristic often found in metastatic cells is the loss of key cell-to-cell adhesion molecules, enabling the cells to spread to other tissues and organs of the body (reviewed in [8]).

Enabling replicative immortality

Most normal cells are only able to go through a certain number of divisions before they enter senescence, a non-proliferative state, or crisis, which leads to cell death. Evidence suggests that telomeres at the chromosome ends are responsible for the limited number of divisions, as they are shortened for each round of replication. The enzyme telomerase is able to elongate the telomeres by adding repeating segments to the chromosome ends, but in most normal cells it is inactivated. In cancer cells, however, telomerase is often found to be activated, resulting in elongation of telomeres and thus avoidance of senescence (reviewed in [8]).

Tumour-promoting inflammation

In addition to cancer cells, most tumours have also been found to contain immune cells in variable numbers. This is considered to be an attempt of the immune system to combat the disease, but the inflammatory effect has also been found to promote tumour growth. This is because the immune cells deliver many signalling molecules to the tumour, including growth factors, survival factors, and proangiogenic factors. In addition, the immune cells can release reactive oxygen species (ROS) that are mutagenic, leading to a further accumulation of mutations (reviewed in [8]).

Avoiding immune destruction

An increasing amount of evidence points to the possibility that the immune system acts as a brake or barrier to tumorigenesis. Some cells are able to disable parts of the immune system, thus enabling them to avoid destruction by immune cells. This, however, is still not an established hallmark, and more evidence is needed to confirm its position as an important characteristic of carcinogenesis (reviewed in [8]).

1.1.2 Colon cancer

Colon cancer is one of the most prevalent cancer types, especially in industrialised countries. In 2014, 2801 patients were diagnosed with colon cancer in Norway. Out of these, 1442 were women and 1359 were men, making it the second and third most common cancer type among the genders [5]. This is a small increase from the years before, and it is likely to be associated with a westernised lifestyle with lack of exercise, a high intake of saturated fats and other dietary factors, obesity, and smoking (reviewed in [5, 9]).

Some mutations have been found to increase the risk of colon cancer, including mutations in the adenomatous polyposis coli (APC) gene, causing familial adenomatous polyposis, and in the mismatch repair genes, causing Lynch syndrome, but these inherited cases can only account for about 10% of all colon cancer cases. Thus, the environmental factors mentioned above seem to be of high importance in the development of colon cancer. These environmental factors contribute to a change in the balance between cell proliferation and cell death in the epithelium of the colon by introducing new mutations that promote carcinogenesis. It has been found that colon cancers are some of the most genetically complex cancers, but some common driver mutations include the APC gene, the rat sarcoma family of genes (RAS) genes, and the phosphatidyl inositol-3-kinase (PI3K) gene, all of which are considered to be either tumour-suppressor genes or proto-oncogenes (reviewed in [10]).

1.2 Fatty acids

1.2.1 Structure and nomenclature

Fatty acids (FAs) consist of a hydrocarbon chain with a methyl group (-CH_3) attached in one end and a carboxyl (-COOH) group at the other end. Whereas SFAs contain single bonds between the carbon atoms in the chain and are saturated with hydrogen atoms, unsaturated FAs (UFAs) contain one or more double bonds (figure 3). UFAs are further classified according to the number of double bonds. Monounsaturated FAs (MUFAs) contain one double bond, while PUFAs have two or more [11].

The International Union of Pure and Applied Chemists' (IUPAC) system for naming FAs is based on the number of carbon atoms in the FA chain, the position of double bonds, if present, as well as the configuration of the double bonds. Carbon atoms are numbered starting from the carboxyl group. Thus, the IUPAC name of α-linolenic acid is *cis, cis, cis*-9, 12, 15-octadecatrienoic acid. Because of the complexity of this system, trivial names are often used. The most common system is the C:D (n minus) system, where C denotes the number of carbon atoms, D is the number of double bonds, and n minus refers to the position of the double bond closest to the methyl end of the FA. By using this system, α-linolenic acid is denoted as 18:3(n-3) [11].

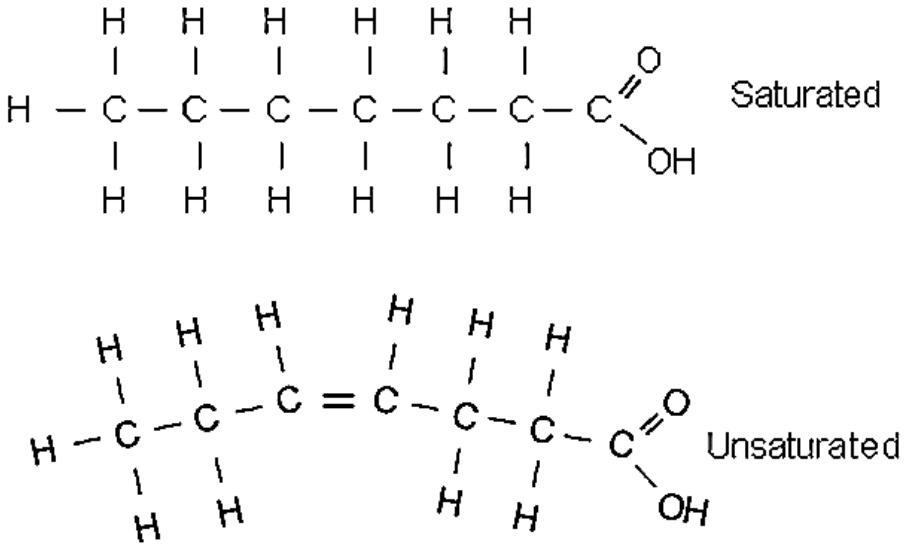

Figure 3: The chemical structure of saturated and unsaturated fatty acids (the figure is modified with permission from [11]).

1.2.2 Fatty acid metabolism

Fatty acid synthesis

In a normal westernised diet fat constitutes about 35-40% of the daily energy intake, and in general this covers the body's need for FAs [12]. Therefore, *de novo* synthesis of FAs in the body usually only occur when there is an excess intake of energy. Carbon atoms from the energy source, usually carbohydrates, are first converted to pyruvate in the cytosol. The pyruvate is transported to the mitochondria where the pyruvate dehydrogenase enzyme complex oxidises pyruvate to form acetate. Acetate is then esterified to form acetyl coenzyme A (CoA), enters the Krebs cycle in the mitochondrion, and condensates with oxaloacetate to form citrate, which can exit from the cycle if the conditions are set for FA synthesis [13].

Citrate is transported to the cytoplasm and cleaved to form acetyl CoA and oxaloacetate. To obtain some of the energy that is required for the FA synthesis to occur the oxaloacetate molecule is cleaved to yield nicotinamide adenine dinucleotide phosphate (NADPH). The rest of the energy required, both in the form of NADPH and adenosine triphosphate (ATP), originates from the pentose phosphate pathway [13].

Acetyl CoA is used as starting point in the synthesis of FAs. Two enzymes are essential to this process – Acetyl CoA carboxylase and the fatty acid synthase (FAS) complex. The former is responsible for the carboxylation of acetyl CoA to form malonyl CoA, whereas the latter uses malonyl CoA as a donor for 2-carbon units that is added to a growing FA chain. The enzymes are held in a complex together with the growing FA chain. When the synthesis has ended, usually when palmitic acid (16:0) has been formed, the FA is cleaved from the complex by an internal thioesterase. Following this, other FAs, like UFAs, can be formed by elongation and desaturation processes [13].

Elongation and desaturation

The enzymes responsible for the elongation and desaturation of FAs are named elongases and desaturases, and they use both FAs synthesised in the body and obtained from the diet as substrates. These processes occur in the membrane of the endoplasmic reticulum (ER) membrane. Elongases utilise malonyl CoA to elongate the FA chain by adding 2-carbon units to form longer FAs, whereas desaturases use O_2 and NADH to introduce double bonds into the FA chain. The desaturases in humans are not able to introduce double bonds beyond C-9 in the FA chains, and this is why linoleic acid and α-linolenic acid are essential in the diet [13].

Absorption, transport, and oxidation of fatty acids

The digestion of FAs occurs in the intestinal lumen, where lipases from the pancreas degrade triacylglycerol (TAG) to FAs and monoacylglycerol (MAG) by the help of micelles of bile salts from the gall bladder. The digested fats are then transported to the intestinal epithelium to cross the brush border membrane and enter the intestinal mucosal cells, where they are resynthesised to form TAGs that enters the ER where they are packed into chylomicrons [12]. Chylomicrons consist of the protein apolipoprotein B-48 as well as other fats and fat-soluble vitamins, and are released into the lymph system before entering the blood in order to transport the FAs around the body. Recipient cells contain membrane-bound lipases that bind chylomicrons and degrade TAG to FAs and MAG that can enter the cell [13].

As FAs enter the recipient cells they can either be used as an energy source, or they can be stored as fat in adipocytes. The latter requires esterification of the FA to TAGs, and this conversion can be done by two different pathways – the MAG pathway or the *sn*-glycero-3-phosphate pathway (reviewed in [14]). The MAG pathway is located in the smooth ER, whereas the *sn*-glycero-3-phosphate pathway occurs in the rough ER. The stored TAGs can be mobilised at a later point if the energy demand increases, and enter a process called lipolysis. This process requires the enzymes hormone-sensitive lipase, adipose triglyceride lipase, and MAG lipase, and results in the conversion of TAGs to free FAs and glycerol [13].

The energy-yielding process is called β-oxidation, and it occurs mainly in the mitochondria. Before the FAs can enter the mitochondria they are linked to CoA, a reaction catalysed by acyl CoA synthase on the outer mitochondrial membrane. The newly formed fatty acyl CoA is transported into the mitochondria by a translocase, where it is degraded by repeated cleavage that forms acetyl CoA units, as well as NADH and Flavin adenine dinucleotide ($FADH_2$). Acetyl CoA is then oxidised in the citric acid cycle, where each acetyl CoA is generating 10 ATP molecules. In addition, each NADP and $FADH_2$ generate approximately 2.5 and 1.5 molecules of ATP, respectively [13].

UFAs require two additional enzymes to be fully oxidised, an isomerase and a reductase. FAs with an odd number of double bonds only require the isomerase, which converts *cis* double bonds into *trans* double bonds, making the FA an available substrate for the oxidation process. However, if the FA has an even number of double bonds, both a reductase, which uses NADPH to reduce double bonds, and an isomerase are required [13].

1.2.3 Polyunsaturated fatty acids

The three main groups of PUFAs include the n-3 PUFAs, the n-6 PUFAs, and the n-9 PUFAs. All of the FAs in these groups derive from α-linolenic acid (ALA, C18:3 n-3), linoleic acid (LA, C18:2 n-6), and oleic acid (OA, C18:1 n-9), respectively (reviewed in [11]). Among these, ALA and LA are considered to be essential in mammals, as mammals lack the ability to introduce double bonds in FAs beyond carbon 9 and 10. Both ALA and LA are synthesised in plants and vegetables, and are therefore mainly consumed through vegetable oils and seeds in the diet [4].

In addition to ALA the most important n-3 PUFAs in human diet include eicosapentaenoic acid (EPA, C20:5 n-3) and docosahexaenoic acid (DHA, C22:6 n-3). The main dietary sources of EPA and DHA include fatty fish and fish oils, but the body is also able to synthesise these FAs to a certain degree by using ALA as a starting point [12].

PUFA mechanism and function

The three main functions of FAs in the body are to serve as an energy source, as a part of membranes and as signalling molecules in the body (reviewed in [11]). PUFAs are especially important in the latter two categories, but are also used as fuel in times of need.

The composition of FAs in membranes has an impact on the fluidity of the membrane. A high number of SFAs in the membrane decreases the membrane fluidity, whereas a high number of UFAs increases it. This in turn affects the number and affinity of the receptors found in the membrane. Membrane-bound PUFAs are also important as precursors for eicosanoids, derived from the C:20 PUFAs arachidonic acid (AA, 20:4 n-6) and EPA, and docosanoids, derived from DHA. These second messengers are involved in a variety of mechanisms in the body, including inflammation, immune responses, blood clotting, smooth muscle contraction, cell growth and proliferation (reviewed in [14]).

Synthesis of eicosanoids starts when the enzyme phospholipase A_2 releases AA or EPA from glycerol in the membrane. Following this, the FA can enter one of several pathways in eicosanoid production. One of these pathways is the cyclooxygenase (COX) pathway that leads to the production of prostaglandins. One of the prostaglandins deriving from AA is prostaglandin E_2 (PGE_2), which is pro-inflammatory, stimulates platelet aggregation, and serves as a vasoconstrictor. However, the enzyme responsible for this can also use EPA as a substrate, which gives rise to the less potent prostaglandin E_3 (PGE_3). PGE_3 promotes vasodilation and is an anti-aggregator, meaning it holds the opposite effects of PGE_2.

Therefore, a higher concentration of EPA relative to AA can be beneficial because the two FAs compete for conversion by the same enzyme. In addition, n-3 PUFAs are preferred over n-6 PUFAs by the elongases and desaturases, meaning that higher levels of n-3 PUFAs competitively inhibit the desaturation of LA to AA (reviewed in [11]).

Another group of n-3 PUFA derived eicosanoids are the resolvins, which have been shown to have potent anti-inflammatory effects. The resolvins are found in both a D- and an E-series, which derive from DHA and EPA, respectively. E-series resolvins are produced by the aspirin-treated COX-2 and lysyl oxidase (LOX) enzymes, whereas D-series resolvins are produced by LOX enzymes. In addition to being anti-inflammatory, the resolvins also modulate the immune system and seem to reduce inflammatory pain (reviewed in [15]).

1.2.4 Omega-3 PUFAs and cancer

Though somehow inconsistent, epidemiological studies point to a link between high n-3 PUFA intake and lower cancer risk. The anticancer effect of n-3 PUFAs has also been documented by a large number of both *in vitro* and *in vivo* studies. Several studies support the use of n-3 PUFAs in cancer therapy, and especially in combination with other traditional treatments, including radiation therapy and chemotherapeutic drugs like 5-fluoracil and tamoxifen. In addition, n-3 PUFAs may reduce some of the side-effects of cancer treatment, as well as cachexia (reviewed in [16]).

Several of the studies done on cancer and n-3 PUFAs point to a large number of molecular pathways and mechanisms involved in the anticancer properties, including modulation of cell proliferation, differentiation and survival. However, the main hypotheses regarding the mechanisms involved are the possible conversion of n-3 PUFAs into resolvins and changes in COX activity, alterations in membrane composition and membrane constituents, and increased oxidative stress (reviewed in [3]). Other proposed mechanisms include the regulation of certain transcription factors, modulation of proteins and pathways involved in apoptosis, and the regulation of signalling pathways and cell cycle regulatory proteins (reviewed in [17]).

COX-modulation and resolvin production

As described above, EPA can compete with AA as a substrate for the COX enzyme, producing PGE_3 instead of PGE_2. PGE_2 seems to play a role in the early stages in colorectal carcinogenesis, whereas PGE_3 exhibits anticancer properties. The metabolism of DHA and EPA by LOX and aspirin-modified COX enzymes, respectively, also produces resolvins,

which show anti-inflammatory activity. No direct antineoplastic function has yet been identified, but a resolvin known as resolvin E1 inhibits the activation of the nuclear factor kappa-light-chain-enhancer of activated B cells (NF-κB) when signalling through the chemokine-like receptor 1. NF-κB is known to be of importance in the early stages of carcinogenesis (reviewed in [17, 18]). In addition, the anti-inflammatory effect of the resolvins may also suppress carcinogenesis, as inflammation is counted as one of the emerging hallmarks of cancer (reviewed in [8]).

Alterations in membrane composition and dynamics

The incorporation of PUFAs in membranes, especially DHA, alters the membrane fluidity and regulates the membrane function. The changes in fluidity can alter the position of membrane-bound proteins in lipid rafts, which lead to altered signalling through these receptors. One such receptor is the epidermal growth factor receptor. When the enzyme's ligands, the growth factors, bind to these receptors, they start a signalling cascade that leads to variable cellular responses, including cell proliferation. Treatment with DHA has been shown to exclude this receptor from the lipid rafts in some cancer types. Another protein that is affected by the membrane composition is RAS, which is often mutated in colon cancers. In cells treated with DHA it has been found that RAS localisation is restricted, as it is found only in the membrane and not in the cytosol. This prevents the activation of RAS (reviewed in [17, 18]).

Generation of oxidative stress

Compared to normal cells, colon cancer cells are considered to be more sensitive to oxidative stress [19]. N-3 PUFAs are highly peroxidable, and their oxidation by cellular oxidants produces ROS that increases the oxidative stress. This is considered to be a direct route for n-3 PUFAs action on cancer cells, as it induces the activation of a variety of intracellular pathways related to cell proliferation or apoptosis (reviewed in [3, 16]).

Modulation of transcription mediators

The activity of several transcription mediators are affected by the action of n-3 PUFAs. One family of such mediators is the peroxisome proliferator-activated receptors (PPAR) family, which is involved in the regulation of lipid storage and metabolism. Impaired function of one of the members of the PPAR family, PPARγ, has been associated with colon cancer. DHA can interact with and activate this receptor, and this action has been reported to be an important part of the anticancer role of n-3 PUFAs (reviewed in [17]).

DHA can also have an effect on the transcription factor NF-κB. DHA suppresses the activation of NF-κB, which leads to a reduction in the transcription of NF-κB induced genes, including cancer-promoting cytokines and genes involved in cell proliferation and cell death. It has also been shown that cancer cells are more sensitive to radiation treatment when the concentration of NF-κB is decreased (reviewed in [17]).

As previously mentioned, the tumour-suppressor APC has been found to be mutated in many colon cancer tumours. The APC protein is a part of a wingless-type MMTV integration site (Wnt) signalling cascade, where v-myc avian myelocytomatosis viral oncogene homolog (cMyc) is a downstream effector of APC. It has been shown that DHA treatment increases the concentration of cMyc in the cells, and this sensitises the cells to anticancer treatment. In addition, it has been shown in mice with a defective APC gene that the formation of new tumours is suppressed if they were treated with DHA (reviewed in [17]).

Several transcription modulators involved in ER stress, described in section 1.3.1, has been shown to be upregulated in colon cancer cells after treatment with DHA [20]. These transcription factors activate transcription of genes involved in protein folding, translation-associated genes, anti-oxidant genes, and genes involved in apoptosis [21].

1.3 The integrated stress response

The integrated stress response (ISR) is an intracellular signalling system that responds to a variety of stresses in the cells. These stresses often involve fluctuations above normal in a variety of physical factors, including pathogens, ion concentrations, metabolite concentrations and redox potentials. Upon stress, the ISR activates one of four kinases, which phosphorylates the α subunit of the eukaryotic initiation factor 2 (eIF2α). This is a hallmark of ER stress, and it initiates a signalling pathway called the unfolded protein response (UPR) that slows down the rate of the translation of new proteins and protects the cell against oxidative stress [22]. This does not only affect the ER, but can also lead to stress responses in other cellular structures depending on the cellular needs, including oxidative stress, Golgi stress, mitochondrial stress and autophagy (reviewed in [21]).

1.3.1 Endoplasmic reticulum stress

The ER is made of membrane sacs and tubules, and it includes the nuclear envelope and cytoplasmic ER. Two types of the ER exist; rough ER and smooth ER, both of which are responsible for important processes in the cell. Whereas smooth ER is involved in the metabolism of fats, rough ER is involved in protein production and modification, as well as

the shipping of these proteins to other cellular locations. The ER also has an important function in storing calcium in the cell (reviewed in [23]).

The production, folding and modification of proteins in the ER are tightly regulated by a number of enzymes, like chaperones that assist in the folding process. This processing system is, together with environmental factors, important to maintain a normal function in the ER. Different environmental factors like oxidative stress, hypoxia, and nutrient deficiencies can disrupt this system and lead to an accumulation of unfolded and misfolded proteins. This will activate the ER stress response, which consists of three different pathways; the activating transcription factor 6 (ATF6) pathway, the inositol-requiring enzyme 1 (IRE1) pathway, and the PKR-like ER kinase (PERK) pathway (figure 4). Under normal conditions, these sensor molecules are bound to a type of HSP70 protein named the heavy chain binding protein/glucose-related protein of 78 kDa (Bip/GRP78), but when unfolded proteins accumulate in the ER, Bip detaches and the stress sensor proteins are activated. The activation of these pathways ultimately leads to the activation of the UPR that works to restore normal function in the ER or, if the system is beyond repair, induces apoptosis (reviewed in [24].

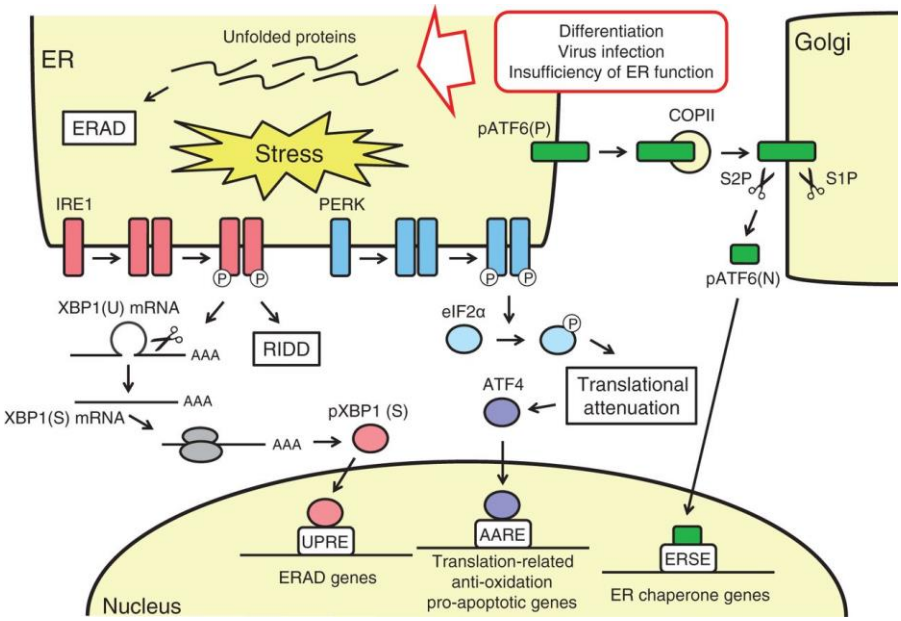

Figure 4: The stress response pathways in the ER (the figure is copied with permission from [21]).

The ATF6 pathway

ATF6 is a transmembrane protein found in the ER membrane that in its phosphorylated form (pATF6) functions as an ER stress sensor protein. Upon stress, pATF6 is translocated by the action of a COPII vesicle to the Golgi apparatus (GA), where it is cleaved by two proteases named Site-1 protease and Site-2 protease [25, 26]. Cleavage of ATF6 releases the

cytoplasmic domain of the protein, which translocates to the nucleus and binds to the ER stress response element (ERSE). This *cis*-acting response element then enhances the transcription of certain ER chaperone genes, producing glucose-regulated proteins (GRPs) that are important for correct protein folding [27].

The IRE1 pathway

In addition to being the stress sensor in the IRE1 pathway, the ER transmembrane protein IRE1 acts as a kinase and an endoribonuclease. IRE1 is activated by dimerisation and auto-transphosphorylation of the protein, and this causes an activation of its RNase domain due to conformational changes in the protein [28]. The active RNase domain acts on the pre-mRNA of the transcription factor X-box binding protein-1 (XBP1), catalysing a splicing process that leads to the expression of this transcription factor [29]. XBP1 then binds to the *cis*-acting enhancer element called the unfolded protein response element and induces transcription of these genes. This leads to the production of proteins important for the UPR, including ER chaperones and glycosylation enzymes [30].

The PERK pathway

The transmembrane protein PERK is the sensor protein in the PERK pathway. It is localised in the membrane of the ER, and is especially common in the mitochondria-associated ER membrane [31]. Heath shock protein 90 (HSP90) and binding immunoglobulin protein are bound to PERK under normal cellular conditions, but release PERK when stress occurs. PERK, which is also a kinase, is then able to phosphorylate itself and undergo dimerization to become activated (reviewed in [32]). Activated PERK then phosphorylates eIF2α, and this attenuates the translation of new proteins and thus reduces the accumulation of unfolded proteins in the ER [33].

Activating transcription factor 4 (ATF4) is activated by a general attenuation of protein translation, which means that activation of PERK eventually leads to the activation of ATF4 [22]. Activated ATF4 then enters the nucleus and starts transcription of an amino acid response element that includes a set of anti-oxidant genes, translation-associated genes, and genes involved in apoptosis, including C/EBP homologous protein (CHOP), a potent mediator of ER stress-induced apoptosis. The activation of these genes ensures a decrease in oxidative stress during ER stress, prepares the cell for translation of proteins after translational attenuation, and ensures removal of severely stressed cells by apoptosis, respectively (reviewed in [21]).

One of the genes activated by ATF4 and involved in restoring normal translation after translation attenuation is growth arrest and DNA damage-inducible protein 34 (GADD34). The GADD34 protein is a phosphatase that dephosphorylates eIF2α, thereby restoring normal protein translation (reviewed in [32]).

Tribbles-related protein 3 (TRIB3) is induced via ATF4 and CHOP, and is involved in ER stress-induced apoptosis together with CHOP. TRIB3 downregulates the transcriptional activity induced by CHOP, and is also a negative inducer of its own activity [34]. It functions as a pseudokinase, and is involved in the inactivation of several transcription factors and signalling proteins. One of the most studied mechanisms of action of TRIB3 is the targeting of the PI3K/protein kinase B (Akt)/ mammalian target of rapamycin (mTOR) pathway leading to autophagy. Activated mTOR phosphorylates certain proteins involved in translation and cell growth, and suppresses autophagy by the phosphorylation and inhibition of a protein complex involved in the initiation of the autophagosome known as autophagy-related 1 (ATG1)/unc-51-like kinase (ULK) complex. TRIB3 has been shown to be a negative regulator of both mTOR and Akt, meaning that activated TRIB3 leads to increased autophagy via its action on mTOR (reviewed in [21, 35]).

In addition to its action on ATF4, activation of PERK also leads to the activation of nuclear factor (erythroid-derived 2)-related factor 2 (NFE2L2). In its inactive form NFE2L2 is found in the cytosol bound to another protein named kelch-like-ECH-associated protein 1 (Keap1), but when phosphorylated by activated PERK it translocates to the nucleus and initiates transcription of a set of genes mainly involved in the protection against and management of oxidative stress [36].

1.3.2 Golgi apparatus stress

The GA consists of several cisternae organised into stacks that are connected by tubules. The main function of this organelle is to receive and sort proteins from the ER, to execute post-translational modifications to proteins and lipids, and to forward these modified proteins and lipids to their final destination by vesicular transport [37]. It is also involved in intracellular signalling, mitosis, apoptosis and autophagy, among other things.

The cellular requirements in relation to growth and energy demands are an important factor in deciding the dimensions of the size and work rate of the GA [21]. This has been shown in several cases. Campadelli et al. showed that in some cell lines the GA becomes fragmented and dispersed when the cell is infected with a virus [38]. It has also been found that the GA in

prolactin-secreting cells in the pituitary gland and acinar cells in the mammary glands are larger and more functional in lactating female mice than in non-lactating mice, and that this changes dynamically with the presence or absence of pups [39, 40]. Thus, the GA is dynamically changing to meet the requirements of the cell, and if these requirements overwhelm the capacity of the GA it will induce the Golgi stress response. This response can lead to an upregulation of a group of Golgi-related genes regulated by an enhancer element called the Golgi apparatus stress response element (GASE) [41], induction of apoptosis, or transcription of certain proteins (reviewed in [21]). Recently, three different pathways involved in the Golgi stress response have been identified [42-44]. This includes the transcription factor binding to immunoglobulin heavy constant Mu (IGHM) enhancer 3 (TFE3) pathway, HSP47 pathway, and the cathelicidin antimicrobial peptide responsive element binding protein 3- ADP-ribosylation factor 4 (CREB3-ARF4) pathway (figure 5). However, it is likely that many pathways are still undiscovered, as the GA is a very complex organelle.

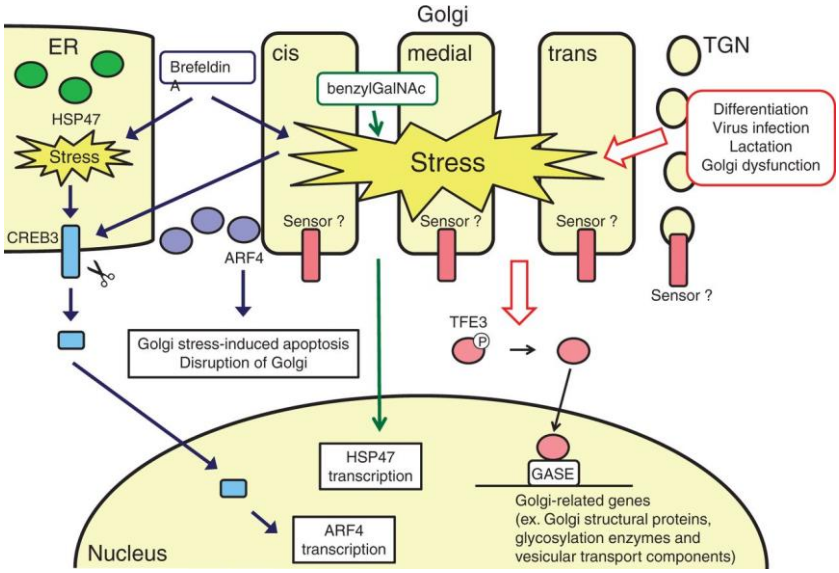

Figure 5: The stress response pathways in the GA (the figure is copied with permission from [21]).

The TFE3 pathway

It has recently been discovered that during Golgi stress, transcription of a set of Golgi-related genes is upregulated through GASE [41]. Taniguchi et al. found that this element is regulated by the transcription factor TFE3. Under normal conditions, TFE3 is found in a phosphorylated form in the cytoplasm, but during Golgi stress the TFE3 is activated by dephosphorylation and is translocated to the nucleus [44].

A new paper by Martina et al. also points to TFE3 as an important component of the ISR. In addition to being a transcriptional regulator of GASE, TFE3 also promotes expression of autophagic and lysosomal genes, as well as UPR genes, in response to ER stress [45].

The HSP47 pathway

The GA is responsible for several post-translational modifications, including O-glycosylation, and Miyata et al. found that when treating cells with benzyl-acetyl-galactosaminide to inhibit this glycosylation, the expression of HSP47 was increased. Further, they found that by giving the same treatment to HSP47-suppressed cells, the GA was fragmented and apoptosis was induced. This induction of apoptosis was due to activation of caspase-2 when HSP47 was inhibited in the GA. Thus, it seems as if the HSP47 pathway is important in protecting the GA against stress [42].

The CREB3-ARF4 pathway

Reiling et al. recently discovered the CREB3-ARF4 signalling pathway involved in GA stress. After treating cancer cells with Brefeldin A (BFA), which inhibits ER-Golgi transport and thus induces GA stress, they found that the ARF4 was upregulated. ARF4 is found on the ER-GA interface, and is involved in the transport of COP-I vesicles between the two organelles [46]. The induction of ARF4 is dependent on the CREB3 transcription factor, a transmembrane protein found in the ER membrane. Upon stress, CREB3 is activated by proteolysis, and the cytoplasmic domain translocates to the nucleus to upregulate the transcription of ARF4. The function of this upregulation is not fully known, but it is speculated that it induces disruption of the GA and GA-stress induced apoptosis [43].

1.3.3 Autophagy

Autophagy includes the three processes microautophagy, macroautophagy, and chaperone-mediated autophagy (figure 6), and involves the lysosomal breakdown of cellular structures. The main focus here will be macroautophagy, hereafter referred to as autophagy, which is a cellular process that removes damaged cellular components to maintain the stability of the cell, and that breaks down these or other components to ensure turnover of proteins and to provide the cell with nutrients during starvation (reviewed in [47]). Autophagy is initiated by the formation of structures called autophagosomes – double-membraned vesicles – around the cellular components that are to be degraded. The autophagosomes later fuse with lysosomes, forming autolysosomes, and the cargo are targeted and broken down by hydrolase enzymes (reviewed in [48]).

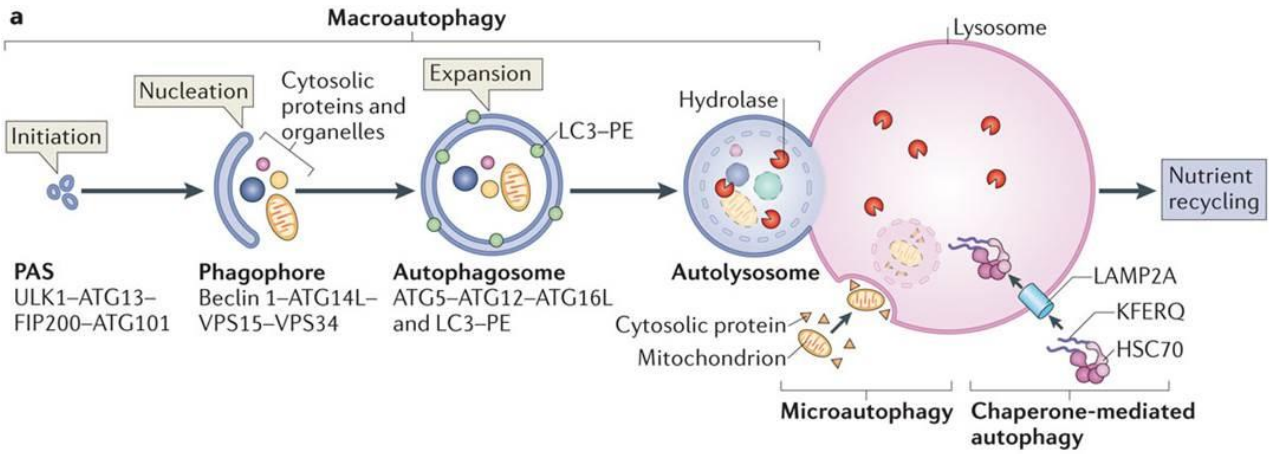

Figure 6: Overview of the different autophagy pathways (the figure is adapted with permission from [49]).

More than 30 different autophagy-related genes (ATG) have been discovered. These genes encode proteins involved in all steps of the autophagy process, including initiation, vesicle formation, fusion of the autophagosome with the lysosome, and degradation of the cargo. ATG genes also encode proteins responsible for the release of the degradation products into the cytosol so they can be exploited by the cell. These genes are activated when the cell receives signals of starvation or of intracellular stress (reviewed in [50]).

The initiation phase of autophagy is regulated by two protein complexes, the first one known as the ULK complex and a second complex consisting of a PI3K catalytic subunit type 3 protein known as vacuolar protein sorting 34 (VPS34) and ATG6/Beclin-1, as well as a protein known as p150 (reviewed in [51]). When dephosphorylated, the ULK complex is activated and assembles at the isolation membrane to initiate autophagosome formation (reviewed in [49]). The complex phosphorylates other proteins involved in autophagy, including Beclin-1. This enables the activation of the VPS34-containing complex [52]. The activated PI3K subunit catalyses the production of phosphatidylinositol 3-phosphate (PI3P), and this recruits other proteins to the phagophore, including the ubiquitin-like protein microtubule-associated protein 1 light chain 3 (LC3). LC3 is then conjugated to phosphatidyl-ethanolamine (PE). The LC3-PE conjugate is necessary for the expansion of the isolation membrane of the phagophore as well as the completion of the autophagosome. LC3 has therefore been widely used to monitor autophagosome formation. LC3-PE is also necessary for the fusion of the autophagosome with lysosomes to create the autolysosome (reviewed in [49, 51]).

Selective autophagy is mediated through specific receptor proteins called autophagy cargo receptors. These receptors have a domain called the ubiquitin-binding domain (UBD) that binds to ubiquitinated proteins marked for degradation. Another important domain on these receptors is the LC3 interacting region which binds to LC3 on autophagosomes. One such receptor is sequestosome 1 (SQSTM1/p62) that bind protein aggregates marked for destruction [49].

It has been discovered that p53 acts as a master regulator of autophagy, and it functions both as an initiator and an inhibitor of autophagy depending on its localisation in the cell. When p53 is located in the nucleus it works as a transcription factor, and many of its target genes are autophagy-stimulating genes. One of these activating pathways ends in the downregulation of mTOR via the activation of AMP-activated protein kinase (AMPK), leading to increased autophagy due to decreasing inhibitory effects of mTOR. On the other hand, if p53 is localised in the cytosol, it acts as an inhibitor of autophagy (reviewed in [53]).

It has been shown that autophagy can be induced by several stimuli other than damaged cellular components and starvation, including ER stress, the UPR, and ROS (reviewed in [51]).

1.3.4 PUFAs and the integrated stress response

Previous work published by our group show that the expression of ER stress-related genes are upregulated in the colon cancer cell line SW620 after treatment with DHA [20]. This includes increased levels of phosphorylated eIF2α (peIF2α), which is involved in the ISR and is considered to be a hallmark of ER stress. Other important ER stress regulators that were found to be upregulated included ATF6, PERK, and ATF4, as well as NFE2L2 that is involved in the protection against oxidative stress.

Both SFAs and UFAs have been shown to induce autophagy, but they do so by different mechanisms. The SFA palmitate induces autophagy through the canonical pathway and relies on the activation of the protein complex consisting of beclin-1 and VPS34, whereas autophagy is induced by a non-canonical pathway in response to the UFA oleate. The mechanism of activation in this non-canonical pathway is not known, but it requires an intact GA and does not rely on beclin-1 to induce autophagy [54].

A recent paper suggests that the basal level of autophagy in colon cancer cells is important for the DHA sensitivity [55]. Two cell lines were used, one DHA sensitive and one DHA

tolerant, and when investigating the basal level of autophagy they found that a low level correlated with DHA sensitivity, whereas the DHA tolerant cells showed a high level of basal autophagy. Lim et al showed that in prostate cancer cells expressing mutated p53, autophagy was induced via mitochondrial ROS after treatment with DHA [56]. Further, the results indicated that the induction of autophagy was due to a ROS-mediated inactivation of the Akt-mTOR signalling pathway. Another paper published by the same group explored DHA-induced cell death in non-small cell lung cancer cells [57]. Here, they showed that DHA treatment activated AMPK and thus inactivated mTOR via Akt.

1.4 Aim of study

The aim of this study was to identify the molecular mechanisms involved in the anticancer properties of DHA in human colon cancer cell lines, with special focus on pathways in the integrated stress response. Previous work done by our group showed that treatment with DHA in DHA sensitive colon cancer cell lines led to an induction of both ER- and oxidative stress, and found differences in the basal autophagy levels between sensitive and less sensitive cell lines. In this study we wanted to investigate whether the activity of integrated stress pathways could explain differences in DHA sensitivity between colon cancer cell lines. We especially wanted to focus on the relationship between DHA treatment and oxidative stress, ER stress, Golgi stress, and autophagy.

2. Method

2.1 Cell cultivation

2.1.1 Cell lines

Two colon cancer cell lines, DLD-1 and LS411N, were used in this project. DLD-1 originates from a Dukes' type C human colon adenocarcinoma, whereas LS411N originates from a Dukes' type B colon carcinoma. The cells were obtained from American Type Culture Collection (ATCC, USA) and stored in an N_2-container.

2.1.2 Thawing of cells

The cells were retrieved from the N_2- container, and thawed in a water bath (37°C) for five minutes (min). The cell suspension was then resuspended in 1 ml medium and added to a 15 ml tube containing 9 ml of medium, before centrifuged at 125 g for six min to remove DMSO residues from the freezing media. The supernatant was removed and the cell pellet resuspended in 12 ml medium and transferred to a 75 cm^2 cell culture flask. The cells were then incubated at 37°C and 5% CO_2, and subcultured at about 70% confluence. All medium used during this procedure was preheated to 37°C in a water bath.

2.1.3 Culturing of cells

DLD-1 and LS411N cells were grown in RPMI 1640x medium from Gibco, supplemented with foetal bovine serum (10% FBS) and gentamicin (0.5%). Both cell lines were cultivated in 75 cm^2 cell culture flasks in 5% CO_2 at 37°C. During subcultivation the growth medium was removed and the cells were washed with phosphate saline buffer (2x5 ml, PBS), before adding trypsin (1 ml) to enzymatically detach the cells from the culture flask. The trypsinated cells were incubated for 8 min before they were resuspended in fresh growth media. The cells were counted using the Moxi Z cell counter (Orflo technologies, USA) with the S-type cassette, before they were added to a new culture flask. Solutions used during cell subcultivation were preheated to 37°C in a water bath.

2.1.4 Treatments

Both DLD-1 and LS411N cells were treated with different solutions, including ethanol (EtOH), docosahexaenoic acid (DHA,70 and 105 µM), butylated hydroxyanisole (BHA, 0.05 mM), butylated hydroxytoluene (BHT, 0.05 mM), N-acetyl-cysteine (NAC, 1 mM), brefeldin A (BFA, 1 µM), thapsigargin (TG, 1 µM), and bafilomycin A1 (BafA1, 0.1 µM).

The different treatments were added to fresh growth medium to obtain the desired concentration using a syringe or a pipette, before the supplemented media was vortexed for 30 seconds (sec) and incubated in a water bath (37°C) for 15 min.

Cells were seeded out 24 hours (h) prior to treatment. During treatment, the medium was removed, and replaced with the supplemented media. The same protocol was used for all treatments.

2.2 Cell counting

The effect of the different treatments used on the cell lines was investigated by comparing cell numbers at different time intervals (24 h, 48 h, and 72 h) after seeding out the cells. All cells were grown under identical conditions with 5% CO_2 at 37°C. Cells were seeded out in 12-well plates, and different treatments were added after 24 h by removing the old medium and adding the supplemented media. 24 h or 48 h after treatment the media was discarded and the cells were washed with PBS (2x0.5 ml), detached by incubation with trypsin (0.3 ml) for 10 min, and resuspended in growth medium (1 ml) before counting the cells using the Moxi Z cell counter with the S-type cassette.

2.3 Protein isolation and quantification

2.3.1 Harvesting of cells for protein analysis

DLD-1 cells were seeded in 155 cm^2 plates and LS411N cells were seeded in 55 cm^2 plates. The cells were incubated for 24 h at 37°C and 5% CO_2 before the growth medium was replaced with supplemented growth medium containing EtOH, DHA (70 µM), NAC (1 mM), BafA1 (1 µM), TG (1 µM), or BFA (1 µM), or a combination of two or more of these treatments. Cells were then incubated and harvested after 3, 6, 12, 24, and 48 h.

2.3.2 Total protein isolation

The medium was removed from the plates and the cells were washed with cold PBS (2x10 ml) before scraped in 6 ml cold PBS. The cell suspension was transferred to a 15 ml tube and centrifuged at 2000 rpm (500 G, 4°C) for 10 min. After centrifugation, the supernatant was removed, and the cell pellet was resuspended in 1 ml cold PBS before the suspension was transferred to cold Eppendorf tubes and centrifuged one more time under the same conditions.

The supernatant was removed, and urea lysis buffer (appendix I) was added (minimum 2x the packed cell volume), before vortexing the cells for 30 sec and placing them on ice for 30 sec repeatedly three times. The cell suspension was then centrifuged for 15 min at 13,000 rpm

(18,000 G, 4°C), before the supernatant was transferred to new Eppendorf tubes and frozen in liquid nitrogen for storage at -80°C.

2.3.3 Protein quantification

Protein concentration was determined using the Bio-Rad Protein Assay (500-0006, BioRad) with the dye Coomassie brilliant blue G-250 that changes colour when binding to basic and aromatic amino acids. When measuring the absorbance at 595 nm a higher concentration of proteins will give a higher absorbance.

The Bio-Rad reagent concentrate was diluted 1:5 with MQ water. Three parallels for each sample were made by adding 1 µl of protein sample to 999 µl Bio-Rad reagent concentrate. The prepared samples were then left for 15 min before measuring the absorbance at 595 nm, using the lysis buffer as a blank measurement. The protein concentrations were then calculated by using the measured absorbance and a standard curve, shown in equation 1.

$$Protein\ concentration\ (\mu g/\mu l) = absorbance\ 595\ x\ 22.02\ x\ dilution \quad (1)$$

2.4 Western Blotting

2.4.1 Sample preparation

The samples used were thawed on ice and then spun down before they were diluted using TRIS-HCL (10 mM, pH 8.0) buffer to achieve the same protein concentration in all samples. NuPAGE LDS buffer (Life technologies, USA) and dithiotreitol (DTT) (Sigma Aldrich, USA) were added. The prepared samples held 70% diluted proteins, 25% NuPAGE LDS 4x sample buffer and 5% DTT. The samples were heated at 80°C for 15 min before they were spun down and put on ice and loaded onto the gel. A protein standard containing Odyssey protein molecular weight marker 928-40000 (Li-cor Biosciences, USA) and a loading mix (75%) were prepared in the same way.

2.4.2 SDS-polyacrylamide gel electrophoresis

10% NuPAGE Novex Bis-Tris 10- or 12 well gels (Life technologies) were used for separation of the total protein extracts. The gels were run in Xcell SureLock Mini-Cell (Life technologies) according to the NuPage Technical guide. NuPAGE MOPS SDS Running buffer was used both in the inner and outer chamber of the Mini-Cell. The proteins were then separated at 200 V for 45 min at room temperature (RT).

2.4.3 Blotting

The gels were placed together with Immobilion Transfer Membranes (Merck Millipore, USA) in the XCell TM blot module according to the NuPage technical guide and put in the XCell SureLock TM Mini-Cell as described in the XCell Surelock TM Minicell user manual. The inner chamber was filled with NuPAGE Transfer Buffer and the outer with ice water. The blotting was done at 30 V for 1 h at RT.

2.4.4 Blocking, hybridisation and detection

The membranes were rehydrated in methanol (MeOH) for 20 sec followed by 30 sec in Tris Buffered Saline with tween (TBST). The membranes were then put, protein side facing in, in a 50 ml tube with 3 ml blocking solution containing equal amounts of TBST and Odyssey blocking buffer, and put on the roller at RT for 1 h.

The primary antibodies (table 1) were spun down and diluted in 3 ml TBST+Odyssey blocking buffer. Membranes were incubated in the primary antibody solution for 1 h on a roller at RT, before they were rinsed in 3 ml TBST for 3x10 min. This was followed by a new incubation step for 1 h at RT with the secondary antibody (table 2) that was spun down and diluted in 3 ml TBST+Odyssey blocking buffer. Due to the light sensitivity of the secondary antibody this was done in a dark room. After incubation the membranes were then rinsed 3x10 min with 3 ml Tris Buffered Saline (TBS) and dried in a dark space.

Detection of the proteins on the membrane was done by using the Oddysey Infrared Imaging System (Li-cor Biosciences, UK).

Table 1: Primary antibodies used in western blotting experiments

Antigen	Primary antibody	Manufacturer (Cat. No)	Dilution
Arf4	Rabbit monoclonal	Abcam Ab171746	1:20,000
ATF4	Rabbit monoclonal	Cell Signaling D4B8	1:1000
β-actin	Mouse monoclonal	Abcam Ab6276	1:20,000
CHOP	Mouse monoclonal	ThermoFisher MA1-250	1:333
Cox IV	Rabbit monoclonal	LI-COR 926-42214	1:1000
CREB3	Rabbit polyclonal	Abcam Ab42454	1:2000
EIF2α	Mouse monoclonal	Abcam Ab5369	1:500
LC3BII	Rabbit monoclonal	Cell Signaling 3868S	1:1000
NFE2L2	Rabbit polyclonal	Cell Signaling D1Z9C	1:1000
p53	Mouse monoclonal	Dako M7001	1:3000
pEIF2α	Rabbit monoclonal	Cell Signaling D9G8	1:200
PERK	Mouse monoclonal	Abcam Ab105929	1:500
p-PERK	Rabbit polyclonal	Santa Cruz SC-32577	1:100
SQSTM1 (p62)	Guinea pig polyclonal	Progen Biotechnik GP62-C	1:1000
TFE3	Rabbit polyclonal	Abcam Ab93808	1:3000
TRIB3	Rabbit polyclonal	Sigma-Aldrich HPA 015272	1:200

Table 2: Secondary antibodies used in western blotting experiments

Antigen	Secondary antibody	Manufacturer (Cat. No)	Dilution
Rabbit anti Arf4	IRDye 800 CW donkey anti-rabbit IgG	Licor Odyssey (926-32213)	1:10,000
Rabbit anti ATF4	IRDye 680 CW goat anti-rabbit IgG	Licor Odyssey (926-68071)	1:20,000
Mouse anti β-actin	IRDye 680 CW goat anti-mouse IgG	Licor Odyssey (926-68070)	1:20,000
Mouse anti CHOP	IRDye 680 CW goat anti-mouse IgG	Licor Odyssey (926-68070)	1:20,000
Rabbit anti Cox IV	IRDye 680 CW goat anti-rabbit IgG	Licor Odyssey (926-68071)	1:20,000
Rabbit anti CREB3	IRDye 800 CW donkey anti-rabbit IgG	Licor Odyssey (926-32213)	1:10,000
Mouse anti EIF2α	IRDye 800 CW donkey anti-mouse IgG	Licor Odyssey (926-32212)	1:10,000
Rabbit anti LC3BII	IRDye 800 CW donkey anti-rabbit IgG	Licor Odyssey (926-32213)	1:10,000
Rabbit anti NFE2L2	IRDye 680 CW goat anti-rabbit IgG	Licor Odyssey (926-68071)	1:20,000
Mouse anti p53	IRDye 800 CW donkey anti-mouse IgG	Licor Odyssey (926-32212)	1:10,000
Rabbit anti pEIF2α	IRDye 680 CW goat anti-rabbit IgG	Licor Odyssey (926-68071)	1:20,000
Mouse anti PERK	IRDye 800 CW donkey anti-mouse IgG	Licor Odyssey (926-32212)	1:10,000
Rabbit anti p-PERK	IRDye 680 CW donkey anti-rabbit IgG	Licor Odyssey (926-68071)	1:20,000
Guinea pig anti SQSTM1	IRDye 800 CW donkey anti-guinea pig IgG	Licor Odyssey (926-32411)	1:10,000
Rabbit anti TFE3	IRDye 800 CW donkey anti-rabbit IgG	Licor Odyssey (926-32213)	1:10,000
Rabbit anti TRIB3	IRDye 800 CW donkey anti-rabbit IgG	Licor Odyssey (926-32213)	1:10,000

2.4.5 Analysis of the data

Quantification of the band signals from the hybridised membranes was done by using the Image Studio Lite version 3.1 software. Band signals were normalised against their respective loading controls, and the fold change values of untreated samples versus treated samples were calculated. The significance level was calculated by using a t-test (paired, one-tailed distribution) in the Microsoft Excel 2010 software, and a P-value below 0.05 was considered to be statistically significant from the control.

2.5 Confocal Microscopy

2.5.1 Treatment and fixation

Cells were seeded out in 8 well confocal plates (Nunc, Germany) 24 h before treatment, and treated according to the treatment protocol (paragraph 2.1.4) until fixation. Fixation was done by removing half of the media, and adding the equivalent amount of paraformaldehyde (PFA, 8%), giving the desired concentration of 4% PFA. The cells were then left for 10 min at RT before discarding all solutions, and the wells were washed with PBS (200 µl). The wells were filled with 400 µl PBS and the plates were then packed in aluminium foil and stored at 4°C.

2.5.2 Permeabilisation, blocking, and staining

PBS was removed from the confocal wells, and cold methanol (-20°C, 200 µl) used to permeabilise the cells was added to each well before 10 min incubation on ice. Cells were washed with PBS (200 µl) before adding a blocking solution (goat serum (3%) and PBS, 200 µl). The cells were left on a shaker at RT for 1 h.

The blocking solution was removed and primary antibody solution (goat serum (1%), PBS, and antibody, 100 µl) (table 3) was added, before the cells were incubated for 1 h on a shaker at RT. The primary antibody solution was removed, the cells were washed with PBS (200 µl, 3x5 min) on the shaker, and the secondary antibody solution was added (goat serum (1%), PBS, and secondary antibody, 200 µl) (table 4). The cells were left for incubation for 30 min on the shaker at RT, before the solution was removed, and the wells were washed with PBS (400 µl, 5x5 min) on the shaker.

The PBS was removed, and Draq5 (100 µl, 5µM), used for nuclear staining, was added to each well, before incubation on the shaker at RT for 10 min. The solution was then removed, and each well was washed with PBS (200 µl, 10 min) on the shaker. The PBS was removed, and 400 µl of PBS was added. The plates were packed in aluminium foil and stored in the fridge until microscopy.

Table 3: Primary antibodies used in immunofluorescent staining for confocal microscopy

Antigen	Primary antibody	Manufacturer (Cat. No)	Dilution
ATF4	Rabbit monoclonal	Cell signaling D4B8	1:150
LC3BII	Rabbit monoclonal	Cell signaling 3868	1:200
NFE2L2	Rabbit polyclonal	Cell Signaling D1Z9C	1:50
p53	Mouse monoclonal	Dako M7001	1:200
SQSTM1 (p62)	Guinea pig polyclonal	Progen Biotechnik GP62-C	1:2000
TRIB3	Rabbit polyclonal	Sigma-Aldrich HPA 015272	1:1000

Table 4: Secondary antibodies used in immunofluorescent staining for confocal microscopy

Antigen	Secondary antibody	Manufacturer (Cat. No)	Dilution
Rabbit anti ATF4	Alexa Fluor 488 goat Anti Rabbit IgG	Fisher Scientific (10729174)	1:5000
Rabbit anti LC3BII	Alexa Fluor 488 goat Anti Rabbit IgG	Fisher Scientific (10729174)	1:5000
Rabbit anti NFE2L2	Alexa Fluor 488 goat Anti Rabbit IgG	Fisher Scientific (10729174)	1:5000
Mouse anti p53	Alexa Fluor 488 goat Anti Mouse IgG	ThermoFisher (A11001)	1:5000
Guinea pig anti SQSTM1	Alexa Fluor 555 goat Anti Guinea Pig IgG	Fisher Scientific (A-21435)	1:5000
Rabbit anti TRIB3	Alexa Fluor 488 goat Anti Rabbit IgG	Fisher Scientific (10729174)	1:5000

2.5.3 Imaging

For imaging of the immunofluorescent stained proteins an Axiovert 200 microscope with confocal module LSM 510 Meta with a Plan-Apochromat 63x/1.2 water objective or a Plan-Apochromat 63x/1.4 oil objective (Carl Zeiss) was used. The images were analysed using the ZEN 2012 (blue edition) software version 1.1.2.0.

2.6 Flow cytometry

2.6.1 Measuring oxidative stress

The ROS production in the cells following treatment with different solutions was measured by using the mitochondrial oxidative stress marker MitoSOX (MitoSOX Red Mitochondrial superoxide, M36008, Life technologies) which produces red fluorescence when oxidised by mitochondrial superoxide, and the cellular oxidative stress marker dichlorohydrofluorescein diacetate (H2DCF) (ROS detection kit, C6827, Life technologies) which is converted to fluorescent dichlorofluorescein (DCF) when cleaved by esterases and oxidised. The two markers are used to measure mitochondrial oxidative stress and ROS in cells, respectively.

DLD-1 and LS411N cells were seeded in 12-well plates and incubated for 24 h at 37°C and 5% CO_2. The growth medium was replaced with supplemented growth media containing either EtOH, DHA (70 µM), DHA (70 µM) and NAC (1 mM), or NAC (1 mM). Cells where then incubated for 6 and 24 h before washed with PBS (2x0.5 ml) and labelled with 500 µl DCF (0.3 µM) or 500 µL MitoSOX (5 µM). The labelled cells were incubated at 37°C and protected from light for 30 min. The labelling solution was removed, and the cells were washed with PBS (2x0.5 ml) before the cells were detached by incubation with trypsin (0.3 ml) for 10 min. The trypsin was neutralised by adding 1 ml growth media, and the cell suspension was transferred to Eppendorf tubes and centrifuged at 1200 rpm (150 G) for 5 minutes before the media was replaced with cold PBS (500 µl). The fluorescence levels were then measured by using flow cytometry (BD FACSCanto, VWR International), following the instrument manual. Fold change values of untreated versus treated samples were calculated, and the significance level was calculated by using a t-test (paired, one-tailed distribution) in the Microsoft Excel 2010 software. P-values below 0.05 were considered to be statistically significant from the control.

2.6.2 Measuring autophagy with Cyto-ID

The autophagy level in DLD-1 and LS411N cells were measured by flow cytometry using the Cyto-ID autophagy detection kit (ENZ-51031-K200, Enzo) that measures the amount of autophagic vacuoles in the cells.

The cells were seeded in 12-well plates and incubated for 24 h at 37°C and 5% CO_2 before the growth medium was discarded and replaced with growth media supplemented with either EtOH, DHA (70 µM), NAC (1 mM), BafA1 (1 µM), chloroquine (10 µM), rapamycin (50 nM), DMSO (50 nM) or a combination of two or more of these solutions. Rapamycin induces

an upregulation of autophagy via mTOR, whereas chloroquine raises the pH in lysosomes and inhibits the fusion of auotphagosomes with lysosomes. Both were used as controls for autophagy.

The treated cells were incubated for 24 h at 37°C and 5% CO_2 before the media was discarded and the cells washed with PBS (2x0.5 ml) and detached by trypsination (0.3 ml, 10 min). The cells were resuspended in growth medium (1 ml) in Eppendorf tubes and centrifuged at 4°C and 1200 rpm (150 G) for 5 min. The supernatant was removed, and the cell pellet was resuspended in 1 ml PBS before centrifugation was repeated. The cell pellets were then resuspended in 250 µl 1x Assay buffer, and diluted Cyto-ID detection reagent (250 µl) from the kit was added. After incubation at 37°C and protected from light for 30 min the cells were centrifuged, washed with 1x Assay buffer, and resuspended in 500 µl 1x Assay buffer. The samples were then analysed using flow cytometry. Fold changes were calculated for untreated versus treated samples. The significance level was calculated by using a t-test (paired, one-tailed distribution) in the Microsoft Excel 2010 software, and P-values below 0.05 was considered to be statistically significant from the control.

2.7 Protein knockdown by siRNA

P53 small interfering RNA (siRNA) was used to knock down p53 mRNA in DLD-1 cells to investigate whether the knockdown of p53 had any effect on DHA-mediated growth inhibition. Growth inhibition was measured by cell counting, and p53 protein expression was investigated using western blotting and confocal imaging.

2.7.1 siRNA transfection

To find the correct concentration of siRNA, DLD-1 cells were transfected with siRNA (10, 20 or 40 nM) by using the Lipofectamine RNAiMax transfection reagent (Fisher Scientific). SiRNA for p53 (#SI00011655, Qiagen), AllStars Negative control (#1027280, Qiagen), and AllStars Hs Cell Death Control (positive transfection control, #1027298, Qiagen) was used in the experiment. The manufacturer's protocol was followed (Fisher Scientific). Cells were seeded out and transfected in 6 well plates by using 2.5 mL growth medium and 500 µL transfection buffer (5 µL Lipofectamine, siRNA/water, and Opti-MEM).

Before treatment, siRNA (p53 and negative control) or RNA-free water was added to Opti-MEM together with Lipofectamine (5 µL) and left for incubation at RT for 20 min. The solution was then added to the wells (500 µL/well), before cells diluted in 2.5 mL antibiotic free growth medium was added. The cells were left for incubation at 37°C and 5% CO_2 for 24

h. The cells were harvested by removing the growth media, washing with cold PBS (2x2 mL), and scraped with 1 mL PBS before they were centrifuged at 1500 rpm (240 G) for 10 min. The PBS was removed, and protein isolation and western blotting was done as described in section 2.5 and 2.6. SiRNA for the positive transfection control was, together with the negative control, prepared in the same way as described above. The positive and negative control was used to evaluate transfection efficiency by using a light microscope to observe cell survival 48 h after transfection.

After the correct concentration had been established, cells were seeded in 55 cm^2 plates and transfected as described above, with a siRNA concentration of 10 nM. After 24 h of incubation the growth medium was removed, cells were washed with PBS, trypsinated, and seeded out in 55 cm^2 plates for protein expression analysis and 12-well plates for counting. The cells were then incubated for 24 h at 37°C and 5% CO_2 before the growth medium was replaced with supplemented growth media containing EtOH (70 µM), DHA (70 µM), BafA1(1 µM), or a combination of these treatments. After incubation at 37°C and 5% CO_2 for 24 h the cells were harvested and total proteins isolated and used for western blotting as described above. 12 well plates were used to measure the effect of p53 knockdown on cell growth. 48 h after treatment the cells were counted following the above protocol (section 2.2).

3. Results

3.1 The human colon cancer cell lines DLD-1 and LS411N responded differently to treatment with DHA

Cell counting was used to examine the effect of DHA treatment on cell growth of the human colon cancer cell lines DLD-1 and LS411N, which were cultivated in the same growth medium. The results showed that DLD-1 cells are DHA sensitive with a growth inhibition of about 35% after 48 h of treatment with 70 µM DHA (figure 7A and B), whereas LS411N cells showed little or no growth inhibition after the same treatment (figure 7C and D). EtOH was used as a control.

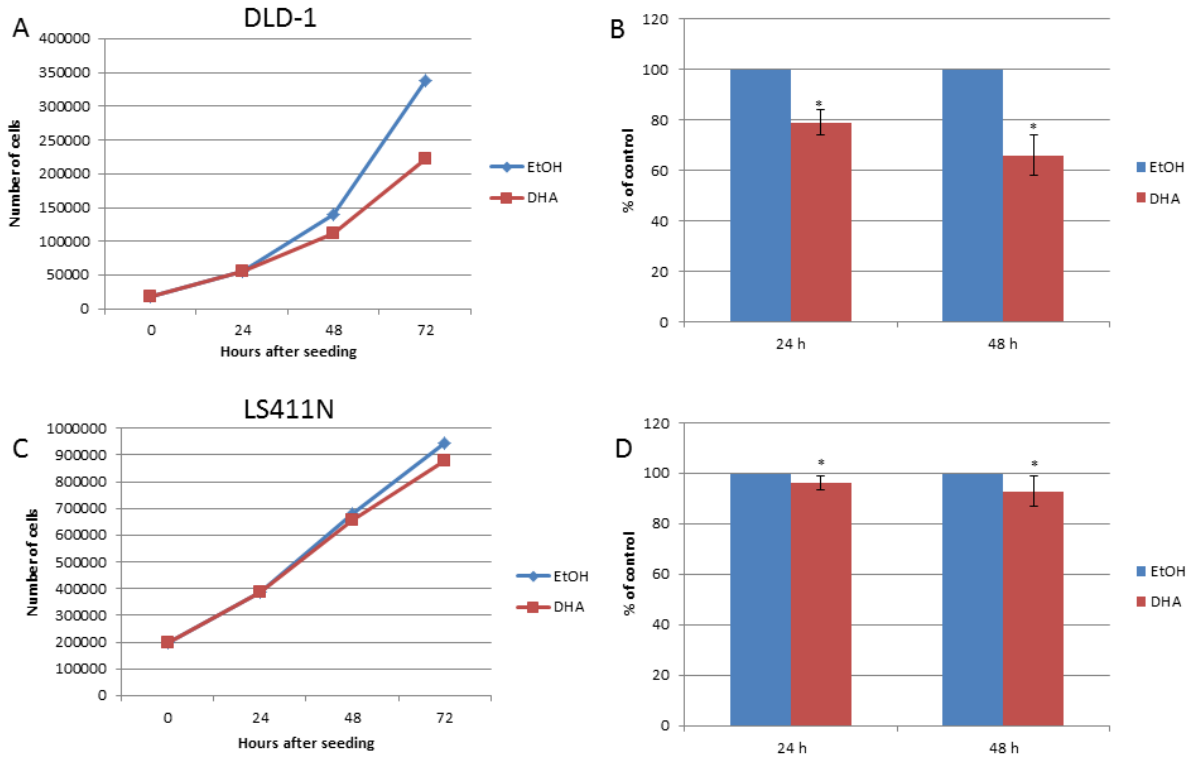

Figure 7: The effect of DHA treatment (70 µM) on growth of cell lines DLD-1 (A and B) and LS411N (C and D). Cells, DLD-1 (A) and LS411N (N), were seeded 24 h prior to treatment and counted 24 and 48 h after treatment. Mean percent of control and standard deviation are shown for DLD-1 cells (B) and LS411N cells (D). The results are based on four independent experiments. *Significantly different from control ($p<0.05$)

3.2 Effect of antioxidants on DHA-induced growth inhibition

Co-treatment with DHA and the antioxidants BHA, BHT and NAC on DLD-1 and LS411N cells were used to investigate whether the growth inhibitory effect of DHA on DLD-1 cells was due to ROS or lipid peroxidation. The effect of antioxidant treatment was measured by

cell counting. The different antioxidants gave variable effects on DHA-induced growth inhibition.

3.2.1 BHA increased the DHA-induced growth inhibition in DLD-1 cells

BHA is a synthetic fat soluble antioxidant that acts as a free radical scavenger and stabilises free radicals [58]. The results showed that co-treatment with BHA and DHA increased the growth inhibitory effect of DHA on DLD-1 cells, with a growth inhibition of about 50% after 48 h compared to 35% growth inhibition with DHA treatment alone. BHA treatment alone on DLD-1 cells resulted in a growth inhibition of about 10% (figure 8A and B). A similar effect was observed in LS411N cell. BHA treatment alone and in combination with DHA also resulted in growth inhibition (figure 8C and D).

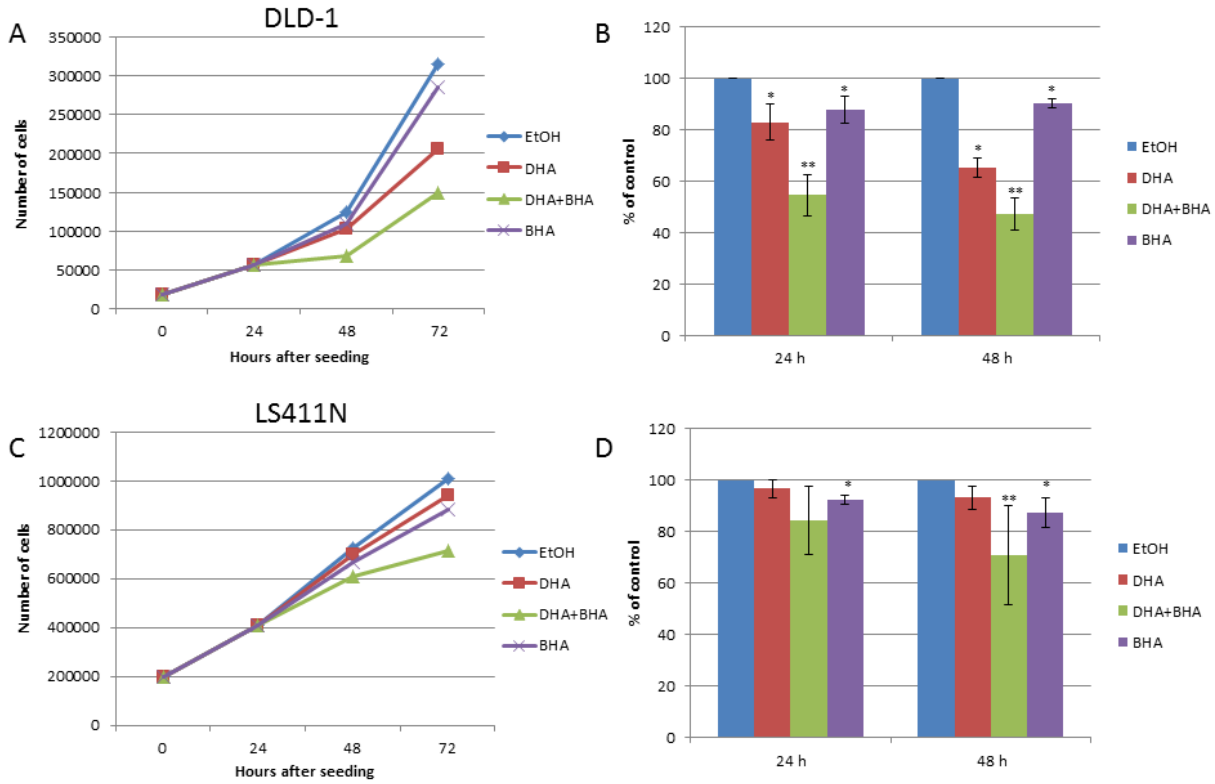

Figure 8: The effect of BHA (0.05 mM) alone or in combination with DHA (70 µM) on growth of DLD-1 and LS411N cells measured by cell counting. DLD-1 (A) and LS411N (C) cells were treated 24 h after seeding, and counted 24 and 48 h after treatment. Mean percent of control and standard deviation of DLD-1 (B) and LS411N (D) cells are based on three independent experiments. *Significantly different from control, **significantly different from control and DHA treatment ($p<0.05$).

3.2.2 BHT did not affect DHA-induced growth inhibition in DLD-1 cells

The synthetic, fat soluble antioxidant BHT acts as a peroxyl radical scavenger by donating a hydrogen atom to the peroxyls to form non-radical hydroperoxides [59]. A combinatory

treatment of DLD-1 cells with BHT and DHA resulted in an increase in growth inhibition (30%) compared with DHA treatment alone (16%) after 24 h. This effect was not seen after 48 h (figure 9A and B). LS411N cells did not seem to be affected by co-treatment with BHT and DHA (figure 9C and D).

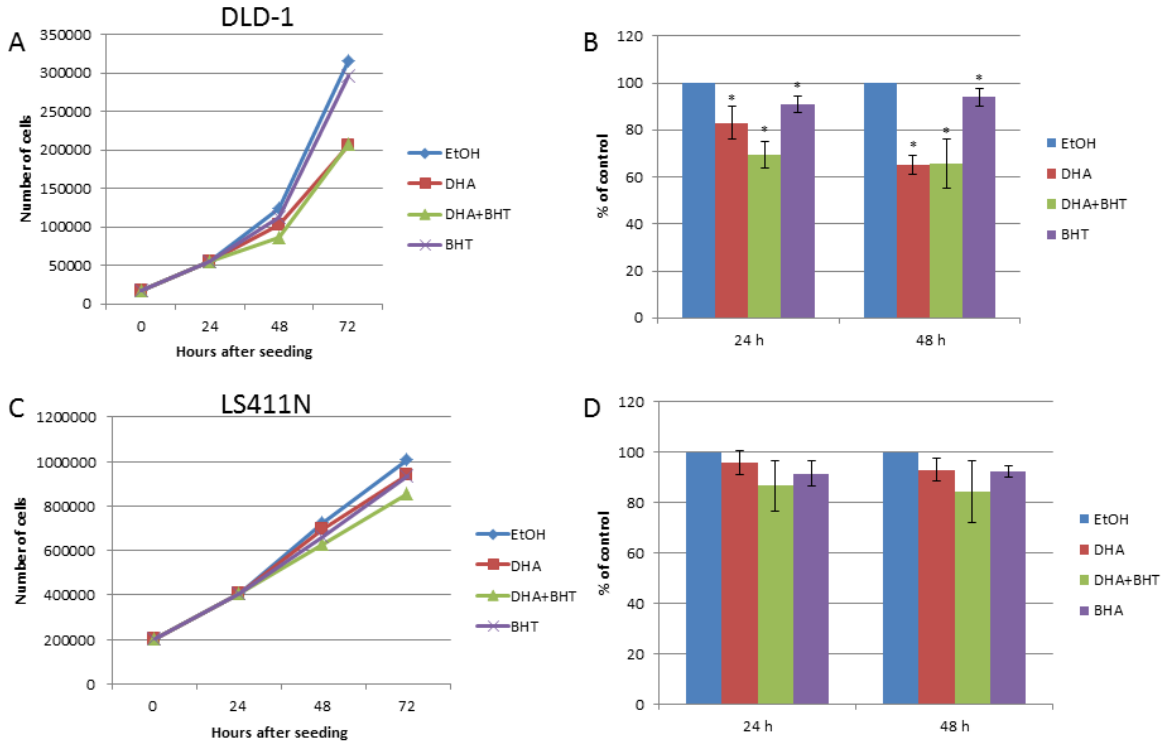

Figure 9: The effect of BHT (0.05 mM) on DHA (70 µM)-mediated growth inhibition in DLD-1 and LS411N cells measured by cell counting. DLD-1 (A) and LS411N (C) cells were treated 24 h after seeding, and counted 24 and 48 h after treatment. Mean percent of control and standard deviation of DLD-1 (B) and LS411N (D) cells are based on three independent experiments. *Significantly different from control ($p<0.05$).

3.2.3 NAC partially counteracted DHA-induced growth inhibition in DLD-1 cells

NAC is an antioxidant consisting of a thiol group, and a precursor of L-cysteine and reduced glutathione. In addition to its direct antioxidant activity through its thiol group, it can also be converted to glutathione, an antioxidant that minimises the lipid peroxidation of cellular membranes [60]. Its antioxidant properties also include the ability to reduce other molecules due to its thiol-disulphide exchange activity. The results showed that a co-treatment with NAC and DHA in DLD-1 cells to some extent counteracted the DHA-mediated growth inhibition, with a reduction of 16% (figure 10A and B). LS411N cells seemed unaffected by the same treatment (figure 10C and D).

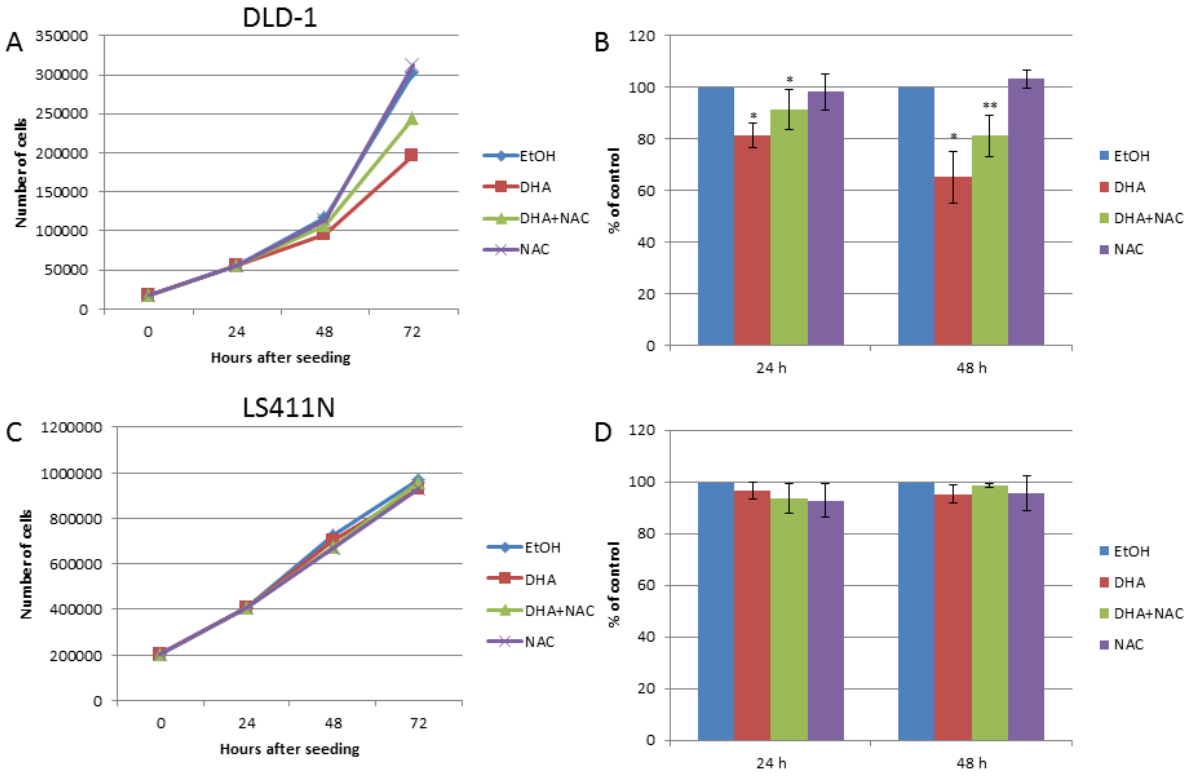

Figure 10: The effect of NAC (1mM) on DHA (70 µM)-mediated growth inhibition in DLD-1 and LS411N cells measured by cell counting. DLD-1 (A) and LS411N (C) cells were treated 24 h after seeding and counted 24 and 48 h after treatment. Mean percent inhibition and standard deviation are based on three independent experiments for DLD-1 (B) and LS411N (D) cells. *Significantly different from control, **significantly different from control and DHA treatment ($p<0.05$).

To examine whether other concentrations of NAC could reverse the DHA-induced growth inhibition completely, a titration with higher NAC-concentrations was done. The results showed that higher concentrations of NAC alone resulted in growth inhibition of DLD-1 cells.

3.3 Induction of ER stress at early time points in DLD-1 cells after treatment with DHA

Our group has previously shown that there is an upregulation of ER stress-related genes after DHA treatment in several colon cancer cell lines. Previous gene expression experiments indicated an upregulation of genes in PERK-eIF2α pathway leading to UPR in DLD-1 cells [61], and this pathway was therefore chosen for further analysis. Protein expression analysis was used to investigate the effect of DHA treatment on ER stress pathways in DLD-1 and LS411N cells. Proteins were isolated at several time points after treatment, and protein expression was examined by western blotting. TG, a known inducer of ER stress, was used as a positive control. Confocal imaging was used to investigate expression changes and cellular localisation of proteins.

PERK is one of three sensor proteins involved in the UPR, and is activated by autophosphoryalation. Results, presented in figure 11, showed that there was a significant increase in PERK levels after 3 h of DHA treatment in DLD-1 cells. Accordingly, a significant increase in pPERK was also observed after 3 and 6 h in the same cell line, before levels decreased after 12 h. No significant change was observed for either PERK or pPERK in LS411N cells.

In its active form, PERK phosphorylates eIF2α, leading to translational attenuation and a possibility for the ER to restore normal function by reducing the amount of misfolded or unfolded proteins. In DLD-1 cells, peIF2α was found to be significantly upregulated 3 h after DHA treatment. Protein expression levels in LS411N cells remained unchanged at all time points (figure 11).

The attenuation of protein translation induced by the phosphorylation of eIF2α leads to the activation of ATF4. Upon activation, ATF4 enters the nucleus and starts transcription of genes involved in translation, anti-oxidants defence, and apoptosis. ATF4 was found to be significantly upregulated at all time points after DHA treatment in DLD-1 cells, but not in LS411N (figure 11). CHOP, an apoptotic inducer that is activated by ATF4, also showed a significant increase in protein expression levels at all time points after DHA treatment in DLD-1 cells. No such change was found in LS411N cells (figure 11).

TRIB3 is also involved in ER stress-induced apoptosis. It is activated by ATF4 and CHOP together, and acts as a negative regulator on both CHOP and itself. Another important function of TRIB3 is to act as a negative regulator of Akt and mTOR, and, because of the inhibitory effect on mTOR, to increase autophagy. A significant increase in TRIB3 levels was observed at all time points after DHA treatment in DLD-1 cells, but not in LS411N cells (figure 11).

The phosphorylation of PERK also leads to the activation of NFE2L2. When NFE2L2 is phosphorylated by PERK, it translocates to the nucleus and initiates transcription of a set of anti-oxidant genes. Results showed a significant increase in NFE2L2 levels in both DLD-1 and LS411N cells at all time points after DHA treatment (figure 11).

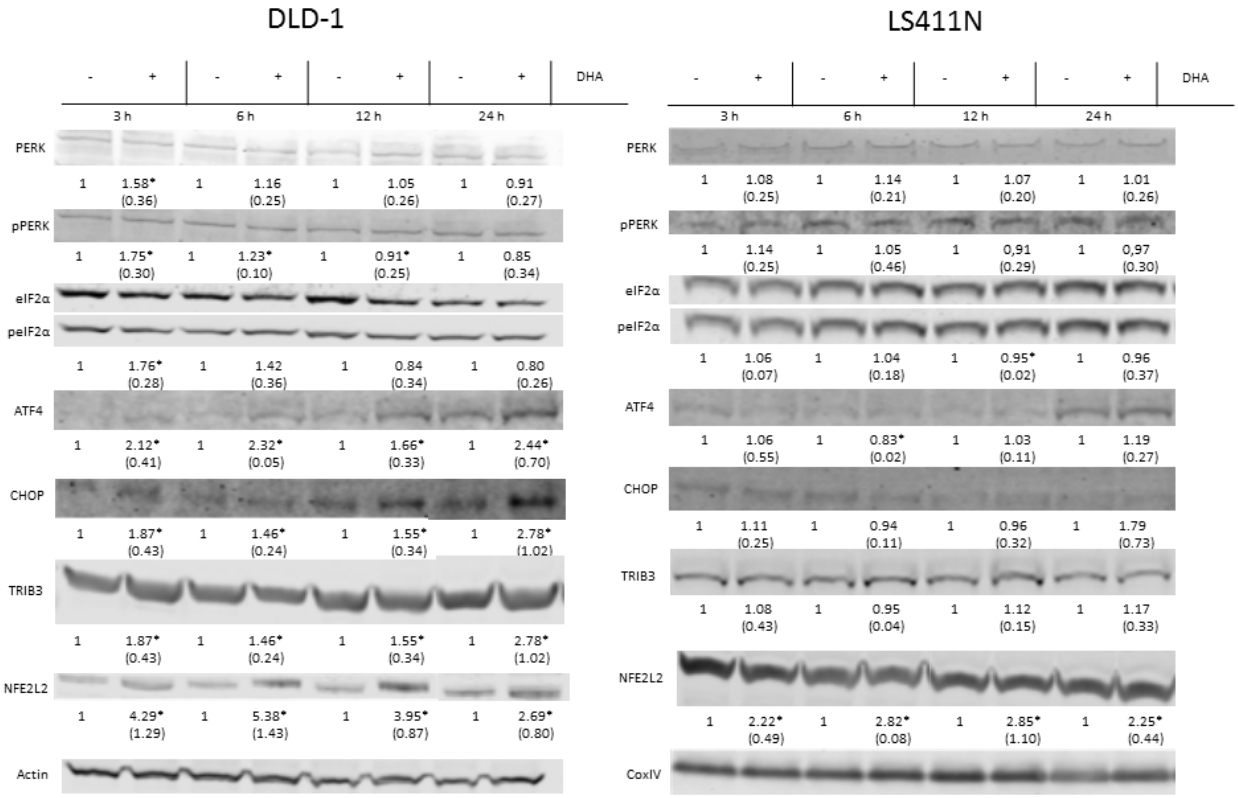

Figure 11: Protein expression levels of PERK and phosphorylated PERK, eIF2α and peIF2α, ATF4, CHOP, TRIB3 and NFE2L2 before and after DHA treatment (70 µM) in DLD-1 and LS411N cells. TG (1 µM) was used as a positive control, but is not included in the figure. Band intensities are normalized against CoxIV/actin and shown as mean fold change of treated samples compared to controls. Band intensities for peIF2α are in addition normalized against eIF2α. Results are based on three independent experiments, and representative bands are shown. *Significantly different from control samples ($p<0.05$).

ATF4, TRIB3 and NFE2L2 are all transcription factors, and confocal imaging was used to investigate cellular protein levels and localisation of these proteins after DHA treatment in DLD-1 and LS411N cells. Results showed that the protein levels were upregulated in the nucleus in DLD-1 cells, but not to the same extent in LS411N cells (figure 12).

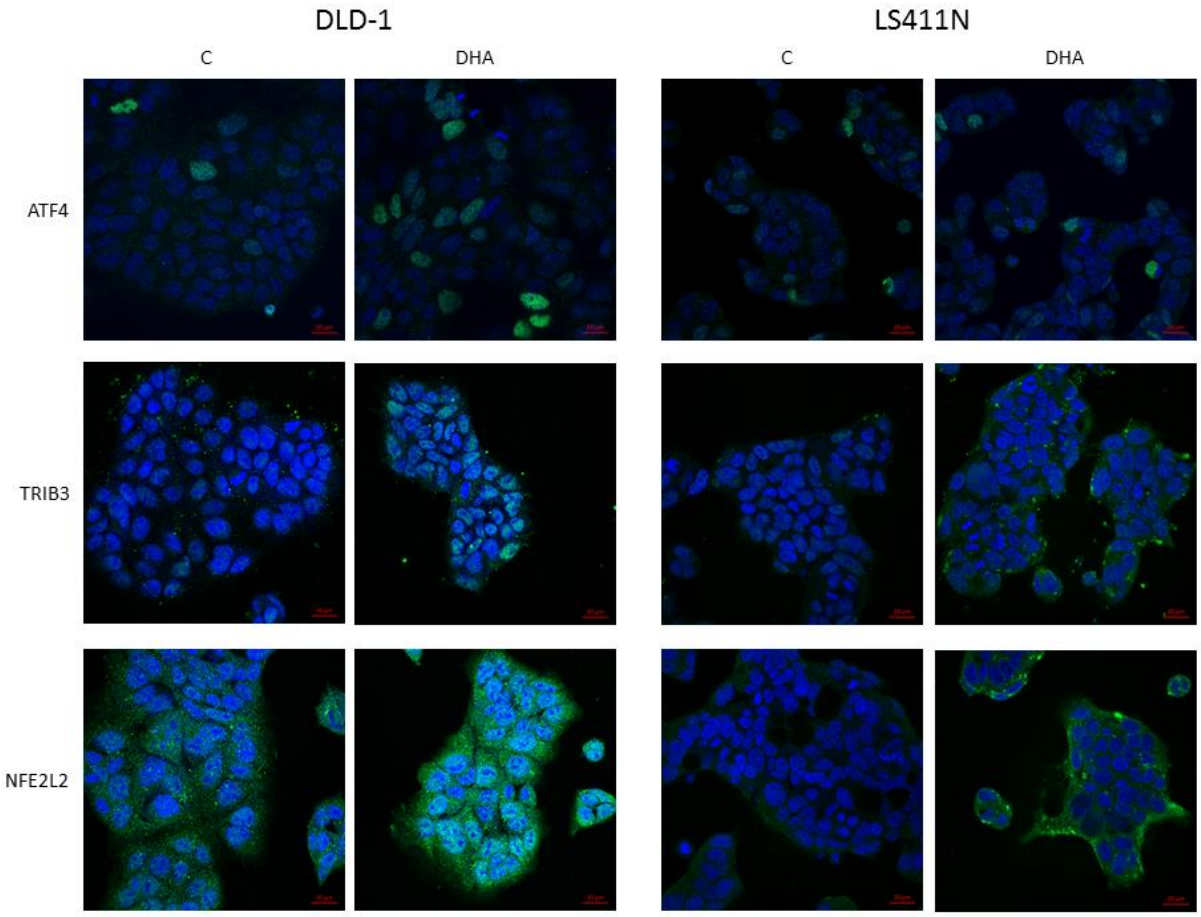

Figure 12: Cellular localisation of immunostained ATF4, TRIB3 and NFE2L2 after 6 h (ATF4) or 12 h (TRIB3 and NFE2L2) of DHA treatment (70 µM) in DLD-1 and LS411N cells. Draq5 is stained in blue. Results are based on three independent experiments, representative images are shown. TG (1 µM) was used as a positive control, but is not included in the figure.

Because NAC partially reversed DHA-induced growth inhibition in DLD-1 cells we wanted to investigate whether expression levels of ER stress-related proteins also changed in response to co-treatment with DHA and NAC compared to DHA treatment alone. ATF4 was chosen due to its important role as a transcription factor in the UPR and its link to autophagy. Although not significant, a decrease in protein level of ATF4 can be observed in both cell lines when treated with both DHA and NAC compared to cells treated with DHA alone, as presented in figure 13.

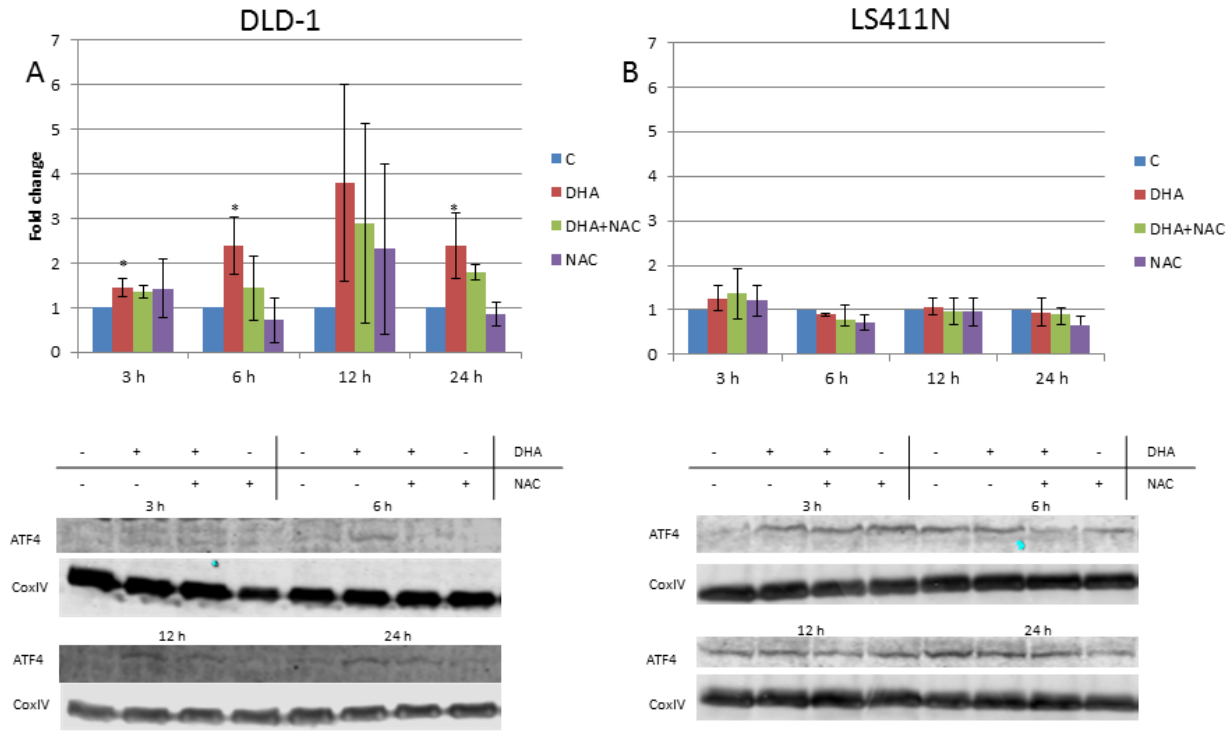

Figure 13: Protein expression levels of ATF4 after 3, 6, 12 and 24 h of treatment with DHA (70 µM), NAC (1 mM), or a combination of the treatments in DLD-1 and LS411N cells. Results represent band intensities normalised against CoxIV, shown as fold changes of treated samples compared to controls. Results are based on three independent experiments, and one representative band is shown. *Significantly different from control ($p<0.05$).

PUFAs are potent inducers of oxidative stress, and because NFE2L2 induces transcription of anti-oxidant genes, we wanted to examine the effect of co-treatment with NAC on DHA-induced increase in the protein expression level of NFE2L2. A significant decrease in NFE2L2-levels was observed after co-treatment with DHA and NAC compared to DHA treatment alone after 3, 6, and 12 h in DLD-1 cells. The same trend was seen in LS411N cells, but not to the same degree (figure 14).

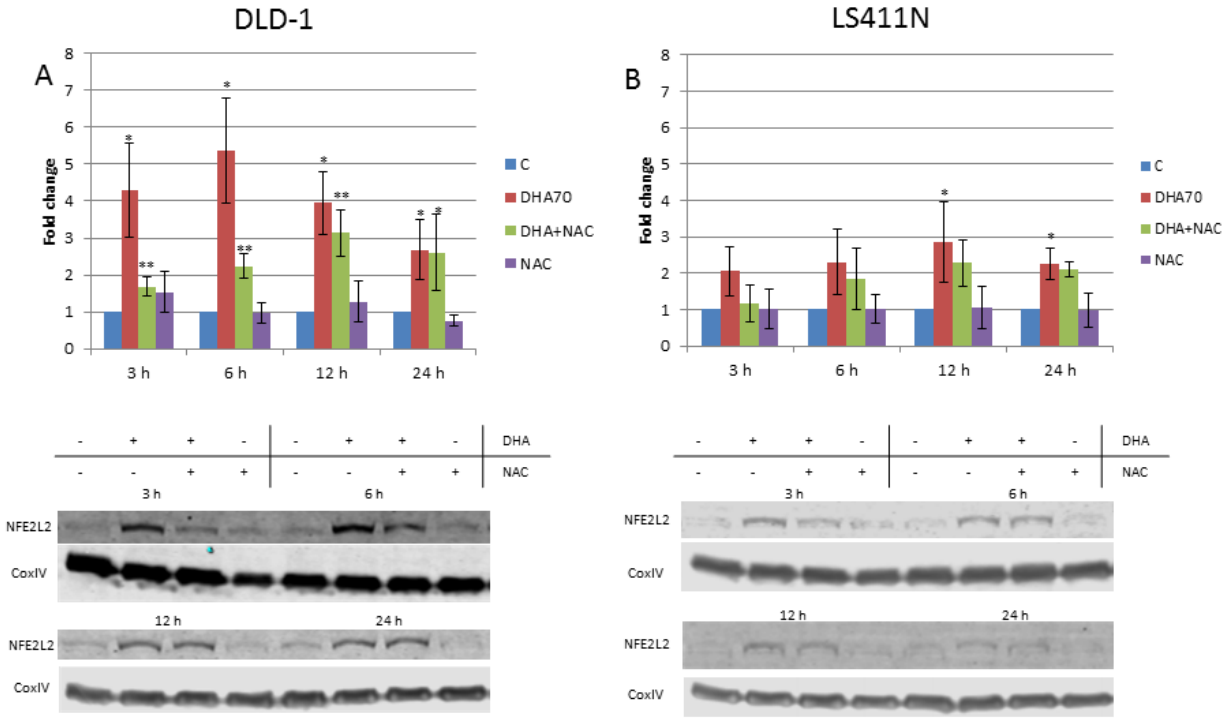

Figure 14: Protein expression levels of NFE2L2 in DLD-1 (A) and LS411N (B) cells 3, 6, 12, and 24 h after treatment with EtOH (C), DHA (70 µM), NAC (1 mM), or a combination of these. Band intensities are normalised against CoxIV and shown as mean fold change of treated samples compared to control samples. Results are based on three independent experiments, one representative band is shown. *Significantly different from control samples, **significantly different from control and DHA-samples ($p<0.05$).

3.4 Expression level of Golgi stress proteins upon DHA treatment in DLD-1 and LS411N cells

To investigate the effect of DHA treatment on Golgi stress signalling pathways in DLD-1 and LS411N cells, the expression of Golgi stress-related genes was analysed by measuring protein expression in both cell lines at different time points after DHA treatment. BFA and TG, known inducers of Golgi and ER stress, respectively, were used as positive controls in both cell lines.

Due to its role as a transcription factor that upregulates the expression of genes involved in the Golgi stress response, the protein expression of TFE3 was investigated. The protein level of TFE3 remained unchanged at all time points after treatment with DHA in both cell lines (figure 15). CREB3 is another transcription factor involved in the Golgi stress response. After activation by proteolysis, the cytoplasmic domain moves to the nucleus to activate target genes. The protein levels of CREB3 were investigated, and for both cell lines and at all time

points, no significant changes in protein expression were detected (figure 15). One of the target genes of CREB3 is ARF4, which is involved in transport between the ER and the GA and is speculated to be involved in the disruption of GA stress-induced apoptosis. Protein expression analyses showed no significant changes in expression in neither cell line at any time points (figure 15).

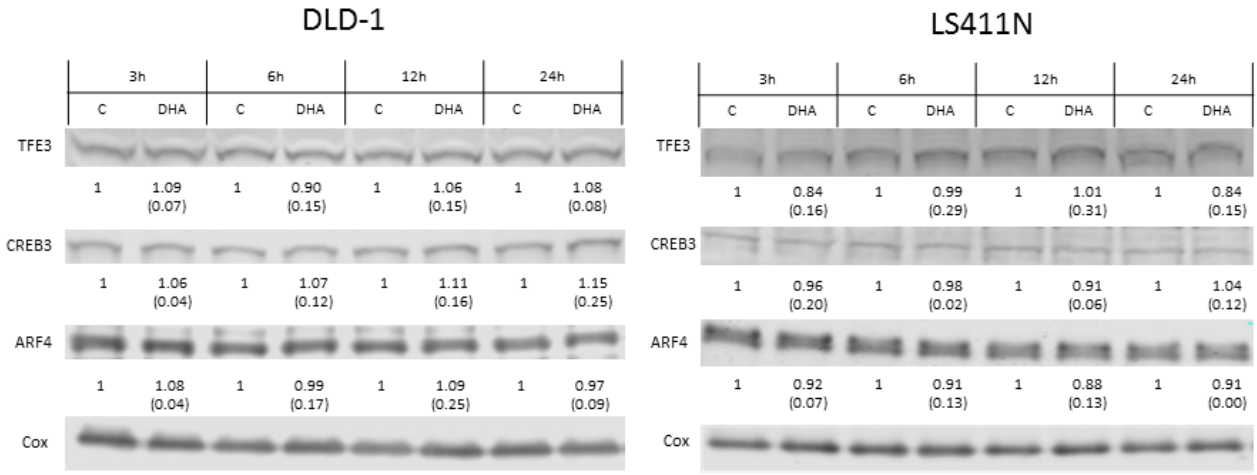

Figure 15: The protein expression level of TFE3, CREB3 and ARF4 at different time points after treatment with EtOH (70 µM) and DHA (70 µM) in DLD-1 and LS411N cells. TG (1 µM) and BFA (1 µM) were used as positive controls, but are not included in the figure. Results are based on three independent experiments for both cell lines, one representative blot is shown. Blot intensities are normalized against CoxIV and shown as mean fold change (SD) of DHA samples compared to controls.

3.5 Oxidative stress was increased after DHA treatment of DLD-1 and LS411N cells

PUFAs are highly peroxidable and can induce oxidative stress. To investigate whether differences in levels of oxidative stress in the cell lines DLD-1 and LS411N after DHA treatment could explain the differences in DHA sensitivity, the levels of two oxidative stress markers were measured by flow cytometry after 6 and 24 h.

3.5.1 Mitochondrial oxidative stress was increased after DHA treatment

Mitochondrial oxidative stress was examined by using MitoSOX as a marker for mitochondrial superoxide activity in DLD-1 and LS411N cells before and after treatment with DHA. The antioxidant NAC was used in combination with DHA to investigate whether it had any effect on the oxidative stress levels compared to DHA treatment alone. Results, displayed in figure 16, show that MitoSOX level significantly increased in DLD-1 cells both 6 and 24 h

after treatment with DHA, and co-treatment with NAC further increased the MitoSOX signal. Similar results were observed in LS411N cells, but not to the same extent as DLD-1 cells.

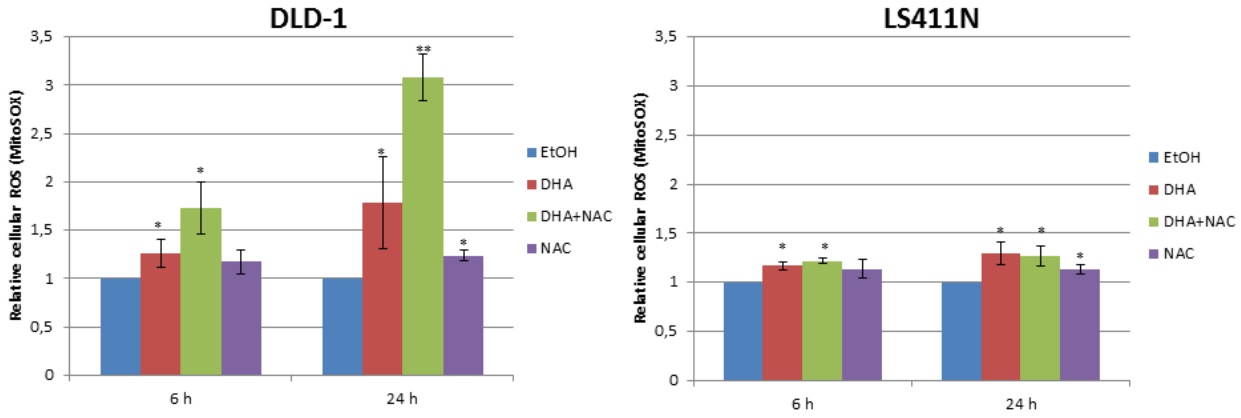

Figure 16: Differences in mitochondrial oxidative stress after treatment with EtOH, DHA (70 µM), NAC (1 mM), or a combination of these treatments in DLD-1 (A) and LS411N (B) cells as measured with the mitochondrial oxidative stress marker MitoSOX by flow cytometry. Data represents mean fluorescence intensities of triplicates of 10,000 cells from three independent experiments, and are shown as mean fold change of treated samples compared to controls. *Significantly different from control, **significantly different from control- and DHA-sample ($p<0.05$).

3.5.2 Cellular oxidative stress was increased after DHA treatment

When the cellular oxidative stress marker H2DCF is cleaved by esterases and oxidised in the cells, it is converted to fluorescent DCF. This marker was used to investigate whether cellular oxidative stress was increased after DHA treatment in DLD-1 and LS411N cells. Co-treatment with NAC was used to examine possible antioxidant effects on cellular oxidative stress levels. Results showed a significant increase in DCF in DLD-1 cells after 6 h, and a markedly increase after 24 h. This increase was partially counteracted after 6 h and 24 h when cells were treated with both DHA and NAC. No significant changes in DCF fluorescence levels were found in LS411N cells (figure 17).

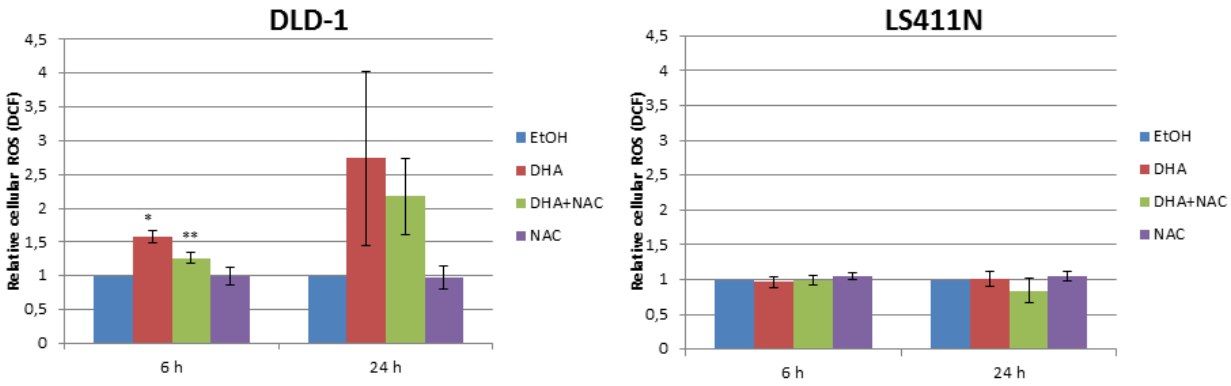

Figure 17: Differences in relative cellular stress measured by flow cytometry with the cellular stress marker DCF in DLD-1 (A) and LS411N (B) cells 6 and 24 h after treatment with DHA (70 µM), NAC (1 mM), or a combination of these treatments. Data represents mean fluorescence intensity from three independent experiments with triplicates of 10,000 cells. Results are shown as mean fold change of treated samples compared to controls. *Significantly different from controls, **significantly different from control- and DHA-sample ($p<0.05$).

3.6 Autophagy level increased after DHA treatment in DLD-1 cells

To investigate whether differences in DHA sensitivity between the two cell lines DLD-1 and LS411N could be explained by differences in the ability to induce autophagy, the autophagy level before and after treatment with DHA, NAC, BafA1, DMSO, rapamycin, chloroquine, or a combination of these treatments were measured by using the fluorescent autophagic marker Cyto-ID. When inside autophagic vesicles, the Cyto-ID marker fluoresces, and fluorescence intensity was measured by flow cytometry. BafA1, rapamycin, DMSO and chloroquine were used as controls. The antioxidant NAC was used alone and in combination with DHA to investigate possible effects of NAC on autophagy. Results, presented in figure 18, showed that DHA treatment significantly increased the autophagy level compared to controls in DLD-1 cells. LS411N cells also showed a significant increase in autophagic vesicles after DHA treatment, but to a much smaller extent than in DLD-1 cells. Treatment with NAC together with DHA led to a decrease in autophagy levels compared to DHA treatment alone in both DLD-1 and LS411N cells. DHA- and BafA1-treatment together led to a higher increase in autophagy than BafA1 alone in DLD-1, but not in LS411N cells.

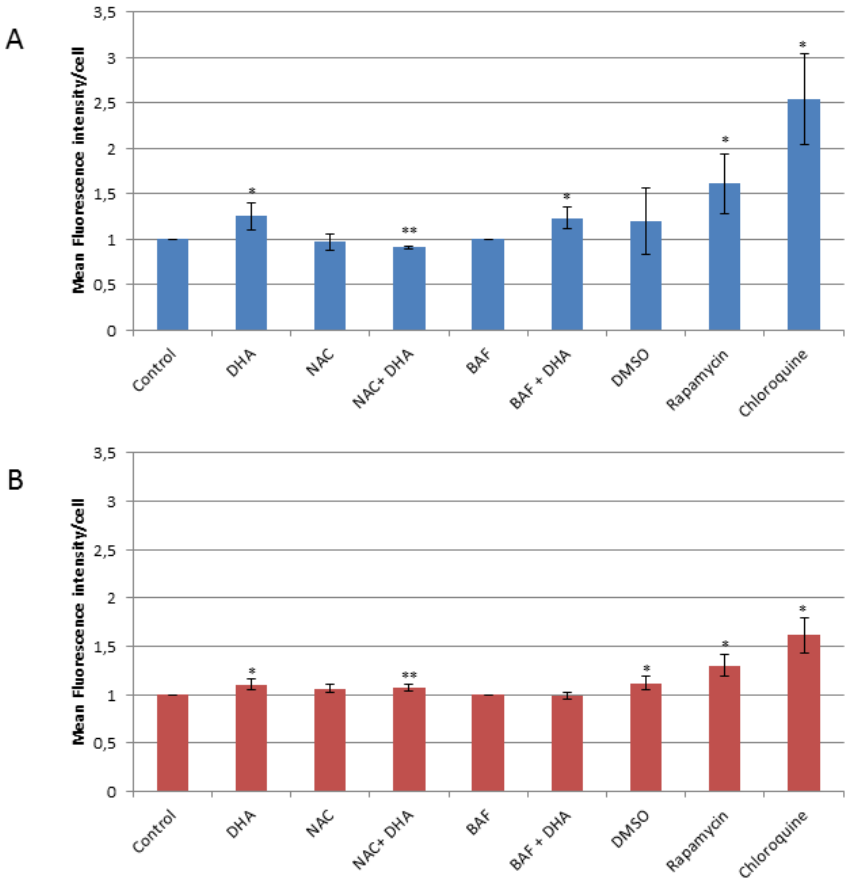

Figure 18: Differences in mean fluorescence intensity levels after incorporation of the fluorescent autophagy marker Cyto-ID in DLD-1 (A) and LS411N (B) cells after treatment with DHA (70 µM), NAC (1 mM), BafA1 (0.1 µM), DMSO (50 nM), rapamycin (50 nM), chloroquine (10 µM) or a combination of these treatments. Results are shown as the mean intensities and standard deviations of triplicates of 10,000 cells from three independent experiments. Results are shown as mean fold change of treated samples compared to respective controls (EtOH or Baf). *Significantly different from respective control, **significantly different from control and DHA treatment ($p<0.05$).

3.7 Basal autophagy level is higher in LS411N cells compared to DLD-1 cells

A recent paper by our group points to differences in the basal autophagy level as a possible cause for dissimilarities in DHA sensitivity between colon cancer cell lines [55]. To investigate the basal autophagy level DLD-1 and LS411N cells, the autophagy levels in untreated cells were measured by using the autophagic marker Cyto-ID. This marker emits fluorescence when inside autophagic vesicles. Fluorescence intensities were measured by flow cytometry. Results showed that mean fluorescence intensity was 2.5-fold higher in LS411N cells than in DLD-1 cells. This indicates a higher basal autophagy level in LS411N cells than in DLD-1 cells (figure 19).

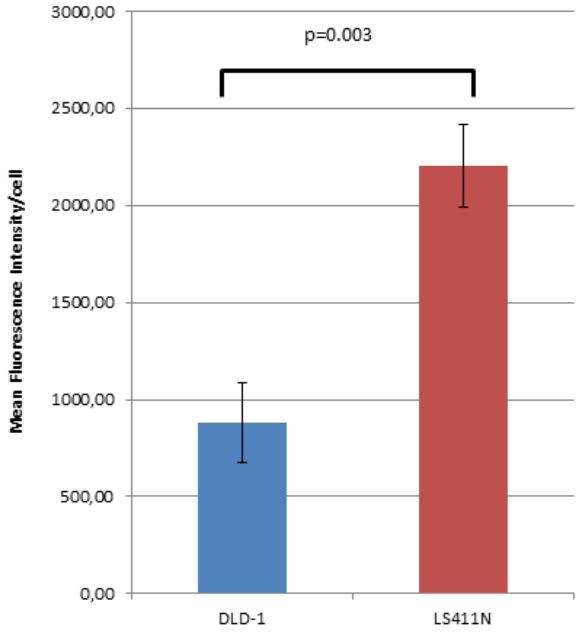

Figure 19: Differences in mean fluorescence levels after incorporation of the autophagy marker Cyto-ID in untreated DLD-1 and LS411N cells measured by flow cytometry. Results show the mean intensities and standard deviations of triplicates of 10,000 cells from three independent experiments.

3.8 Treatment with DHA increased the autophagic flux only in DLD-1 cells

To check whether DHA treatment affected the autophagic process in DLD-1 and LS411N cells, expression levels of some autophagy-related proteins were investigated after 24 and 48 h of treatment with DHA, NAC, or BafA1, or a combination of two or more of these. BafA1 was added to inhibit fusion of autophagosomes with lysosomes and thus stop lysosomal degradation of proteins. Protein expression was analysed by western blotting, and confocal imaging was used to investigate protein expression and cellular localisation of proteins.

LC3BII is found on the membrane of autophagosomes and is necessary for both the elongation of the isolation membrane and the fusion of autophagosomes with lysosomes. It is therefore often used to monitor the autophagic flux in cells. DHA treatment led to an increase in LC3BII expression levels in DLD-1 cells 24 h after treatment, while it remained unchanged in LS411N cells (figure 20).

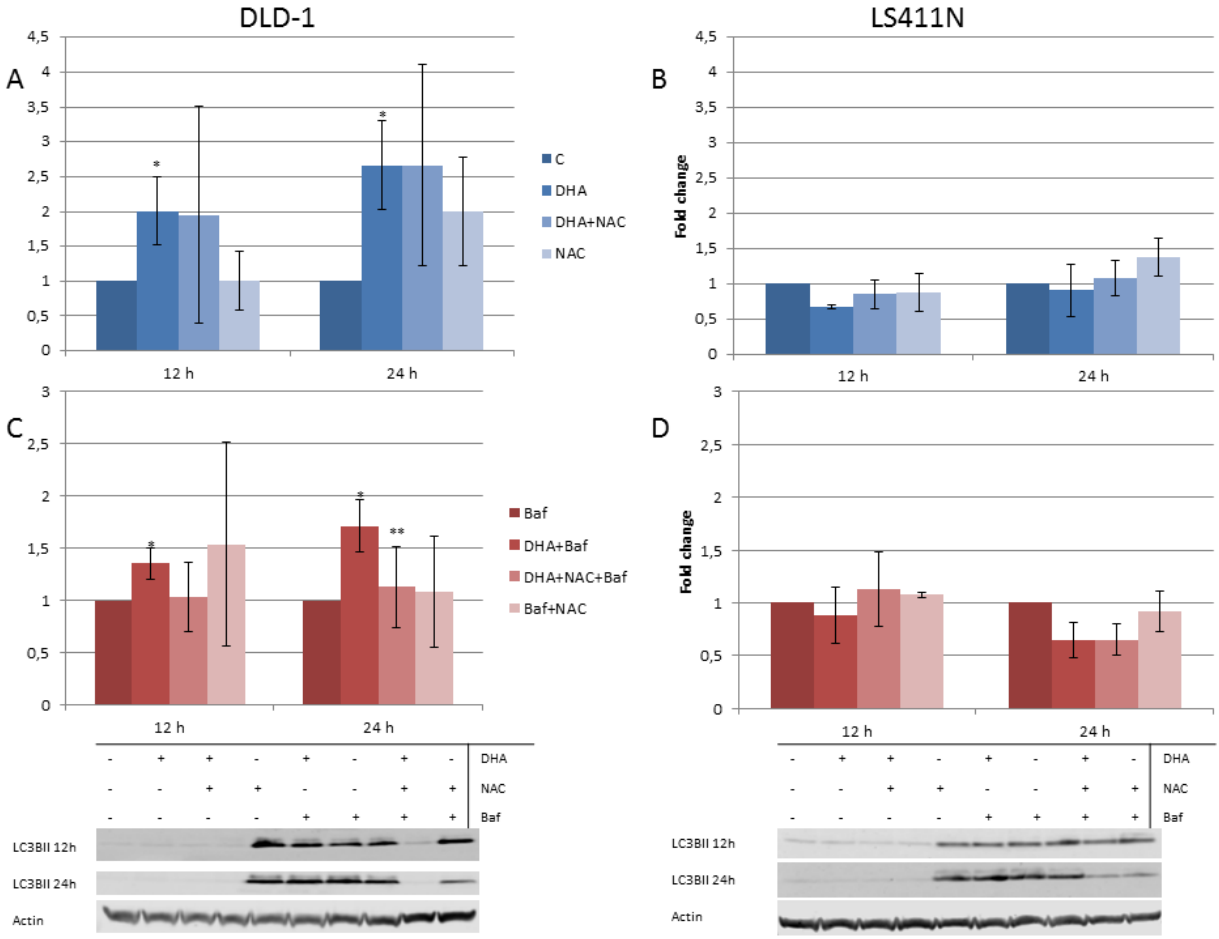

Figure 20: Protein expression level of LC3BII in DLD-1 (A and B) and LS411N (C and D) cells after treatment with DHA (70 µM), NAC (1 mM), BafA1 (0.1 µM), or a combination of these treatments. One representative band is shown from three independent experiments. Results represent band intensities normalised against actin and shown as mean fold change of treated samples compared to controls (EtOH or BafA1). *Significantly different from control, **significantly different from control- and DHA-samples ($p<0.05$).

P62 is a receptor that is involved in selective autophagy, and when activated, it binds to LC3 and is incorporated into autophagosomes. Results showed that DHA treatment of DLD-1 cells increased p62 levels in DLD-1 cells after 12 and 24 h, and the accumulation of p62 induced by BafA1 treatment increased. Co-treatment with NAC reduced this increase after 12 h, but not after 24 h. The same trend was seen in LS411N cells, but not to the same extent.

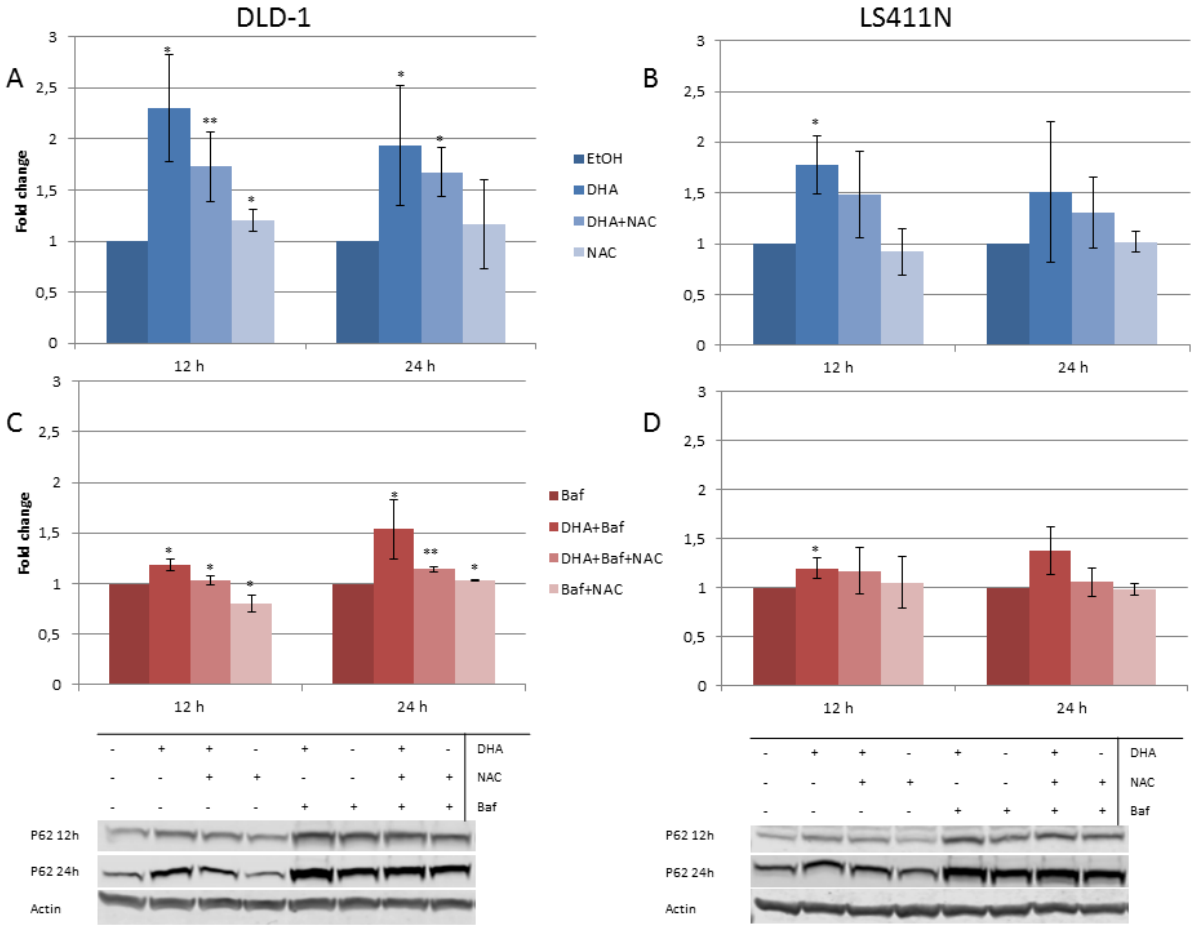

Figure 21: Protein expression level of p62 at 12 and 24 h after treatment with EtOH, DHA (70 µM), NAC (1 mM), BafA1 (0.1 µM), or a combination of these treatments in DLD-1 (A and B) and LS411N (C and D) cells. Results are based on three independent experiments, and representative bands are shown. Band intensities are normalised against actin and shown as mean fold change of treated samples compared to controls (EtOH or BafA1). *Significantly different from control treatment, **significantly different from control and DHA treatment ($p<0.05$).

Confocal imaging of cells immunostained for p62 and LC3BII was performed 12 and 24 h after DHA treatment to investigate levels and cellular localisation of the proteins. Both p62 and LC3BII levels seemed to increase after DHA treatment in DLD-1 cells, but not to the same extent in LS411N cells. However, initial LC3BII levels in control LS411N cells seemed to be higher than in control DLD-1 cells. Results also indicated a co-localisation of p62 and LC3BII. BafA1 was used to inhibit lysosomal degradation, and thus led to an accumulation of autophagic vesicles. This was observed in both DLD-1 and LS411N cells, but to a higher degree in LS411N cells. DHA treatment combined with BafA1 seemed to increase the accumulation of autophagic vesicles further in DLD-1 cells (figure 22 and 23).

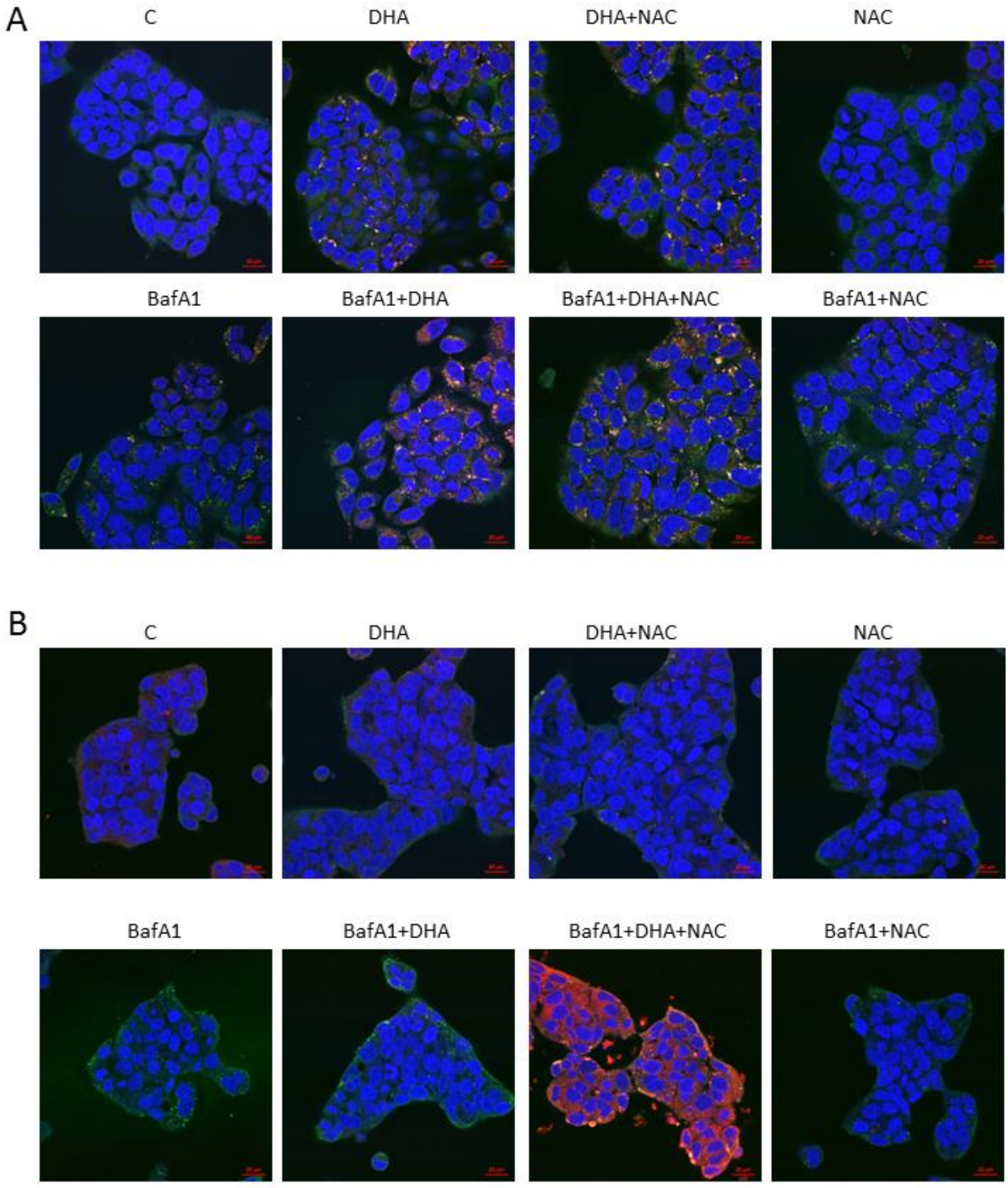

Figure 22: Cellular localisation of LC3BII and p62 in DLD-1 (A) and LS411N (B) cells 12 h after treatment with DHA (70 µM), NAC (1 mM), BafA1 (0.1 µM), or a combination of these treatments, shown by confocal images of cells immunostained with LC3BII (red) and p62 (green). Draq5 is stained in blue. Results are based on three independent experiments, representative images are shown.

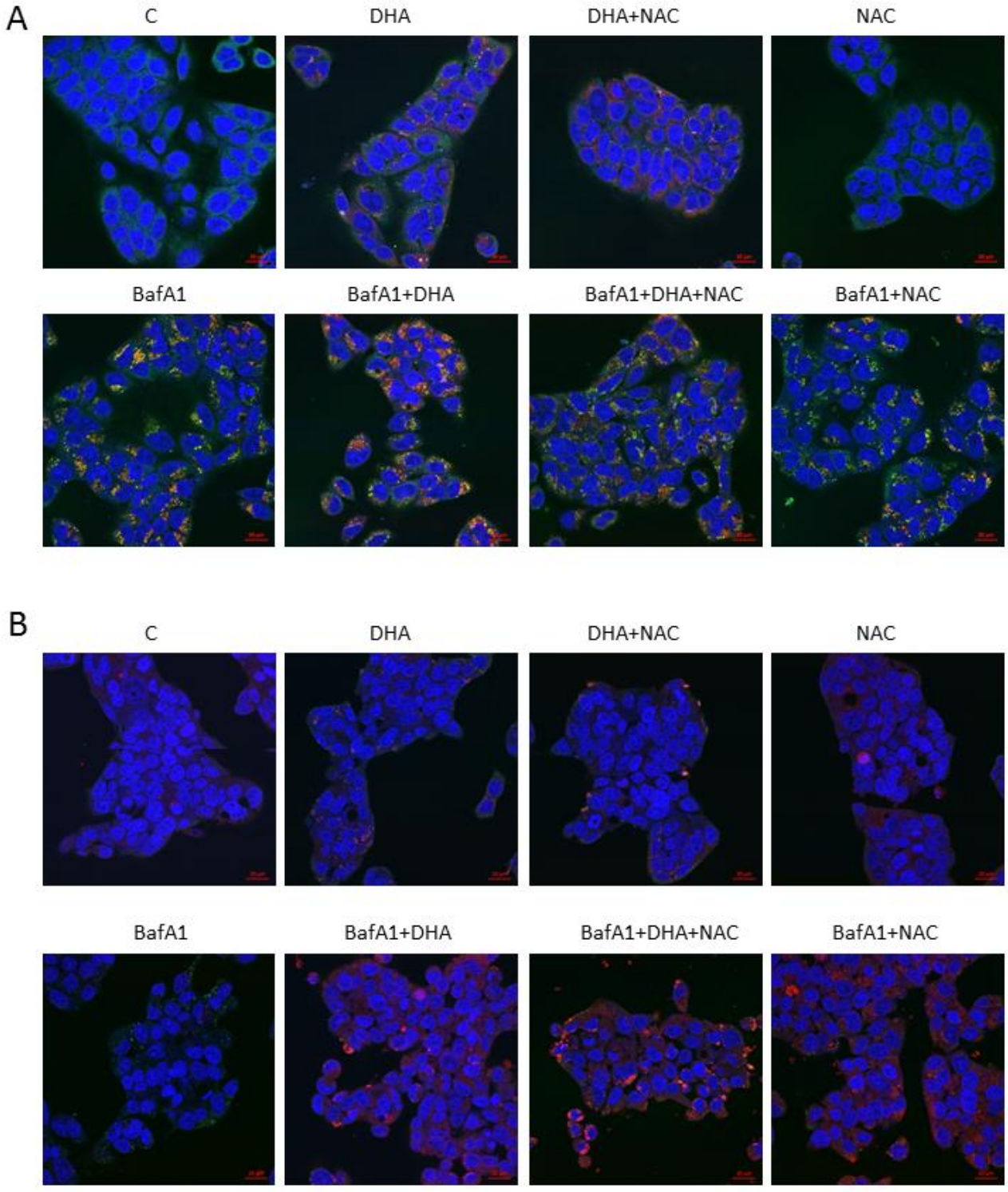

Figure 23: Cellular localisation of LC3BII and p62 in DLD-1 (A) and LS411N (B) cells 24 h after treatment with DHA (70 µM), NAC (1 mM), BafA1 (0.1 µM), or a combination of these treatments, shown by confocal images of cell immunostained with LC3BII (red) and p62 (green). Draq5 is stained in blue. Results are based on three independent experiments, representative images are shown.

3.9 DHA decreased the protein level of p53, and induced formation of p53 aggregates

The p53 status in the two cell lines DLD-1 and LS411N is different. In DLD-1 cells p53 is present in a mutated form, whereas in LS411N cells the gene has a nonsense mutatation and the protein is not expressed [62]. Because p53 is activated in response to ROS [63] and acts as a regulator of autophagy, we wanted to investigate the level of p53 protein after treatment with DHA and NAC in the DHA sensitive cell line DLD-1. The expression of p53 was analysed by measuring protein expression at several time points after treatment. Protein expression was measured by using western blot, and confocal imaging was used to investigate protein expression and cellular localisation. The results, presented in figure 24, showed that DHA treatment resulted in an increased expression of p53 in DLD-1 cells after 3 h, but a decreased expression at later time points. Co-treatment with NAC in DHA-treated cells also resulted in a decrease of p53 expression after 24 h treatment, although not to the same extent than DHA treatment alone.

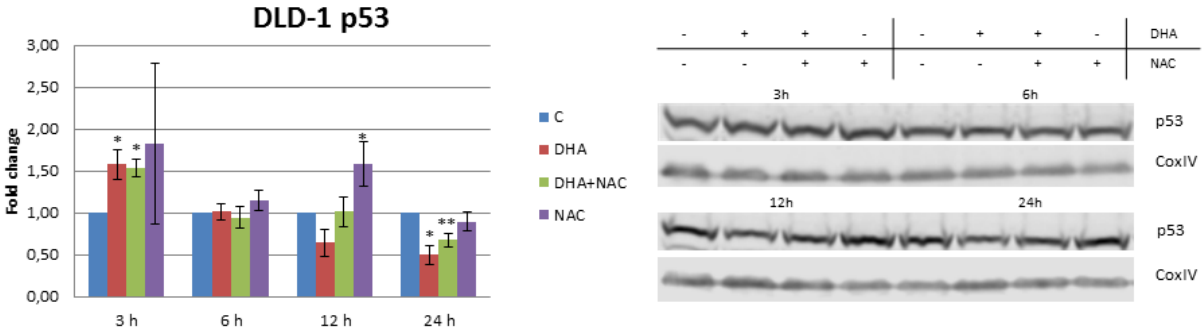

Figure 24: Protein expression levels of p53 in DLD-1 cells at different time points after treatment with EtOH (70 µM), DHA (70 µM), NAC (1 mM), or a combination of these. Results are based on three independent experiments, one representative band is shown. Band intensities are normalised against CoxIV and shown as mean fold change of treated samples compared to controls. *Significantly different from control treatment, **significantly different from control and DHA treatment ($p<0.05$).

Confocal imaging of immunostained cells was performed 12 and 24 h after treatment to investigate the expression level and cellular localisation of p53. The results showed that p53 proteins aggregated after DHA treatment in DLD-1 cells (figure 25).

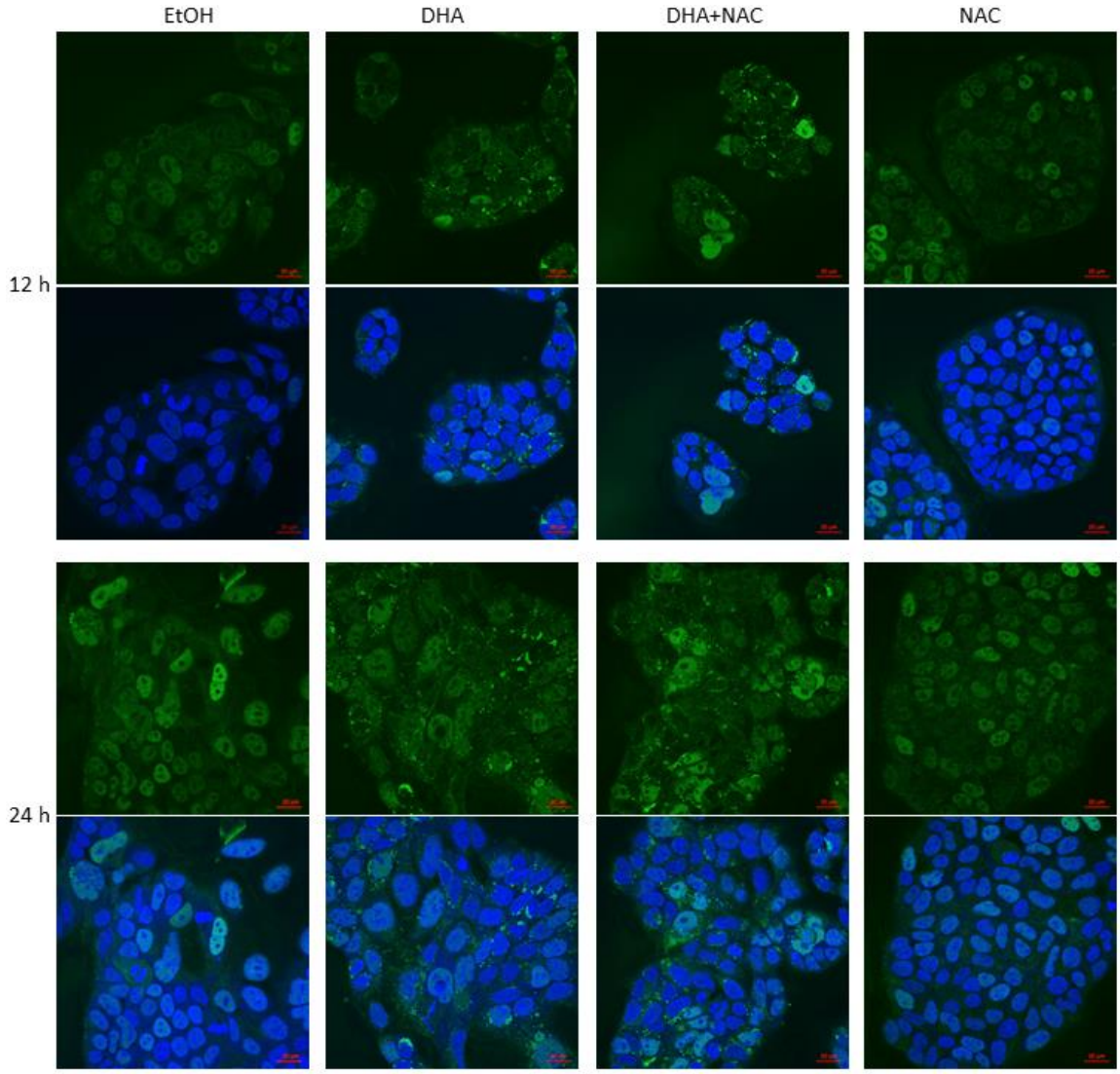

Figure 25: Cellular localisation of p53 in DLD-1 cells 12 and 24 h after treatment with EtOH (70 µM), DHA (70 µM), NAC (1 mM), or a combination of these. P53 is stained in green. Results are based on three independent experiments, representative images are shown.

Due to its role in autophagy regulation, we wanted to investigate the localisation of p53 aggregates relative to the localisation of the autophagy protein LC3BII. Confocal imaging of immunostained p53 and LC3BII was performed 12 and 24 h after treatment with DHA, NAC, BafA1, or a combination of two or more of these. As previously mentioned BafA1 inhibits fusion of autophagosomes with lysosomes, and therefore induced an accumulation of autophagic vesicles in the cells. Results indicated a possible co-localisation of p53 aggregates with LC3BII after DHA treatment in DLD-1 cells. BafA1 treatment alone did not induce p53 aggregation (figure 26 and 27).

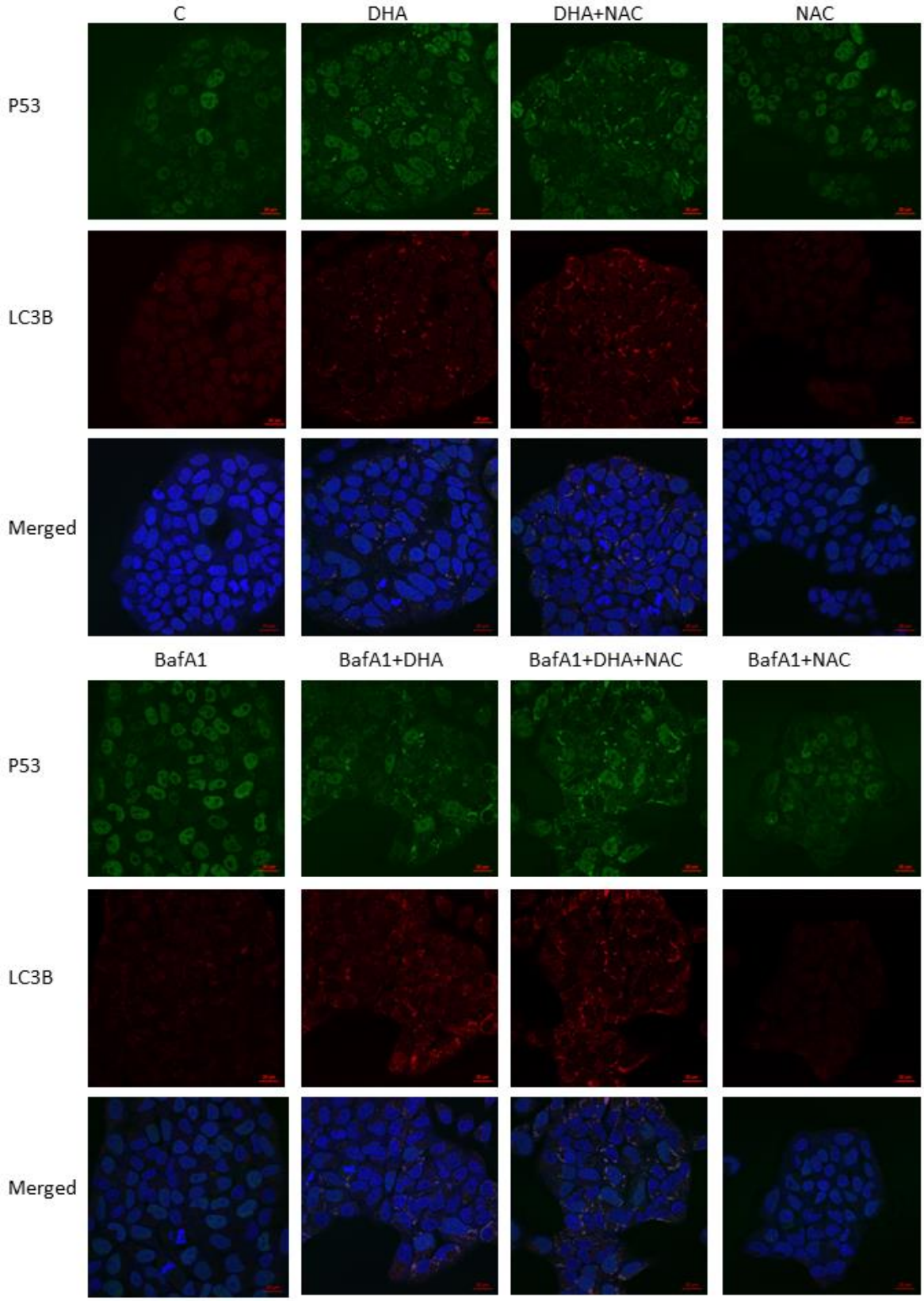

Figure 26: Cellular localisation of immunostained p53 (green) and LC3BII (red) 12 h after treatment with DHA (70 µM), NAC (1 mM), BafA1 (0.1 µM) or a combination of these treatments in DLD-1 cells. Draq5 is stained in blue. Results are based on three independent experiments, and representative images are shown.

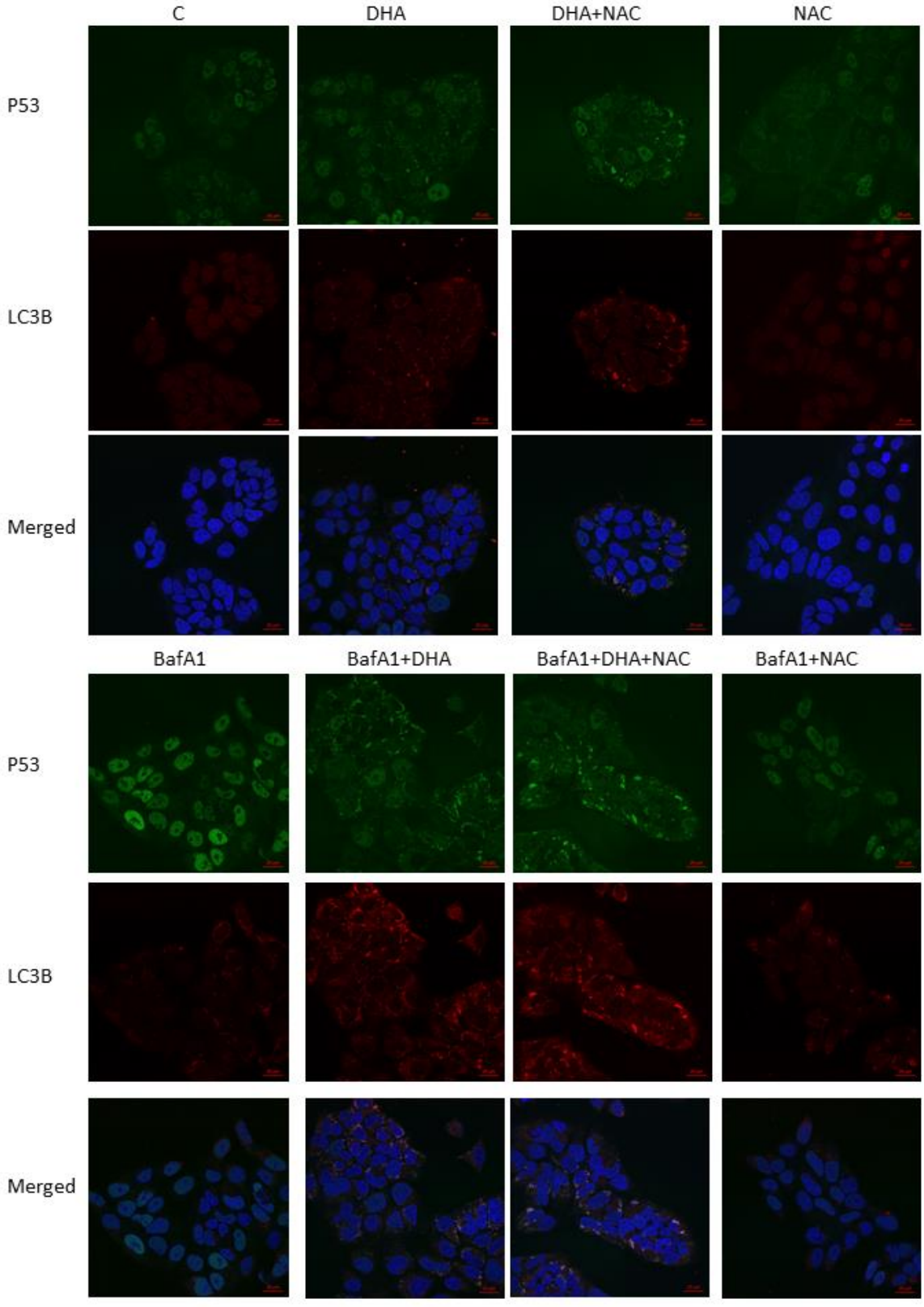

Figure 27: Cellular localisation of immunostained p53 (green) and LC3BII (red) 24 h after treatment with DHA (70 µM), NAC (1 mM), BafA1 (0.1 µM) or a combination of these treatments in DLD-1 cells. Draq5 is stained in blue. Results are based on three independent experiments, and representative images are shown.

3.10 Knockdown of p53 did not affect DHA-induced growth inhibition in DLD-1 cells

Depending on its cellular localisation, p53 can either induce or inhibit autophagy [53]. Nuclear p53 activates autophagy-stimulating genes, whereas cytosolic p53 inhibits autophagy. The DHA sensitive DLD-1 cells express a mutated form of p53, whereas the less sensitive LS411N cells are negative for p53 expression. Results showed that the basal level of autophagy differed in DLD-1 and LS411 cell and that p53 levels were affected by DHA treatment in DLD-1 cells. To further investigate the role of p53 in relation to DHA, we wanted to explore whether p53 knockdown affected DHA-induced growth inhibition in DLD-1 cells. Knockdown of p53 was done with p53-mRNA targeting siRNA. Initial testing of the knockdown effect showed a reduction in the expression of p53 of 92% (figure 28).

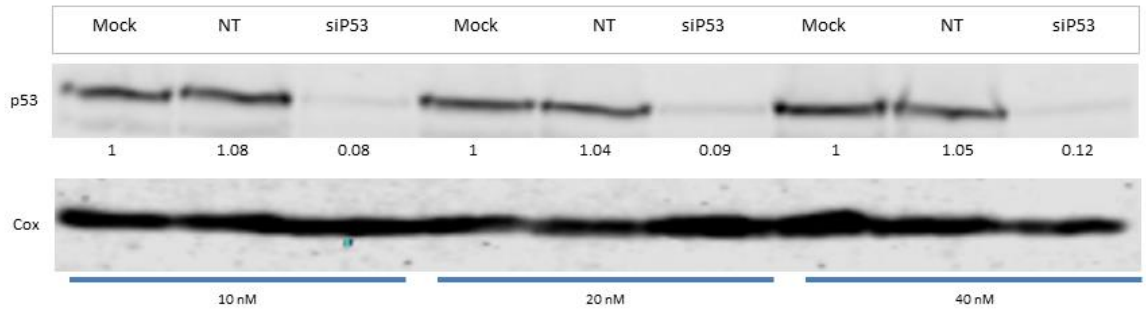

Figure 28: Protein expression level of p53 after initial testing of the knockdown effect of siP53 (10, 20 or 40 nM) transfection in DLD-1 cells. Band intensities are normalised against CoxIV and shown as fold change of siRNA-treated samples compared to Mock samples (only lipofectamine). Results are based on one experiment. NT=non-target siRNA.

Cells with siRNA-mediated knockdown of p53 were treated with DHA 48 h prior to protein harvesting to investigate the effect of DHA. Western blotting analysis showed that the knockdown efficiency of p53 by p53 siRNA was high, with a reduction in p53-expression of 89% compared to the NT-control. Also, the DHA-treated siP53-sample showed a clear reduction in p53 levels compared to the corresponding NT-siRNA sample (figure 29).

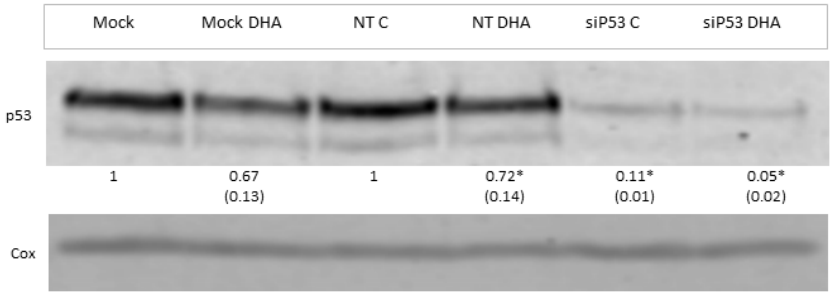

Figure 29: Protein expression level of p53 in DLD-1 cells after Mock treatment (lipofectamine only), NT (non-target) siRNA transfection, and siP53 transfection (10 nM). Band intensities are normalised against cox, and shown as fold change of treated samples compared to controls. NT siRNA C acts as control for siP53-treated samples. Results are based on three independent experiments and are shown as one representative band. *Significantly different from NT control ($p<0.05$).

To examine the effect of p53 knockdown on DHA-mediated growth inhibition cells were counted 48 h after DHA treatment. The siP53-transfected DLD-1 cells were 42% growth inhibited compared to NT-siRNA control cells. DHA-induced growth inhibition of DLD-1 cells did not seem to be affected by siP53 transfection. Compared to siP53 knockdown control cells, DHA treatment of siP53 knockdown led to a growth inhibition of 58 % (figure 30).

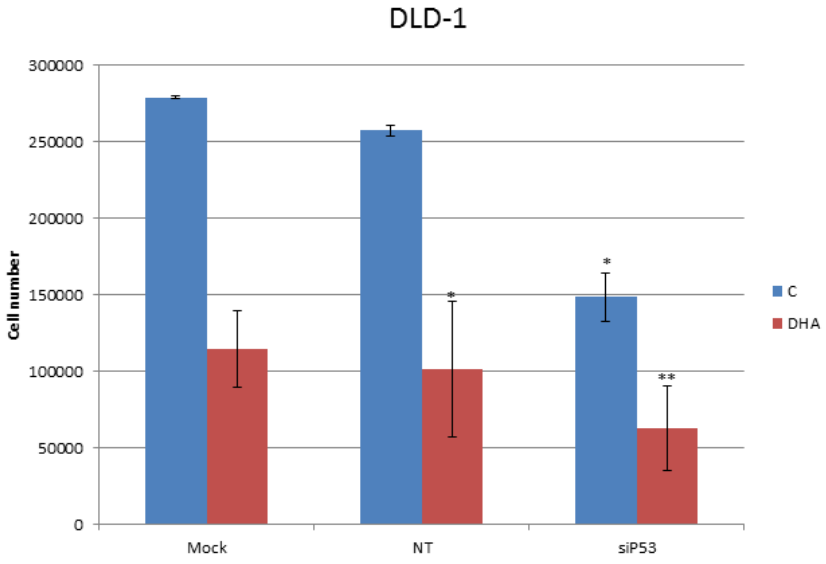

Figure 30: The effect of p53 knockdown by siRNA transfection in DLD-1 cells treated with EtOH (70 µM) or DHA (70 µM) on DHA-mediated growth inhibition. Growth inhibition was measured by cell counting 48 h after treatment. Results are based on three independent experiments. *Significantly different from NT control, **significantly different from NT and siP53 control ($p<0.05$).

4. Discussion

Cancer cells are known to respond differently to DHA treatment. The data presented in this thesis show that treatment with physiologically relevant doses of DHA in the two colon cancer cell lines DLD-1 and LS411N result in different growth responses and suggests that various molecular pathways are involved. DLD-1 cells are sensitive to DHA treatment and the expression level of both ER stress-related proteins and autophagy markers are increased after treatment with DHA. On the other hand, growth of LS411N cells is much less affected by DHA treatment and does not show a notable induction of the same proteins.

4.1 DHA induced different growth responses in DLD-1 and LS411N cells

Previous work done by our group showed that colon cancer cell lines responded differently to DHA treatment. The two cell lines DLD-1 and LS411N were chosen for this project because they display different DHA sensitivity even though they are cultivated in the same growth medium [61]. Results showed that DLD-1 cells were clearly sensitive to DHA, with a growth reduction of about 40-50% after 48 h, whereas LS411N cells were far less sensitive under the same conditions. These results demonstrating differences in DHA-mediated growth inhibition between these cell lines are in accordance with previous studies done on several colon cancer cell lines that show a DHA-induced growth inhibition [64, 65].

Previous studies have shown that the composition of the growth media, and especially the serum concentrations, can affect the DHA-induced growth inhibition [66]. Higher amounts of serum in the medium seem to protect against the cytotoxic effects of DHA [67, 68]. Because the cell lines included in this study were cultivated in the same growth medium and under the same conditions, effects due to differences in cultivation conditions were significantly reduced. Other factors that have been found to influence the effect of DHA treatment is cell density, proliferation state and growth rate [69] (reviewed in [70]). According to these papers, cells seem to be more sensitive to DHA at lower densities, and cells with faster growth rates are generally more sensitive than slower growing cells. This can possibly contribute to the differences in DHA sensitivity observed in DLD-1 and LS411N cells, which have a doubling time of 22 and 40 h, respectively. The papers also mention that cells are more sensitive to DHA treatment in proliferative than dormant phases. To ensure that the cells used in the experiment were in a proliferative phase, DLD-1 and LS411N cells were monitored during the cell counting experiments by counting cells before and 24 and 48 h after treatment.

Previous work performed has shown that the n-9 PUFA OA does not affect the growth of DLD-1 cells and the growth of the colon cancer cell line SW620 [20, 61]. To be certain that the effect is n-3 PUFA specific however; further research should also explore the effect of n-6 PUFAs in these cell lines.

4.2 Antioxidants affected DHA-induced growth inhibition in different ways

The DHA-induced growth inhibition in DLD-1 cells was affected to a different extent by the antioxidants BHA, BHT and NAC. Whereas BHA and DHA together showed a higher growth inhibitory effect than that of DHA treatment alone in DLD-1 cells, NAC partially reversed it. BHT did not seem to have any effect on cell growth in DLD-1 and LS411N cells, neither in combination with DHA treatment or alone. Both BHA and BHT are fat soluble antioxidants, and as neither counteracted the DHA-induced growth inhibition, results indicate that lipid peroxidation is not the cause of DHA-mediated cytotoxicity.

The antioxidant BHT is synthetic and fat soluble, and exerts its antioxidant activity through the donation of a hydrogen atom to free radicals. Through this action, it reduces the formation of ROS, and becomes a radical itself. Even though BHT is considered to be a safe food additive, it has been reported an induction of necrosis and carcinogenic effects on rat livers. However, anticancer effects have also been reported in hepatocytes of rats(reviewed in [59, 71]). The results showed that BHT treatment alone did not affect cell growth in DLD-1 and LS411N cells. Further, BHT did not affect the growth inhibitory effect of DHA treatment in DLD-1 cells. As BHT is a powerful antioxidant, this indicates that the reduction in cell growth after DHA treatment is not due to lipid peroxidation.

The synthetic fat-soluble antioxidant BHA is known to suppress the formation of free radicals and to prevent lipid oxidation, and is therefore much used as a food additive to stabilise fats [58]. However, BHA is also known to exert a wide range of other biological activities in addition to its antioxidant action. The results showed that BHA rather than reversing the DHA-induced growth inhibition induced it further in DLD-1 cells, and a growth inhibition due to BHA treatment alone was observed in both DLD-1 and LS411N cells. This indicates an additive effect when combined with DHA and a growth inhibitory effect of BHA alone, which is in agreement with previous papers showing a BHA-induced growth inhibition of HeLa cells [58, 72]. These papers found that BHA induces growth inhibition via caspase-induced apoptosis and cytotoxic effects of BHA in A549 lung cancer cells.

NAC is an antioxidant consisting of a thiol group, and a precursor of L-cysteine and reduced glutathione (reviewed in [73]). It can act as an antioxidant in several ways; either the thiol group itself can reduce ROS, or glutathione - which also is an antioxidant, can reduce oxidative stress, especially lipid peroxidation of cellular membranes (reviewed in [74]). In addition, NAC has been shown to increase the activity of superoxide dismutase, catalase, and glutathione peroxidase in cells from the jejunum in piglets [75]. All of these enzymes exert antioxidant action. A possible cause of the decrease in DHA-induced growth inhibition in DLD-1 cells after co-treatment with NAC is therefore a reduction in the level of oxidative stress in the cells. Oxidative stress is further discussed below. However, NAC is also known to affect cells in other ways. Several papers show that NAC has growth-promoting activities, either by inducing growth directly or by inhibiting apoptosis (reviewed in [73]). One paper showed that NAC activated the extracellular signal-regulated kinases-mitogen activated protein kinases (ERK-MAPK) pathway in articular chondrocytes, a pathway which is known to promote cell survival and growth [76]. Another paper showed that NAC protected against cell death in endothelial cells after an heat shock induction [77]. It has also been reported that NAC-supplementation in piglets increased plasma concentrations of epidermal growth factor, as well as intestinal mRNA levels for epidermal growth factor receptors [75]. Therefore, the partial reversal of the DHA-induced growth inhibition in DLD-1 cells caused by NAC treatment may also be due to growth promoting activity, and not necessarily the antioxidant effect alone. However, only a small non-significant increase in cell growth were found after treatment with NAC alone in DLD-1 cells, and no such increase was found in LS411N cells. This indicates that the growth-promoting activity of NAC reported by several papers may not be of importance in the partial reversal of DHA-induced growth inhibition in DLD-1 cells.

4.3 DHA treatment activated pathways of the integrated stress response

As described in the introduction, the ISR is activated by a variety of cellular stressors, and acts to restore normal cellular function. Previous work done by our group has shown an induction of ER stress after DHA treatment in several colon cancer cell lines, and preliminary results suggested an upregulation of autophagy in DLD-1 cells [20, 55, 61]. Based on this, we wanted to explore whether differences in the induction of ISR-signalling pathways in DLD-1 and LS411N cells after DHA treatment could explain the differences in DHA sensitivity between these two cell lines. Indeed, results showed an induction of ER stress, oxidative stress, and autophagy in DLD-1 cells. In addition, DHA treatment in DLD-1 cells affected expression levels of the protein p53, a protein important for regulation of cell survival and

apoptosis. Expression levels were found to increase shortly after treatment, before a decrease was observed at later time points. Some of these pathways were also affected in LS411N cells, but to a much lesser extent, and at later time points. Golgi stress was not found to be induced in neither cell line. Results are further discussed below.

4.3.1 DHA treatment induced ER stress in DLD-1 cells

To complete previous work done by our group, the expression of several important ER stress related proteins were investigated. RT-PCR analysis of mRNA-transcripts showed an upregulation of several UPR-related genes in DLD-1 cells after treatment with DHA, and protein expression analyses and confocal imaging of immunostained proteins showed the same trend [61]. The results presented in this thesis confirm an early upregulation of proteins in the PERK-eIF2α pathway of the UPR in DLD-1 cells after DHA treatment. This was not observed in LS411N cells. These findings agree with previous work published by Jakobsen et al. that showed an induction of ER stress in the colon cancer cell line SW620 in response to DHA treatment [20], as well as a paper published by Slagsvold et al. which demonstrated an activation of UPR genes in the human leukaemia cell line HL60 after treatment with the n-3 PUFA EPA. However, the DHA-induced upregulation of the UPR is not restricted to cancer cells, as ER stress-related genes have also been shown to be upregulated in peripheral blood mononuclear cells from healthy subjects after DHA treatment [78]. Even so, in normal cells ER stress has a protective role and acts to restore normal cellular function, but if the stress is too severe and the system is beyond repair, ER stress can induce apoptosis. It can therefore be speculated that cancer cells, which are more unstable than normal cells due to its higher growth rate, might not be able to restore the system to the same degree as normal cells, which could results in ER stress-related cell death.

Since cell counting experiments showed that the DHA-induced growth inhibition in DLD-1 cells was partially counteracted after treatment with NAC, we wanted to explore whether this could also be seen at protein level. Indeed, results showed a smaller increase in protein expression levels of ATF4 and NFE2L2 after treatment with both NAC and DHA compared to DHA alone. As oxidative stress is known to be a possible inducer of ER stress, this can be due to the antioxidant activity of NAC. Also, it has been shown that the levels of HSP70 in the intestinal mucosa of piglets are reduced after NAC-supplementation [75]. Elevated levels of HSP70 are indicative of oxidative stress, and act to promote refolding and prevent aggregation of damaged proteins (reviewed in [60]). It can also be speculated that the effect on HSP70 has a direct effect on the PERK-eIF2α pathway, as PERK is bound to a HSP70

protein named Bip in its inactive form. Upon stress, Bip detaches, and PERK is released and activates the downstream signalling pathway leading to UPR. Bip has also been found to have an important role in the induction of apoptosis in DHA-treated colon cancer cells. Calviello et al. showed that cells expressing low levels of Bip were more likely to undergo apoptosis after DHA treatment than those expressing higher levels [79]. Further, they showed that DHA treatment decreased the levels of Bip in the three colon cancer cell lines used in the experiments, making them more prone to apoptotic cell death. On the contrary, preliminary mRNA-expression analyses in DLD-1 cells performed by our group did not show a decrease in the expression of Bip after DHA treatment; rather, the expression was increased 1.4-fold [61]. This indicates that the induction of this specific apoptotic pathway is not involved in DHA-induced cell growth inhibition in DLD-1 cells, but this should be further investigated by protein expression analyses and the preliminary mRNA-expression analyses should be completed.

4.3.2 DHA treatment did not seem to induce Golgi stress

The ISR includes many intracellular pathways that are connected. Several ER stress-related proteins were found to be upregulated after DHA treatment, and because ER stress can lead to stress responses in the GA, protein expression levels of several Golgi stress-related proteins were investigated. Especially TFE3 is known to be activated in response to ER stress [45]. Brefeldin A was used as a positive control, and showed an increase in protein levels of the selected Golgi stress markers TFE3, CREB3, and ARF4. No significant changes in expression of these proteins were detected after DHA treatment in DLD-1 and LS411N cells, indicating that Golgi stress is not induced after DHA treatment in these cell lines. However, the protein levels were only investigated after total protein isolation. All of the investigated proteins act as transcription factors, and a conclusion about the possible activation of these proteins can therefore not be made based on the current data. To further investigate the role of Golgi stress-related proteins in DHA-induced growth inhibition, the cellular localisation of these proteins should be investigated before and after DHA treatment, either by a nuclear protein extract or confocal imaging for immunostained proteins.

4.3.3 DHA treatment induced oxidative stress in DLD-1 and LS411N cells

As discussed above, antioxidant treatment affected the DHA-induced growth inhibition in DLD-1 cells in different ways. Whereas BHA and BHT did not reverse the growth inhibition, it was partially reversed by treatment with NAC. To further investigate whether increases in

oxidative stress could explain some of the observed differences in growth reduction between DLD-1 and LS411N cells, we measured the level of mitochondrial oxidative stress and ROS.

Results showed that mitochondrial oxidative stress was increased after DHA treatment in DLD-1 and LS411N cells. This was investigated by using the marker MitoSOX that when oxidised by mitochondrial superoxide becomes fluorescent. Therefore, the fluorescence intensity reflects the levels of mitochondrial superoxide present in the cells. As mentioned above, fluorescence intensity levels were increased in DLD-1 cells after DHA treatment, both after 6 and 24 h. A small increase was also observed in LS411N cells. This is in agreement with previous work published by our group, that show a substantial increase in MitoSOX fluorescence intensity after DHA treatment in the DHA sensitive cell line SW620, and a smaller increase in the less sensitive cell line Caco2 [55]. Co-treatment with the antioxidant NAC did not reduce the mitochondrial oxidative stress level; on the contrary, it increased the fluorescence levels. This is in conflict with the findings of Lim et al. that showed a reduction in mitochondrial oxidative stress in prostate, ovarian, lung, and cervical cancer cells after treatment with both NAC and DHA compared to DHA alone [56, 80]. The results indicate that the DHA-induced growth inhibition in DLD-1 cells is not exclusively due to increased mitochondrial oxidative stress, as the observed reduction in growth inhibition after co-treatment with NAC is not reflected by measurements of mitochondrial oxidative stress after the same treatment. On the other hand, it has been demonstrated that mild mitochondrial ROS stress might improve cell survival (reviewed in [81]). It can therefore be speculated that the increase in mitochondrial oxidative stress after co-treatment with NAC in DHA-treated cells may actually be responsible for the observed reduction in DHA-induced growth inhibition.

The cellular oxidative stress marker H2DCF2 was used to measure the level of oxidative stress in DLD-1 and LS411N cells before and after treatment with DHA. When this marker is oxidised, it becomes fluorescent. Therefore, the level of ROS in the cells can be investigated by measuring the fluorescence level. Results showed an increase in fluorescence intensity after DHA treatment in DLD-1 cells, indicating an increase in ROS. This was not seen in LS411N cells. These findings agree with results previously found by our group, which showed an increase in ROS measured by DCF in SW620 cells after DHA treatment, but not in Caco2 cells [55]. Further, the results presented herein showed that co-treatment with NAC decreased the fluorescence intensity compared to DHA treatment alone, but not to control levels. This suggests that the observed partial reversal in DHA-induced growth inhibition after co-treatment with NAC is due to a reduction in oxidative stress in the cells. Co-treatment with

NAC also affects protein expression levels of ER stress-related proteins, autophagy proteins and p53. This can be due to a reduction in oxidative stress. It has previously been shown that the glutathione levels in the cells act as a buffer for cellular stress, and that the action of glutathione is important for the management of ROS (reviewed in [82]). By adding NAC, glutathione levels may increase, leading to a reduction in ROS levels in the cells.

An important factor regarding these experiments is that the DCF marker is commonly used to investigate the cellular level of ROS, a somewhat vague description. A paper by Karlsson et al. explores what the DCF marker really shows [83]. Indeed, they found that DCF-induced fluorescence is not necessarily a product of total cellular ROS, but is caused by enzymatic oxidation by cytochrome C and by the impact of hydroxyl radicals in the cytosol. Thus, the observed increase in fluorescence intensity after DHA treatment in DLD-1 cells may not necessarily reflect the total amount of ROS in the cell, but can be caused by the specific action of cytochrome C and hydroxyl radicals.

It is established that ER stress can lead to increased oxidative stress due to an accumulation of ROS (reviewed in [82]). ER stress signalling is connected to oxidative stress signalling by the action of ATF4 and NFE2L2 via PERK activation, all of which were found upregulated in protein expression analyses after DHA treatment in DLD-1 cells. Therefore, it is a possibility that the first response to DHA treatment in these cells is ER stress, which leads to increased oxidative stress. On the other hand, oxidative stress is also a known inducer of ER stress. Whether the oxidative stress induces or is a result of ER stress has yet to be explored in this cell line. However, the observation that treatment with the antioxidant NAC reduced the expression levels of ER stress proteins in addition to a reduction in cellular oxidative stress may suggest that oxidative stress occurs first.

4.3.4 DHA treatment affected autophagy levels and vice versa

Autophagy can be induced by several types of cellular stress, and are integrated with the stress responses of other cellular structures, including ER and oxidative stress (reviewed in [48]). Thus, autophagy is an important player in the ISR. As both ER stress related proteins and oxidative stress were induced in DLD-1 cells after DHA treatment, we wanted to explore whether the autophagy level in the cells also was affected. Indeed, results showed that DHA treatment increased both the autophagy level and the autophagic flux in DLD-1 cells, measured by fluorescence intensity of the autophagic marker Cyto-ID and by protein

expression levels of LC3BII, respectively. This was also seen to some degree in LS411N cells, although to a much smaller extent.

Autophagy measurements were done by using the probe Cyto-ID that becomes highly fluorescent when entering autophagic vesicles [84]. Even though this is a good tool to monitor autophagic activity, one important limitation is that it reflects only the number of autophagosomes in the cell and not necessarily autophagy induction, as the number of autophagosomes can also increase as a result of blocked conversion to autolysosomes. Therefore, the autophagic flux was also investigated by monitoring the expression of LC3BII. However, increased levels of LC3BII can be a result of both increased autophagy or reduced degradation of the protein (reviewed in [85]). Thus, even though DHA treatment increased LC3BII levels in DLD-1 cells, this does not necessarily implicate increased autophagic flux. By using BafA1 to inhibit the fusion of autophagosomes and lysosomes the degradation of LC3BII was inhibited, leading to an accumulation of the protein in the cells. To evaluate whether the autophagic flux was affected, DLD-1 and LS411N cells were treated with a combination of BafA1 and DHA. Because the degradation of LC3BII is inhibited by BafA1, an increase in expression levels of LC3BII compared to control treatments indicate increased autophagic flux as a result of DHA treatment.

As mentioned above, ER stress is a known inducer of autophagy. Especially the PERK-eIF2α-ATF4 branch of the UPR has been shown to induce autophagy, which was found upregulated in protein expression analyses in DLD-1 cells after DHA treatment. A paper by Bruhat et al. showed that eIF2α and ATF4 induce transcription of several autophagy genes, and that, PERK and CHOP are required to increase the translation of genes involved in the function of autophagosomes [86]. Further, PERK has been shown to mediate the conversion of cytosolic LC3BI to the membrane-bound LC3BII, a necessary step for autophagy induction [87]. Another paper discusses the relation between autophagy and TRIB3. By referring to unpublished results, the author claims that TRIB3 links ER stress to autophagy via the inhibition of mTOR activity [88]. Protein expression analyses showed an upregulation of all of these ER stress-related proteins in DLD-1 cells after DHA treatment, and together with an increased autophagic flux in the same cell line, results indicate a connection between the induction of ER stress and autophagy.

Autophagy is also linked to both ER and oxidative stress via NFE2L2. Johansen et al. showed that NFE2L2 induces the activity of the autophagic cargo receptor protein p62 [89]. NFE2L2

can be activated both by PERK and by oxidative stress, and activates transcription of a set of antioxidant genes. Both NFE2L2 and p62 protein expression levels were upregulated after DHA treatment in DLD-1 cells and to a lower degree in LS411N cells, providing a possible link between oxidative stress and the induction of autophagy in these cell lines. Additionally, co-treatment with NAC reduced the expression levels of both NFE2L2 and p62 compared to expression levels after DHA treatment alone. This might indicate that the antioxidant action of NAC reduced oxidative stress and thus the induction of NFE2L2, which further led to a reduction in p62 expression levels. Another link between autophagy and oxidative stress is through a DHA-mediated increase in mitochondrial ROS. Lim et al. found that increased mitochondrial oxidative stress lead to a reduction in protein levels of phosphorylated Akt and phosphorylated mTOR in prostate cancer cells [56]. This leads to the inactivation of mTOR, followed by an activation of autophagy. Similarly, we found an increase in mitochondrial oxidative stress after DHA treatment in DLD-1 cells and to some degree in LS411N cells, as well as an increase in autophagic flux in both cell lines. On the other hand, Lim et al. found that co-treatment with NAC reduced the mitochondrial oxidative stress, but this was not observed in DLD-1 cells.

An interesting finding is that the basal autophagy level in LS411N cells is 2.5-fold higher than that in DLD-1 cells. This agrees with previously reported findings from our group, which showed that the DHA sensitive cell line SW620 had a much lower basal autophagy than the less sensitive Caco2 cells [55]. As autophagy is a process that removes and recycles damaged cellular components, a process necessary for the survival of the cell, it may be hypothesised that cell lines with higher basal autophagy levels are in a better position to handle stress such as that produced by DHA.

4.3.5 The role of p53 in DHA-induced growth inhibition

According to the international agency for research on cancer (IARC) p53 database, the p53 mutation in DLD-1 cells is on codon 241, with an amino acid substitution from serine to phenylalanine [90]. This codon lies in the DNA-binding domain of p53, and might affect the DNA-binding properties of the protein (reviewed in [91]). The IARC database classifies the transcriptional activity of proteins with this specific mutation as non-functional. However, even though p53 is a transcription factor, it can also possess non-transcriptional activities in the cell (reviewed in [92]). These include interaction with both other transcription factors and non-transcription factors. For example, mutated p53 has been found to interact with and inhibit the activity of two of its family members, p63 and p73, both of which act as

transcription factors and function in a similar way as p53 [93]. Thus, even though the specific mutation in DLD-1 cells is listed as a non-functional transcription factor, it is possible that it exerts other functions in the cells. The degree of growth inhibition when knocking down p53 also indicates that it is not only functional, but also important for survival in DLD-1 cells.

As previously mentioned, LS411N cells do not express the p53 protein due to a missense mutation in the gene. Because of the different p53 status in DLD-1 and LS411N cells, we wanted to investigate the effect of DHA treatment on p53 expression levels in DLD-1 cells. Protein expression analyses showed an early increase followed by a later decrease in p53 levels after DHA treatment. This conflicts with findings from Tsuzuki et al. that showed an increase in p53 levels 24 h after treatment with conjugated EPA in DLD-1 cells [94]. On the contrary, our findings agree with a previous paper by Jing et al. showing an increase in p53 at early time points followed by a reduction at later time points after DHA treatment in three human cancer cell lines with wild type p53 [95].

As mentioned above, p53 protein expression levels decreased in DLD-1 cells after DHA treatment. A large number of proteins have been shown to interact with p53 and regulate its degradation (reviewed in [96]). This regulation occurs through ubiquitination of p53, as ubiquitin marks proteins for degradation. One such ubiquitin ligase is the carboxyl terminus of HSP70-interacting protein (CHIP), which causes poly-ubiquitination and degradation of p53. The activity of this protein is dependent on both HSP70 and HSP90, both of which are involved in ER stress. ER stress has also been shown to accelerate p53 degradation through the combined action of human Mdm2 (Hdm2) and glycogen synthase kinase 3β (GSK3β) [97]. In response to ER stress nuclear p53 is phosphorylated by GSK3β, and this enables Hdm2 to start ubiquitination of p53 and to transport p53 from the nucleus to the cytoplasm for its degradation. Results presented in this project show an increase in ER stress proteins, and it can therefore be speculated that the above mechanisms are important in the observed decrease in p53 levels. This is also supported by the confocal images that showed a nuclear localisation of p53 in untreated cells, whereas in DHA-treated cells p53 was found in the cytosol.

Wild type p53 has been found to have important functions in the management of ROS in the cells, and can act as both an antioxidant and a pro-oxidant depending on the cellular levels of the protein [63]. If present at normal cellular levels, p53 is able to upregulate the expression of several antioxidant genes to counteract increasing ROS levels. However, if p53 levels are downregulated, ROS levels increase and may cause oxidative damage to DNA. Protein

expression analysis showed an increase in p53 after 3 h of DHA treatment, but at later time points the p53 levels were decreased. Analyses of mitochondrial oxidative stress and cellular oxidative stress by the fluorescent markers MitoSOX and DCF, respectively, showed a gradual increase in fluorescence intensity, indicating increased ROS levels in the cells. It can therefore be speculated that the increase in ROS can be connected with the decreasing levels of p53. Protein expression levels of NFE2L2, a transcription factor important for the induction of the antioxidant defence, showed an early increase in NFE2L2 after DHA treatment, with a gradual decrease after 12 and 24 h. A paper published by Chen et al. show a connection between p53 and NFE2L2, and proposes a two-phase regulation of NFE2L2 by p53 [98]. At low levels, p53 increased NFE2L2 levels, but increasing levels of p53 showed a dose-dependent decrease in the levels of NFE2L2. They also showed that inhibition of the p53 protein resulted in a downregulation of NFE2L2. This conflicts with the results presented in this thesis, which showed a gradual decrease in NFE2L2 levels as p53 levels declined in DLD-1 cells. However, p53 is mutated in DLD-1 cells, which might lead to other activities compared to wild type p53.

A recent paper published by our group focused on the two colon cancer cell lines SW620 and Caco2. These two cell lines display differences in DHA sensitivity in the same way as DLD-1 and LS411N cells; SW620 is sensitive to DHA treatment, whereas Caco2 cells are less sensitive [55]. Interestingly, the p53 status in these two cell lines is also similar to DLD-1 and LS411N cells. Whereas DHA sensitive SW620 cells have a missense mutation, but still express the protein, the p53 gene in Caco2 cells has a nonsense mutation and is not expressed [62, 99]. The mutation in SW620 cells is found in the DNA-binding domain, and causes an amino acid substitution from arginine to histidine on codon 273. Like the p53 mutation found in DLD-1 cells, its transcriptional activity is classified as non-functional by the IARC p53 database [90]. A paper published by Montero et al. shows that p53 is involved in the regulation of a type of necrotic cell death induced by ROS, and that human colorectal and breast cancer cells that have lost p53 function is resistant to this type of cell death [100]. The findings in this paper show that in addition to its more known function in being a regulator of apoptotic cell death, p53 modulates poly (ADP-ribose) polymerase (PARP), which in active form regulates necrotic cell death. The loss of p53 decreases the activity of PARP, which protects against cell death. These findings can be a possible explanation on the observed differences in cell growth and survival after DHA treatment in both DLD-1 and LS411N cells and SW620 and Caco2 cells, as none of the less DHA sensitive cell lines express p53. The

similarities in DHA sensitivity and p53 status between these cell lines, together with the observed effect of DHA treatment on p53 protein levels, led us to explore the effect of DHA treatment on siRNA-mediated p53 knockdown in DLD-1 cells. Results showed that the knockdown of p53 itself led to a substantial growth inhibition in DLD-1 cells, although the degree of DHA-mediated growth inhibition was similar to the growth inhibition observed in non-transfected DLD-1 cells. This indicates an important function of p53 in DLD-1 cells, but not in relation to DHA-induced growth inhibition. Thus, the necrotic cell death induced by p53 may not be of importance, as knockdown of p53 did not affect DHA-induced growth inhibition. However, this should also be tested in cells with wild type p53, and experiments with knockdown of p53 in the p53 wild type colon cancer cell line LS513 have been started in our laboratory.

As previously mentioned, the knockdown of p53 led to reduced cell growth in DLD-1 cells, indicating an important function for p53 on cell growth and/or survival in these cells. A possible explanation for this is the role of p53 as an antioxidant. As mentioned above, downregulation of p53 leads to increasing ROS levels that can cause damage to DNA, mutations, and genome instability [63]. It would therefore be interesting to measure and compare the cellular oxidative stress in p53-knockdown cells compared to normal DLD-1 cells. Another possibility is that the mutation in the p53 gene in DLD-1 cells has led to a "gain of function" property that promotes cell survival. Indeed, several p53 mutations have been shown to affect apoptosis and to regulate metabolism to promote cell survival and proliferation in cancer cells (reviewed in [91]).

Confocal imaging showed that DHA treatment induced aggregation of p53 in DLD-1 cells. Several papers have shown aggregation of mutant p53 and that this aggregation often is accompanied by gain of function of carcinogenic effects [101-103]. Xu et al. showed that mutant p53 aggregated in several cancer cell lines, and that p63 and p73 were included in this aggregates [102]. This co-aggregation inactivated both p63 and p73, which, as mentioned above, act as transcription factors in a similar way as wild type p53. They also showed that p53 aggregation upregulated the expression of HSP70, a protein which is involved in the activation of ER stress responses. Indeed, results showed an induction of ER stress after DHA treatment in DLD-1 cells, which might be connected to the observed p53 aggregation in the same cell line. Further, preliminary mRNA expression analyses previously done by our group showed a 4-fold increase in the HSP70 protein HSPA1B and a 1.4-fold increase in the ER-specific HSP70-protein Bip after 6 h of DHA treatment in DLD-1 cells [61]. However, this

still has to be further investigated, both on mRNA and protein level to confirm a connection between p53 aggregates and increased levels of HSP70 in DLD-1 cells.

4.3.5 The role of p53 in DHA-induced autophagy

Since p53 is known to regulate autophagy, we wanted to investigate whether the observed p53 aggregates could be found in connection with the autophagy marker LC3BII after DHA treatment in DLD-1 cells. Indeed, results suggest a possible co-localisation of p53 and LC3BII, as confocal imaging showed that aggregates of both proteins can be found in the same localisations in the cells. This could be due to degradation of p53 proteins induced by ER stress as discussed above, it may be involved in the regulation of autophagy, or it may be a combination of these two. Kroemer et al. found that induction of autophagy as a response to ER stress required degradation of cytosolic p53 [104]. Results show an induction of both ER stress and autophagy combined with a decrease in p53 levels after DHA treatment in DLD-1 cells. It can therefore be speculated that the decrease in p53 levels is due to degradation induced by ER stress, which then leads to activation of autophagy in these cells. Jing et al. also reported DHA induced autophagy through p53 in human cancer cells harbouring wild type p53 [95]. They found that DHA treatment increased LC3BII protein levels and at the same time decreased p53 protein levels, which is in agreement with the results presented in this thesis. Further, they reported that p53 activated autophagy through AMPK/mTOR signalling, via the inhibition of mTOR. However, unlike the cell lines used by Jing et al., DLD-1 cells express mutated p53, and the role of mutated p53 versus wild type p53 should be further explored. Lim et al. have also shown that DHA induces autophagy via ROS-mediated AKT/mTOR signalling in prostate cancer cells with mutated p53, but the role of p53 in this signalling is less clear [56].

Kroemer et al. also reported that p53 regulates basal autophagy [104]. They found that in unstressed cells, p53 inhibited basal autophagy levels and that silencing p53 lead to an increase in basal autophagy levels. This is in agreement with the p53 status and observed basal autophagy levels in the cell lines used in this project. Whereas DLD-1 cells expressing mutated p53 has low basal autophagy, LS411N cells which lack p53 has a higher level of basal autophagy. To further explore the role of p53 on basal autophagy levels in DLD-1 cells the basal autophagy should be measured after p53 knockdown in these cells.

5. Conclusions and future perspectives

The colon cancer cell lines DLD-1 and LS411N responded differently to treatment with DHA at physiological relevant doses. Whereas DLD-1 cells showed about 40% growth inhibition after DHA treatment, LS411N cells showed almost no growth inhibition. The observed growth inhibition was not due to differences in neither culture media nor culture conditions. The lipid soluble antioxidants, BHA and BHT, did not counteract the growth inhibition induced by DHA, indicating that lipid peroxidation is not the cause of cytotoxicity. However, oxidative stress may be involved, since the antioxidant NAC partially counteracted the growth inhibitory effect of DHA.

ER stress, Golgi stress, and autophagy, all signalling pathways of the integrated stress response, was affected to different extents in the two cell lines. ER stress was induced in DLD-1 cells, but not in LS411N cells. Expression levels of Golgi stress-proteins were not induced in either cell lines by DHA. The basal level of autophagy was higher in LS411N compared to DLD-1 cells, and the autophagic flux was increased in both cell lines after DHA treatment, although to a much smaller extent in LS411N cells. The signalling pathways of the ISR are complex and intertwined, and results suggest that these are involved in DHA-mediated growth inhibition. However, since the antioxidant NAC reduced the expression of ER stress proteins as well as cellular oxidative stress, one may speculate that oxidative stress is the initial ISR trigger.

Wild type p53 has been found to be important in the handling of ROS as well as regulating autophagy. Both DLD1 and LS411N cells have mutations in the p53 gene - a missense and nonsense mutation, respectively. Expression level of p53 increased after DHA treatment in DLD-1 cells up to 3 h, thereafter decreased with time. Also, an accumulation of p53 aggregates in the cytosol was observed. Knocking down p53 did not influence DHA sensitivity of DLD-1 cells. Our results suggest that the DHA sensitivity of the colon cancer cells does not depend on p53 status, at least in our system, but p53 may have a role in the ISR.

The effect of n-6 PUFAs on colon cancer cell lines should be investigated to make sure that the observed effects are n-3 PUFA specific. In addition to the PERK-eIF2α-ATF4 pathway, other ER stress pathways should be investigated further. It would also be interesting to look at gene and protein expression levels of Bip after DHA treatment to determine its role in apoptotic induction in DLD-1 cells. This should also be done in combination with the antioxidant NAC, to see whether this affects expression levels of Bip. Induction of Golgi

stress proteins should be investigated further by analyses of nuclear proteins or by confocal imaging to investigate cellular localisation. It would be interesting to examine the effect of DHA after knockdown of several ER stress proteins on cellular oxidative stress, autophagy induction and on p53 levels. Basal autophagy measurements should be conducted in other colon cancer cell lines to confirm the hypothesis that basal autophagy levels are connected to DHA sensitivity. The function of autophagy levels in the management of DHA treatment should also be investigated by inducing or inhibiting autophagy by rapamycin and chloroquine respectively. Knockdown of p53 in other DHA sensitive cell lines should be done to investigate the role of p53 in DHA-induced growth inhibition. One such experiment has been started in our group, with knockdown of wild type p53 in the colon cancer cell line LS513. The role of p53 in autophagy should be further explored by measuring autophagy levels and investigating autophagic flux after p53 knockdown. Normal cell lines should be included in future experiments to make sure that the observed effects are cancer specific. As DHA has a clear growth inhibitory effect on certain colon cancer cell lines, it would be interesting to explore the effect of DHA as a supplement to conventional cancer treatment.

References

1. *World Cancer Report 2014*, 2015, World Health Organization.
2. Baena Ruiz, R. and P. Salinas Hernandez, *Diet and cancer: risk factors and epidemiological evidence.* Maturitas, 2014. 77(3): p. 202-8.
3. Weylandt, K.H., et al., *Omega-3 Polyunsaturated Fatty Acids: The Way Forward in Times of Mixed Evidence.* Biomed Res Int, 2015. 143109(10): p. 2.
4. Calviello, G. and S. Serini, *Dietary Omega-3 Polyunsaturated Fatty Acids and Cancer*. Diet and Cancer, ed. A. Albini2010: Springer.
5. *Cancer in Norway 2014 - Cancer incidence, mortality, survival and prevalence in Norway*, 2015, Cancer Registry of Norway.
6. Weston, A. and C. Harris, *Holland-Frei Cancer Medicine - Multistage Carcinogenesis*, 2003.
7. Balkwill, F.R., M. Capasso, and T. Hagemann, *The tumor microenvironment at a glance.* J Cell Sci, 2012. 125(Pt 23): p. 5591-6.
8. Hanahan, D. and R.A. Weinberg, *Hallmarks of cancer: the next generation.* Cell, 2011. 144(5): p. 646-74.
9. Zhang, C., et al., *Growth inhibitory effect of polyunsaturated fatty acids (PUFAs) on colon cancer cells via their growth inhibitory metabolites and fatty acid composition changes.* PLoS One, 2015. 10(4).
10. Birt, D.F. and G.J. Phillips, *Diet, genes, and microbes: complexities of colon cancer prevention.* Toxicol Pathol, 2014. 42(1): p. 182-8.
11. Kalish, B.T., E.M. Fallon, and M. Puder, *A tutorial on fatty acid biology.* JPEN J Parenter Enteral Nutr, 2012. 36(4): p. 380-8.
12. *Human Nutrition*2011: Churchill Livingstone Elsevier.
13. Berg, J., J. Tymoczoko, and L. Stryer, *Biochemistry*2012: Freeman.
14. Ratnayake, W.M. and C. Galli, *Fat and fatty acid terminology, methods of analysis and fat digestion and metabolism: a background review paper.* Ann Nutr Metab, 2009. 55(1-3): p. 8-43.
15. Lim, J.Y., C.K. Park, and S.W. Hwang, *Biological Roles of Resolvins and Related Substances in the Resolution of Pain.* Biomed Res Int, 2015. 830930(10): p. 3.
16. Nabavi, S.F., et al., *Omega-3 polyunsaturated fatty acids and cancer: lessons learned from clinical trials.* Cancer Metastasis Rev, 2015. 34(3): p. 359-80.
17. Skender, B., A.H. Vaculova, and J. Hofmanova, *Docosahexaenoic fatty acid (DHA) in the regulation of colon cell growth and cell death: a review.* Biomed Pap Med Fac Univ Palacky Olomouc Czech Repub, 2012. 156(3): p. 186-99.
18. Cockbain, A.J., G.J. Toogood, and M.A. Hull, *Omega-3 polyunsaturated fatty acids for the treatment and prevention of colorectal cancer.* Gut, 2012. 61(1): p. 135-49.
19. Dupertuis, Y.M., M.M. Meguid, and C. Pichard, *Colon cancer therapy: new perspectives of nutritional manipulations using polyunsaturated fatty acids.* Curr Opin Clin Nutr Metab Care, 2007. 10(4): p. 427-32.
20. Jakobsen, C.H., et al., *DHA induces ER stress and growth arrest in human colon cancer cells: associations with cholesterol and calcium homeostasis.* J Lipid Res, 2008. 49(10): p. 2089-100.
21. Sasaki, K. and H. Yoshida, *Organelle autoregulation-stress responses in the ER, Golgi, mitochondria and lysosome.* J Biochem, 2015. 157(4): p. 185-95.
22. Harding, H.P., et al., *An integrated stress response regulates amino acid metabolism and resistance to oxidative stress.* Mol Cell, 2003. 11(3): p. 619-33.
23. Schwarz, D.S. and M.D. Blower, *The endoplasmic reticulum: structure, function and response to cellular signaling.* Cell Mol Life Sci, 2016. 73(1): p. 79-94.
24. Dufey, E., H. Urra, and C. Hetz, *ER proteostasis addiction in cancer biology: Novel concepts.* Semin Cancer Biol, 2015. 33: p. 40-7.
25. Chen, X., J. Shen, and R. Prywes, *The luminal domain of ATF6 senses endoplasmic reticulum (ER) stress and causes translocation of ATF6 from the ER to the Golgi.* J Biol Chem, 2002. 277(15): p. 13045-52.
26. Ye, J., et al., *ER stress induces cleavage of membrane-bound ATF6 by the same proteases that process SREBPs.* Mol Cell, 2000. 6(6): p. 1355-64.

27. Yoshida, H., et al., *Identification of the cis-acting endoplasmic reticulum stress response element responsible for transcriptional induction of mammalian glucose-regulated proteins. Involvement of basic leucine zipper transcription factors.* J Biol Chem, 1998. 273(50): p. 33741-9.
28. Sidrauski, C. and P. Walter, *The transmembrane kinase Ire1p is a site-specific endonuclease that initiates mRNA splicing in the unfolded protein response.* Cell, 1997. 90(6): p. 1031-9.
29. Calfon, M., et al., *IRE1 couples endoplasmic reticulum load to secretory capacity by processing the XBP-1 mRNA.* Nature, 2002. 415(6867): p. 92-6.
30. Lee, A.H., N.N. Iwakoshi, and L.H. Glimcher, *XBP-1 regulates a subset of endoplasmic reticulum resident chaperone genes in the unfolded protein response.* Mol Cell Biol, 2003. 23(21): p. 7448-59.
31. Verfaillie, T., et al., *PERK is required at the ER-mitochondrial contact sites to convey apoptosis after ROS-based ER stress.* Cell Death Differ, 2012. 19(11): p. 1880-91.
32. Wang, M. and R.J. Kaufman, *The impact of the endoplasmic reticulum protein-folding environment on cancer development.* Nat Rev Cancer, 2014. 14(9): p. 581-97.
33. Harding, H.P., Y. Zhang, and D. Ron, *Protein translation and folding are coupled by an endoplasmic-reticulum-resident kinase.* Nature, 1999. 397(6716): p. 271-4.
34. Ohoka, N., et al., *TRB3, a novel ER stress-inducible gene, is induced via ATF4-CHOP pathway and is involved in cell death.* Embo J, 2005. 24(6): p. 1243-55.
35. Mondal, D., A. Mathur, and P.K. Chandra, *Tripping on TRIB3 at the junction of health, metabolic dysfunction and cancer.* Biochimie, 2016. 6(16): p. 00048-1.
36. Cullinan, S.B. and J.A. Diehl, *PERK-dependent activation of Nrf2 contributes to redox homeostasis and cell survival following endoplasmic reticulum stress.* J Biol Chem, 2004. 279(19): p. 20108-17.
37. Nakamura, N., J.H. Wei, and J. Seemann, *Modular organization of the mammalian Golgi apparatus.* Curr Opin Cell Biol, 2012. 24(4): p. 467-74.
38. Campadelli, G., et al., *Fragmentation and dispersal of Golgi proteins and redistribution of glycoproteins and glycolipids processed through the Golgi apparatus after infection with herpes simplex virus 1.* Proc Natl Acad Sci U S A, 1993. 90(7): p. 2798-802.
39. Clermont, Y., et al., *Structure of the Golgi apparatus in stimulated and nonstimulated acinar cells of mammary glands of the rat.* Anat Rec, 1993. 237(3): p. 308-17.
40. Rambourg, A., et al., *Modulation of the Golgi apparatus in stimulated and nonstimulated prolactin cells of female rats.* Anat Rec, 1993. 235(3): p. 353-62.
41. Oku, M., et al., *Novel cis-acting element GASE regulates transcriptional induction by the Golgi stress response.* Cell Struct Funct, 2011. 36(1): p. 1-12.
42. Miyata, S., et al., *The endoplasmic reticulum-resident chaperone heat shock protein 47 protects the Golgi apparatus from the effects of O-glycosylation inhibition.* PLoS One, 2013. 8(7).
43. Reiling, J.H., et al., *A CREB3-ARF4 signalling pathway mediates the response to Golgi stress and susceptibility to pathogens.* Nat Cell Biol, 2013. 15(12): p. 1473-85.
44. Taniguchi, M., et al., *TFE3 is a bHLH-ZIP-type transcription factor that regulates the mammalian Golgi stress response.* Cell Struct Funct, 2015. 40(1): p. 13-30.
45. Martina, J.A., et al., *TFEB and TFE3 are novel components of the integrated stress response.* Embo J, 2016. 25.
46. Nakai, W., et al., *ARF1 and ARF4 regulate recycling endosomal morphology and retrograde transport from endosomes to the Golgi apparatus.* Mol Biol Cell, 2013. 24(16): p. 2570-81.
47. Mizushima, N., et al., *Autophagy fights disease through cellular self-digestion.* Nature, 2008. 451(7182): p. 1069-75.
48. Kroemer, G., G. Marino, and B. Levine, *Autophagy and the integrated stress response.* Mol Cell, 2010. 40(2): p. 280-93.
49. Kaur, J. and J. Debnath, *Autophagy at the crossroads of catabolism and anabolism.* Nat Rev Mol Cell Biol, 2015. 16(8): p. 461-72.
50. He, C. and D.J. Klionsky, *Regulation mechanisms and signaling pathways of autophagy.* Annu Rev Genet, 2009. 43: p. 67-93.

51. Kimmelman, A.C., *The dynamic nature of autophagy in cancer.* Genes Dev, 2011. 25(19): p. 1999-2010.
52. Russell, R.C., et al., *ULK1 induces autophagy by phosphorylating Beclin-1 and activating VPS34 lipid kinase.* Nat Cell Biol, 2013. 15(7): p. 741-50.
53. Maiuri, M.C., et al., *Autophagy regulation by p53.* Curr Opin Cell Biol, 2010. 22(2): p. 181-5.
54. Niso-Santano, M., et al., *Unsaturated fatty acids induce non-canonical autophagy.* Embo J, 2015. 34(8): p. 1025-41.
55. Pettersen, K., et al., *DHA-induced stress response in human colon cancer cells - Focus on oxidative stress and autophagy.* Free Radic Biol Med, 2016. 90: p. 158-72.
56. Shin, S., et al., *The omega-3 polyunsaturated fatty acid DHA induces simultaneous apoptosis and autophagy via mitochondrial ROS-mediated Akt-mTOR signaling in prostate cancer cells expressing mutant p53.* Biomed Res Int, 2013. 568671(10): p. 10.
57. Kim, N., et al., *Docosahexaenoic Acid Induces Cell Death in Human Non-Small Cell Lung Cancer Cells by Repressing mTOR via AMPK Activation and PI3K/Akt Inhibition.* Biomed Res Int, 2015. 239764(10): p. 3.
58. Vandghanooni, S., et al., *Cytotoxicity and DNA fragmentation properties of butylated hydroxyanisole.* DNA Cell Biol, 2013. 32(3): p. 98-103.
59. Yehye, W.A., et al., *Understanding the chemistry behind the antioxidant activities of butylated hydroxytoluene (BHT): a review.* Eur J Med Chem, 2015. 101: p. 295-312.
60. Hou, Y., et al., *N-acetylcysteine and intestinal health: a focus on its mechanism of action.* Front Biosci, 2015. 20: p. 872-91.
61. Samdal, H., *Effect of DHA on growth of two human colon cancer cell lines - the role of ER stress and unfolded protein response*, 2014, NTNU: Trondheim.
62. Liu, Y. and W.F. Bodmer, *Analysis of P53 mutations and their expression in 56 colorectal cancer cell lines.* Proc Natl Acad Sci U S A, 2006. 103(4): p. 976-81.
63. Sablina, A.A., et al., *The antioxidant function of the p53 tumor suppressor.* Nat Med, 2005. 11(12): p. 1306-13.
64. Hossain, Z., M. Hosokawa, and K. Takahashi, *Growth inhibition and induction of apoptosis of colon cancer cell lines by applying marine phospholipid.* Nutr Cancer, 2009. 61(1): p. 123-30.
65. Schonberg, S.A., et al., *Closely related colon cancer cell lines display different sensitivity to polyunsaturated fatty acids, accumulate different lipid classes and downregulate sterol regulatory element-binding protein 1.* Febs J, 2006. 273(12): p. 2749-65.
66. Noding, R., et al., *Effects of polyunsaturated fatty acids and their n-6 hydroperoxides on growth of five malignant cell lines and the significance of culture media.* Lipids, 1998. 33(3): p. 285-93.
67. Griffiths, G., et al., *Effect of n-6 polyunsaturated fatty acids on growth and lipid composition of neoplastic and non-neoplastic canine prostate epithelial cell cultures.* Prostate, 1997. 31(1): p. 29-36.
68. Maehle, L., et al., *Effects of n-3 fatty acids during neoplastic progression and comparison of in vitro and in vivo sensitivity of two human tumour cell lines.* Br J Cancer, 1995. 71(4): p. 691-6.
69. Begin, M.E., et al., *Selective killing of human cancer cells by polyunsaturated fatty acids.* Prostaglandins Leukot Med, 1985. 19(2): p. 177-86.
70. Diggle, C.P., *In vitro studies on the relationship between polyunsaturated fatty acids and cancer: tumour or tissue specific effects?* Prog Lipid Res, 2002. 41(3): p. 240-53.
71. Williams, G.M., M.J. Iatropoulos, and J. Whysner, *Safety assessment of butylated hydroxyanisole and butylated hydroxytoluene as antioxidant food additives.* Food Chem Toxicol, 1999. 37(9-10): p. 1027-38.
72. Moon, H.J. and W.H. Park, *Butylated hydroxyanisole inhibits the growth of HeLa cervical cancer cells via caspase-dependent apoptosis and GSH depletion.* Mol Cell Biochem, 2011. 349(1-2): p. 179-86.
73. Zafarullah, M., et al., *Molecular mechanisms of N-acetylcysteine actions.* Cell Mol Life Sci, 2003. 60(1): p. 6-20.
74. Kerksick, C. and D. Willoughby, *The antioxidant role of glutathione and N-acetyl-cysteine supplements and exercise-induced oxidative stress.* J Int Soc Sports Nutr, 2005. 2: p. 38-44.

75. Hou, Y., et al., *N-acetylcysteine reduces inflammation in the small intestine by regulating redox, EGF and TLR4 signaling.* Amino Acids, 2013. 45(3): p. 513-22.
76. Li, W.Q., F. Dehnade, and M. Zafarullah, *Thiol antioxidant, N-acetylcysteine, activates extracellular signal-regulated kinase signaling pathway in articular chondrocytes.* Biochem Biophys Res Commun, 2000. 275(3): p. 789-94.
77. Abello, P.A., S.A. Fidler, and T.G. Buchman, *Thiol reducing agents modulate induced apoptosis in porcine endothelial cells.* Shock, 1994. 2(2): p. 79-83.
78. Myhrstad, M.C., et al., *Fish oil supplementation induces expression of genes related to cell cycle, endoplasmic reticulum stress and apoptosis in peripheral blood mononuclear cells: a transcriptomic approach.* J Intern Med, 2014. 276(5): p. 498-511.
79. Fasano, E., et al., *DHA induces apoptosis by altering the expression and cellular location of GRP78 in colon cancer cell lines.* Biochimica et Biophysica Acta (BBA) - Molecular Basis of Disease, 2012. 1822(11): p. 1762-1772.
80. Jeong, S., et al., *Docosahexaenoic acid-induced apoptosis is mediated by activation of mitogen-activated protein kinases in human cancer cells.* BMC Cancer, 2014. 14(481): p. 1471-2407.
81. Barbour, J.A. and N. Turner, *Mitochondrial Stress Signaling Promotes Cellular Adaptations.* International Journal of Cell Biology, 2014. 2014: p. 12.
82. Cullinan, S.B. and J.A. Diehl, *Coordination of ER and oxidative stress signaling: the PERK/Nrf2 signaling pathway.* Int J Biochem Cell Biol, 2006. 38(3): p. 317-32.
83. Karlsson, M., et al., *What does the commonly used DCF test for oxidative stress really show?* Biochem J, 2010. 428(2): p. 183-90.
84. Enzo, *Cyto-ID Autophagy Detection Kit Product Manual*, 2015.
85. Mizushima, N., T. Yoshimori, and B. Levine, *Methods in mammalian autophagy research.* Cell, 2010. 140(3): p. 313-26.
86. B'Chir, W., et al., *The eIF2alpha/ATF4 pathway is essential for stress-induced autophagy gene expression.* Nucleic Acids Res, 2013. 41(16): p. 7683-99.
87. Kouroku, Y., et al., *ER stress (PERK/eIF2alpha phosphorylation) mediates the polyglutamine-induced LC3 conversion, an essential step for autophagy formation.* Cell Death Differ, 2007. 14(2): p. 230-9.
88. Cunard, R., *Mammalian tribbles homologs at the crossroads of endoplasmic reticulum stress and Mammalian target of rapamycin pathways.* Scientifica, 2013. 750871(10): p. 30.
89. Jain, A., et al., *p62/SQSTM1 is a target gene for transcription factor NRF2 and creates a positive feedback loop by inducing antioxidant response element-driven gene transcription.* J Biol Chem, 2010. 285(29): p. 22576-91.
90. Petitjean, A., et al., *Impact of mutant p53 functional properties on TP53 mutation patterns and tumor phenotype: lessons from recent developments in the IARC TP53 database.* Hum Mutat, 2007. 28(6): p. 622-9.
91. Freed-Pastor, W.A. and C. Prives, *Mutant p53: one name, many proteins.* Genes Dev, 2012. 26(12): p. 1268-86.
92. Hao, Q. and W.C. Cho, *Battle against cancer: an everlasting saga of p53.* Int J Mol Sci, 2014. 15(12): p. 22109-27.
93. Gaiddon, C., et al., *A subset of tumor-derived mutant forms of p53 down-regulate p63 and p73 through a direct interaction with the p53 core domain.* Mol Cell Biol, 2001. 21(5): p. 1874-87.
94. Tsuzuki, T., et al., *Conjugated EPA activates mutant p53 via lipid peroxidation and induces p53-dependent apoptosis in DLD-1 colorectal adenocarcinoma human cells.* Biochim Biophys Acta, 2007. 1: p. 20-30.
95. Jing, K., et al., *Docosahexaenoic acid induces autophagy through p53/AMPK/mTOR signaling and promotes apoptosis in human cancer cells harboring wild-type p53.* Autophagy, 2011. 7(11): p. 1348-58.
96. Chao, C.C., *Mechanisms of p53 degradation.* Clin Chim Acta, 2015. 438: p. 139-47.
97. Pluquet, O., et al., *Endoplasmic reticulum stress accelerates p53 degradation by the cooperative actions of Hdm2 and glycogen synthase kinase 3beta.* Mol Cell Biol, 2005. 25(21): p. 9392-405.

98. Chen, W., et al., *Does Nrf2 contribute to p53-mediated control of cell survival and death?* Antioxid Redox Signal, 2012. 17(12): p. 1670-5.
99. Rodrigues, N.R., et al., *p53 mutations in colorectal cancer.* Proc Natl Acad Sci U S A, 1990. 87(19): p. 7555-9.
100. Montero, J., et al., *p53 regulates a non-apoptotic death induced by ROS.* Cell Death Differ, 2013. 20(11): p. 1465-74.
101. Rangel, L.P., et al., *The aggregation of mutant p53 produces prion-like properties in cancer.* Prion, 2014. 8(1): p. 75-84.
102. Xu, J., et al., *Gain of function of mutant p53 by coaggregation with multiple tumor suppressors.* Nat Chem Biol, 2011. 7(5): p. 285-95.
103. Lei, J., et al., *Self-aggregation and coaggregation of the p53 core fragment with its aggregation gatekeeper variant.* Phys Chem Chem Phys, 2016. 18(11): p. 8098-107.
104. Tasdemir, E., et al., *Regulation of autophagy by cytoplasmic p53.* Nat Cell Biol, 2008. 10(6): p. 676-87.

Appendix A: Equipment and chemicals

Cell cultivation:

- Cellcultivation flasks (25 cm², 75 cm² and 175 cm²), Costar (USA).
- 6 and 12 well plates, Costar (USA).
- Tissue Culture dish, 150x20 mm, SPL Lifescience Co., Ltd (Korea).
- Clinical tube, 50 ml, SPL Lifescience Co., Ltd (Korea).
- Cellstar® tubes, 15 ml, greiner bio-one.
- Disposable Serological Pipettes (1 ml, 5 ml, 10 ml, 25 ml), Costar (USA).
- RPMI 1640 Medium, Gibco (England).
- Fetal bovine serum (FBS), Gibco (England).
- Phosphate buffered saline (PBS), Oxoid (England)
- Trypsin solution (0.25 %) with EDTA (0,02%), Lonza (Belgium)
- Gentamincin, 10 mg/ml, Gibco (England).

Treatments:

- Docosahexaenoic acid (DHA, 50 mg in 200 µ EtOH), Lot: 0444840-9, Cayman (Ann Harbor, MI)
- Ethanol (Absolute alcohol prima), Arcus (Oslo, Norway)
- Butylated hydroxyanisole (BHA, 138,7 mM), B1253, Sigma-Aldrich (USA)
- Butylated hydroxytoluene (BHT, 226,9 mM), B1378, Sigma-Aldrich (USA)
- N-acetyl cysteine (NAC, 612,78 mM),
- Thapsigargin (TG, 650,75 g/mol), Lot: 052M4144V, Sigma-Aldrich (USA)
- Brefeldin A (BFA,
- Bafilomycin A1 (BafA1, 0.16 mM) B1793-10UG, Sigma-Aldrich (USA)
- Rapamycin (500 nM), R8781, Sigma-Aldrich (USA)
- Chloroquine (60 nM), C6628, Sigma Aldrich (USA)

Imaging:

- Axiovert 200 microscope with confocal module LSM 510 Meta and a 63x1.2 W
- Objective/63x/1.4 oil objective (Carl Zeiss)
- Zeiss LSM Image Examiner Software version 4.2.0.121

Protein isolation:

- EDTA (1M), Sigma-Aldrich (USA)
- Biorad protein assay dye reagent concentrate, Bio-Rad laboratories (USA)

Western blotting:

- NuPAGE reducing agent, Life Technologies (USA)
- NuPAGE Sample buffer, Life Technologies (USA)
- NuPAGE Novex Bis-Tris gels, Life Technologies (USA)
- NuPAGE MOPS Running buffer, Life Technologies (USA)
- NuPAGE Antioxidant, Life Technologies (USA)
- NuPAGE transfer buffer, Life Technologies (USA)
- XCell Mini-Cell, Life Technologies (USA)
- XCell II Blot Module, Life Technologies (USA)
- PDVF membrane, Millipore (USA)
- Odyssey^{R} protein molecular weight marker, 928-40000, LI-COR biosciences (USA)

Immunostaining:

- Odyssey blocking buffer, LI-COR biosciences (USA)

Flow cytometry:

- BD FACSCanto, VWR International (USA)
- MitoSOX Red Mitochondrial superoxide, M36008, Life technologies (USA)
- Dimethyl sulfoxide (DMSO), D2650, Sigma-Aldrich (USA)
- Hanks' balanced salt solution (HBSS) #H8264, Sigma-Aldrich (USA)
- ROS detection kit, C6827, Life technologies (USA)
- Cyto-ID autophagy detection kit, ENZ-51031-K200, Enzo Life Sciences (USA)

Transfection with siRNA:

- Lipofectamine RNAiMax transfection reagent, Fisher Scientific (USA)
- P53 siRNA, #SI00011655, Qiagen (Germany)
- AllStars Negative control, #1027280, Qiagen (Germany)
- AllStars Hs Cell Death Control, #1027298, Qiagen (Germany)

Appendix B: Buffers and solutions used for protein isolation and western blotting

NuPAGE MOPS Running Buffer (1 L)

- 50 mL 20xNuPAGE MOPS running buffer
- 950 mL dH2O

NuPAGE Transfer Buffer (1 L)

- 850 mL dH2O
- 100 mL methanol
- 50 mL NuPAGE Transfer Buffer

Phosphate buffered saline (PBS) washing buffer (1 L)

- 1 L dH2O
- 20 PBS tablets

(Add 10 mL Tween20 to make PBST)

10xTris-buffered saline (TBS)

- 200 mM (0.2 mol/L) Tris (hydroxymethyl)-aminomethan
- 1369 mM (1.369 mol/L) NaCl

Making 1 L

Mix 900 mL dH2O, 24.2 g Tris(hydroxymethyl)-aminomethan and 80 g NaCl. Adjust the pH to 7.6 by using concentrated HCl or NaOH. Add dH2O to get a total volume of 1 L.

Tris-buffered saline (TBS) washing buffer (1 L)

- 100 mL 10xTBS
- 900 mL dH2O

(Add 10 mL Tween20 to make TBST)

Blocking buffer:

- 50 % TBST
- 50 % Odyssey blocking buffer

Primary- and secondary antibody solution:

- Blocking buffer
- Primary/secondary antibody in appropriate dilution

Lysisbuffer for isolation of total proteins (510 µL):

- 400 µL 8M urea-buffer with Triton-x (0.24 g Urea, 5 µL Triton-x, 395 µL MQ water)
- 50 µL 1 M DTT
- 20 µL 25x PI/complete
- 20 µL PIC2
- 20 µL PIC3

Appendix C: Buffers and antibody solutions for immunofluorescent staining

Blocking buffer:

- 3 % Goat serum
- 97 % 1xPBS

Primary/secondary antibody solution:

- 1 % Goat serum
- 99 % 1xPBS
- Primary/ secondary antibody (appropriate dilutions)

Appendix D: Buffers and solutions used for flow cytometry

Cyto-ID 1x Assay buffer (10 mL):

- 1 mL 10x Assay buffer
- 9 ml dH_2O

Cyto-ID Green detection reagent (1 mL)

- 1 µL green detection reagent
- 1 mL 1x Assay buffer

Appendix E: Protein ladders

Figure: Odyssey protein molecular weight marker, 928-40000 (LI-COR biosciences)